**School of Architecture, Construction and Planning**

# DEVELOPMENT OF AN EVALUATION TOOL FOR USE AT THE DESIGN STAGE OF AUDITORIA WITH RESPECT TO UNASSISTED SPEECH REINFORCEMENT

**TERRANCE MC MINN**

**"This thesis is presented as part of the requirements for the award of the Degree of MASTER OF SCIENCE (BUILDING STUDIES) of the Curtin University of Technology"**

**December 1996**

# ABSTRACT

This dissertation describes the development of an evaluation tool that can be used by an acoustican during the design stage of enclosures used for unassisted speech. Enclosures include lecture theatres, lecture halls and speech auditoriums. The tool is designed to enable Acousticians to be able to manipulate various acoustical parameters such as the geometry and the materials or construction selection to gauge the impact on speech performance. The tool can also be used to evaluate the performance of speech privacy within spaces using the Speech Transmission Index.

Computer simulation tools have a number of advantages over existing methods such as physical scale models for this type of evaluation. Typical advantages are in the elimination of the difficult selection of materials with appropriate scale model acoustic performance, resolution of air absorption at scale model frequencies, reduced cost in development of the model, no storage space problems, ease of modifying and duplicating the model.

Scale models also present difficulties in measuring some of the indices such as Speech Transmission Index. Whilst equipment can be purchased for the measurement of STI, scale model equivalents and the impact of the change in frequencies and modulations have not been researched or published. Currently, there are only two methods of evaluating the Speech Transmission of an enclosure: Build a full size enclosure and test; or simulate mathematically to derive the performance. At the time this thesis was commenced there were no commercial simulation programs available that could derive Speech Transmission Index information.

The evaluation tool has been implemented as a computer program, based on IBM® PC type computers running Microsoft WINDOWS® 3.1 or later. The implementation uses the image method for the 'ray trace' algorithm. This basic image method utilises the enhancements made by a number of authors. In particular the Transformation Matrix method and homogenous coordinates have been used to improve the speed of the algorithm. Pre-computation of mutually invisible planes allows trimming the number of possible combination of rays that need to be computed.

Results of physical measurement from two case studies have been compared to results of the simulation. Good correlation between the simulations and the case studies were achieved for the Speech Transmission Index and RASTI values. The accuracy of the simulation, in terms of decay based indices, is limited by the lack of sufficient tail to the calculated number of rays.

Further research and implementation of hybrid techniques utilising both the image method and more traditional ray-tracing algorithms to improve the quality of the calculated decay data are required. Investigation of techniques used in photo-realism 'ray-tracing' may result in far more realistic data which is the basic input to the Speech Transmission Index calculations.

# ACKNOWLEDGMENTS

This thesis would not have been possible without the support, assistance and encouragement of a number of people.

My wife Ann for her support, encouragement and understanding throughout this thesis, and to my children Paul, Kim, Jenny and Tarryn for when I was not ‘there’ to listen to them.

To Andrew Marsh, formerly at University of Western Australia, School of Architecture for his assistance in explaining a number of obtuse mathematical ideas including the derivation of plane equations; hidden line algorithm for tree pruning in the ‘ray trace’; his simple explanation of the Impulse Response methodology.

At Curtin University of Technology;

My research supervisor, Associate Professor Dr. N. A. D'Cruz for his direction, assistance and encouragement.

My associate supervisor, Associate Professor Dr. P. J. Evans for his encouragement and assistance.

Professor L. W Hegvold, Head of the School of Architecture, Construction and Planning for continuing support throughout this project.

# Table of Contents

# Table of Figures

# Table of Tables

# 1. Introduction

This dissertation describes the development of an evaluation tool that can be used by an acoustican during the design stage of enclosures used for unassisted speech. Enclosures would include lecture theatres, lecture halls and speech auditoriums. The tool is designed to enable acousticians to manipulate various acoustical parameters such as material and construction selection in order to gauge the impact on speech performance. The tool could also be used to evaluate the performance of speech privacy within spaces.

For acceptable communication between two people to exist, a number of factors must be accommodated. These factors, which control the overall quality and intelligibility of the communicative effort, are quantified for the particular situations to which they apply.

This research uses computer simulation as a basis for predicting the performance of the enclosure based on the Speech Transmission Index. The Speech Transmission Index is used as it can also be measured in the physical environment, thus providing a convenient and consistent terminology from design through to fine tuning of the constructed building.

To broaden the useability of this tool, a number of other indices are calculated such as Reverberation Time, Early Decay Time, Deutlichkeit, Clarity, Reverberant to Early Sound Ratio, Centre Time and Initial Time Gap. Some are not specific to speech intelligibility but are included to give the Acoustician additional information on which decisions can be made. It is acknowledged that the included indices are a subset of the myriad of indices available, but they do form a broad cross section of those available. These indices have been included as they are readily computed either from the available geometry or from the available ray data, but are not the primary focus.

This research establishes the current position for the computation of the Speech Transmission Index through a review and analysis of the literature, develops a simulation tool and verifies the accuracy of the simulation through a physical measurement case study approach. Comparison of the results from the simulation tool and the case studies are discussed and the limitations are outlined.

## 1.1 Background to the Research

Various methodologies, such as Preferred Speech Interference Level (PSIL); Thiele's 'Deutlichkeit'; Point of Gravity time; Clarity; Early Decay Time; Reverberation Time; Hallmass; Hallabstand; Room Response; Articulation Index; and Speech Transmission Index; have been proposed to quantify and qualify the acoustic performance of spaces, with the major emphasis on quantifying the performance of the space in terms of speech recognition (Jordan 1980). Most of these indices, if not all, tend to specialise on only one or two aspects of the total acoustic performance. Chapter 2 has more details of the indices used in the simulation tool.

French and Steinberg (1947, pp90-91) outline factors which govern the intelligibility of speech as follows:

> *"Speech consists of a succession of sounds varying rapidly from instant to instant in intensity and frequency. Assuming that the various components are received by the ear in their initial order and spacing in time, the success of the listener in recognizing and interpreting these sounds depends upon their intensity in his ear and the intensity of unwanted sounds that may be present, both as a function of frequency."*

In that paper they outline a methodology for predicting speech intelligibility of a transmission system by its parameters, these being the intensities of the speech and the intensity of the unwanted sounds both as a function of frequency. Kryter (1962a) reworked this method into a convenient useable form. In January 1969, the American National Standards Institute adopted it into the S3.5-1969 standard titled *"American National Standard Methods for the Calculation of the Articulation Indexes"*.

Articulation Index is defined as a computed measure of speech intelligibility, based on speech perception tests. To achieve a high degree of repeatability, these tests are quite time consuming requiring a large number of talkers and listeners. (ANSI S3.5-1969)

There are two major limitations to the use of the Articulation Index. Firstly, ANSI S3.5-1969 notes the Articulation Index *"has been principally validated against intelligibility tests involving adult male talkers. The method cannot therefore, be assumed to apply to situations involving female talkers or children"*. Secondly, as Steeneken and Houtgast (1980) point out, the Articulation Index method is not applicable in situations where there is nonlinear distortion (eg. peak clipping as experienced with speech reinforcement systems) or distortions in the time domain (eg. echoes and reverberation).

The early 1970's saw research into other methodologies and indices that might better quantify and qualify acoustical performance. Houtgast and Steeneken (1985a) were able to demonstrate the applicability of using the Modulation Transfer Function in acoustics, as used in the performance assessment of optical systems. The Speech Transmission Index can then be derived from the resultant Modulation Transfer Function.

The Modulation Transfer Function and the derived Speech Transmission Index, is a means of correlating intelligibility with reverberation, echoes and noise (Houtgast and Steeneken, 1973, 1980, 1985a and 1985b). The Modulation Transfer Function provides the means to quantify the extent of modification of the original signal by the enclosure or transmission path between the source and receiver. Most modifications of the signal are related to the carrier frequency; thus the analysis is octave-band specific (Houtgast and Steeneken, 1985b).

Equipment was developed (Steeneken and Agterhuis, 1982) which was able to measure the Modulation Transfer Function over seven octave bands and 14 modulation frequencies (a total of 98 individual measurements). This detailed analysis enables computation of the Speech Transmission Index.

An abbreviated Speech Transmission Index method, known as the Rapid Speech Transmission Index, was devised by Houtgast and Steeneken (1984) to enable faster methods to physically measure auditoria performance. The Rapid Speech Transmission Index was formalised in International Electrotechnical Commission publication 268. Two commercial devices, the Brüel and Kjær Speech Transmission Meter Type 3361 and the Stanley Techron System 12, TEF analyser have been developed. Both devices were designed to measure Rapid Speech Transmission Index.

## 1.2 Research Aim

Equipment is now available to measure both the Speech Transmission Index and the Rapid Speech Transmission Index in completed buildings. What is required is a simulation tool that can be used to predict the expected Speech Transmission Index, or Rapid Speech Transmission Index, from Architect's sketch design concepts drawings. To maximise the design applicability, the simulation tool must be capable of using the gross sketch design parameters, eg. room shape, approximate geometry and suggested surface finishes.

The simulation tool would assist acousticians by calculating not only the Speech Transmission Index and Rapid Speech Transmission Index but include other traditional measures such as Reverberation Time (RT), Early Decay Time (EDT) and Center Time (C). These statistics are calculated from the physical geometry and allow the Acoustican to refine the basic shape and material choices.

Analysis at an early stage in the design process allows basic assessment of various design concepts on the critical speech performance of the space. More elaborate and expensive design tools, both in time and cost, such as scale models can be constructed and tested, based on the final design option.

In special spaces, such as lecture theatres, designed for unassisted speech[1], the speaker relies in part on the 'raw power' of his or her voice and any additional assistance provided by the building enclosure (for example: walls, ceilings and other reflecting surfaces) to provide sufficient signal level above the background noise to allow adequate speech intelligibility.

If it is accepted that the building enclosure is an 'acoustic transmission system' (Houtgast, Steeneken and Plomp, 1980), then its function is to transfer the signal from the source to the listener faithfully. An understanding of the way in which the signal is modified and transmitted to the receiver is essential in designing spaces suitable for natural speech projection.

The signal is transmitted and modified in four ways

a) Directly transmitted (airborne);
b) Reflected differentially by various parts of the enclosure giving a reverberant sound;
c) Modified by ambient noise permeating in from outside the enclosure; and
d) Modified by ambient noise generated within the enclosure.

The traditional global and statistical methods of analysing the acoustic performance of such spaces either do not permit, or only allow a very restrictive scope for the investigation of room's parameters such as:

a) Room dimensions (ratios of length to width to height);
b) Room volume;
c) Surface materials (acoustic absorption characteristics);
d) Locations for the speaker;
e) Locations for the listeners/audience;
f) The transmission performance of the enclosure (how the sound is transmitted from the speaker to the listeners position);
g) Orientation and acoustical performance of surfaces (reflection patterns);

[1] Unassisted speech is defined as the absence of electro-mechanical amplification of the speaker's voice.

Traditional analysis methods, such as:

a) Reverberation Time Calculations (time required for the sound energy to decrease by 60 dB); and
b) Ray Tracing to determine the reflection patterns of various wall surfaces, path lengths and time delays for the reflected sound signals,

were developed for rooms with well defined and simplified acoustic properties, such as uniform distribution of acoustic absorption. In auditoria design, using a uniform distribution of absorption would reduce the overall effectiveness of the space to direct the speaker's voice to the listeners.

This thesis proposal will investigate and produce a simulation tool for use at the design stage of auditoria for unassisted speech reinforcement.

## 1.3 Limitations

This thesis is restricted to developing a simulation tool for the analysis of enclosures used for unassisted speech reinforcement. The rationale behind this is that there is only a single source, of relatively low acoustic power. The maximum sound power of a male voice is approximately 2000μwatts, while vowels may go as high as 50μwatts and soft consonants only 0.03μwatts. *"The high frequency low energy transient consonants are the chief contributors to the intelligibility of speech, and noise will therefore have the greatest masking effect if its spectrum is significant in the frequency range above 500Hz."* (Hassall and Zaveri 1979, p67)

With such low acoustic power, it is vitally important that all building enclosure measures, such as maximising reflections of the sound source into the audience area, lateral reflections and size and placement of reflectors, are utilised to increase the projection capability of the voice whilst maintaining speech intelligibility, particularly in relation to the high frequencies above 500Hz.

With speech reinforcement systems, there are a number of additional complexities. According to Davis and Davis (1989, p1007), the Directivity Factor (Q) of the loudspeaker is *"a fundamental parameter in speech intelligibility in difficult acoustic en-*

*vironments"*. They found that for devices that can be accurately defined, then equally accurate response predictions are possible. *"If the polar response of a loudspeaker is too uneven to derive a single number Q from it … it is impossible to … predict an accurate performance"* (Davis and Davis 1989, p1005).

Another vitally important parameter in speech reinforcement is synchronisation of the speaker array. Mis-synchronisation can lead to degradation of speech intelligibility especially in reverberant spaces (Davis and Davis 1989). Similarly, synchronisation problems occur with the response of microphone arrays. There are other characteristics of microphones which have implicit design considerations, such as their directionality (for example omni-directional, cardioid and ribbon microphones).

Further, there may also be problems in the communications equipment which include:

a) signal clipping;
b) frequency distortions due to incorrect placement of the microphone;
c) feedback;
d) the time intervals between the direct sound from the person speaking and each loudspeaker;
e) use and magnitude of artificial time delays in the speech reinforcement system;
f) the frequency response of the system;
g) the need for operator intervention to control the overall volume as the person speaking moves about;
h) the apparent direction of the sound coming from the person speaking and not the loudspeakers.

These problems are outside the domain of simulation tools such as the one developed in this thesis.

This thesis primary focus is in developing a simulation tool for the *prediction* of the Speech Transmission Index for unassisted speech. Other indices are generated from the available simulation data. Validation will be carried out with no audience present.

## 1.4 Form of the thesis

This thesis is in two parts. This report and the simulation program on the accompanying diskette for IBM compatible PC's. The diskette contains the Microsoft Windows 3.x executable, windows help file and sample data files as used in this report.

Chapter 1 Introduction. States the nature and scope and limitations of the work. This has been the subject of this introductory chapter.

Chapter 2 Literature Review. Reviews the literature and the procedure for the development of the Speech Transmission Index and the Modulation Transfer Function.

Chapter 3 Methodology. States the procedures and theories used in the development of the evaluation tool.

Chapter 4 Results. Discusses the outcomes of the evaluation tool and the comparison of the simulations using this tool and physical measurements for two case studies.

Chapter 5 Conclusions. It compares the aims with the achievements and suggests a number of future developments.

Glossary of Terms provide a brief description of some of the key terms and abbreviations used in the thesis report.

References lists all material cited in this report.

Appendices, contains supplementary information, tables and data.

# 2. Literature Review

The field of scientific study in acoustics, particularly theatre acoustics, can be traced back to the ancient Greek amphitheatres such as Epidauros. Hunt (1978) places the origins of the study of sound to Pythagoras (ca. 570-497 BC). Later in history Roman architects were shown to have developed an understanding of theatre acoustics (open air amphitheatres) as illustrated by the Roman architect Vitruvius in his *De Architectura* books (*Liber V, chapter VII: De locis consonantibus ad theatra eligendis*):

> *"We must chose a site in which the voice may fall smoothly, and not be returned by reflection so as to convey an indistinct meaning to the ear. For there are some places which naturally hinder the passage of the voice, … those (dissonant) places in which the voice, when first it rises upwards, strikes against solid bodies above, and is reflected, interfering as it settles down with the rise of the utterance … those (circumsonant) in which the voice moves around, is then collected in the middle where it dissolves without the case-endings being heard, and dies away in sounds of indistinct meaning … those (resonant) in which the words, striking against a solid body, give rise to echoes and make the case-endings sound double … those (consonant) in which the voice reinforced from below rises with greater fullness, and reaches the ear with clear and eloquent accents. Thus if careful observation is exercised in the choice of sites, such skill will be rewarded by the improved effect of the actor's voices. … Whoever uses these rules, will be successful in building theatres."* (Hunt 1978, p34)
>
> The modern equivalent for the terms of: *dissonant* is interference; *circumsonance* is reverberation; *resonance* is echo and *consonance* is the process where a sound is strengthened by reflection. (Sabine 1913, pp257)

From these early beginnings, the Greek and later Roman amphitheatres were concerned with projecting the voice of the actors to the audience (Jordan 1980). The actors used masks to both enhance expression of the character and to amplify their voices (Jordan 1980; Sabine 1913). Seating was raked and tiered; the audience kept as close as possible to the stage area. Though not all of these early theatres exhibited 'good' acoustics, Vitruvius proposed the use of resonant vases placed in strategic po-

sitions in the audience. This is reported by Sabine (1913) as evidence of the lack of *consonance* in the contemporary Greek theatres.

As the overall noise levels in the markets grew, the need arose to provide some protection to the 'theatre' (Parkin and Humphreys 1958), though this was not the only reason to position walls and buildings behind the stage for the actors. Undoubtedly they did provide some improvement in the distribution of the sound, as the walls of the buildings added reflections to the direct sound projected from the actors. These buildings, positioned behind the stage, grew to incorporate various rooms and features. They became part of the theatre providing alternative views, for example the Roman amphitheatre of Orange in France (Jordan 1980).

The transition from open air theatres to totally enclosed theatres is seen in the Renaissance Teatro Olympico theatre in Vicenza, Italy (Jordan 1980). The plan of the theatre is typical of the Roman amphitheatre 'design' with the major exception being, it is totally enclosed. Another theatre built not long after was the Teatro Farnese in Parma. Here the stage became an elongated shape with what was to develop in a proscenium linking a more traditional stage area and the audience area (Jordan 1980).

History shows that as the music form developed, so did the shape and styles of the auditoria. With the development of the operatic music form, came the need to reduce the reverberation in these auditoria for better understanding of the words. A noteworthy example is Wagner's Festspielhaus in Bayreuth. This operatic theatre deviated from the accepted theatre 'design' of the time. The audience is seated in a fan shaped auditorium, with very large diffusion walls consisting of pillars and niches. The seating is predominantly at floor level which has a steep rake (Jordan 1980).

The development of the music form has out stripped the development of the theatre. There are the differing needs for classical music, opera and symphony. None of these requirements, such as reverberation, articulation, spatial effect, come close to the requirements of the late twentieth century amplified music forms.

To cater for the huge patronage of some groups we now have almost come the complete circle with the outdoor concerts of recent times. Modern groups would be well suited to playing in the ancient Greek amphitheatres with their raked seating. The amphitheatres environment is well suited to this form of music, as it allows for large audiences, situated at considerable distances from the stage, with the visual images projected onto giant video screens, gross amplification can deliver the sound to all patrons for kilometres around. Background noise levels are rarely a problem. The major problem in this environment is how can the sound be restricted to the site!

## 2.1 Auditoriums

Considerable research has been carried out in the field of auditorium acoustics during the past decades. It would seem to some the results of this effort have resulted in auditoriums many feel were only moderately successful. The "*good acoustics is rather a matter of empirical experience and also of good luck than systematic and science-based design.*" (Kuttruff 1994, p27)

A major turning point in the understanding of room acoustics came with Sabine's research in 1895-1898. In 1895, Sabine was instructed, by the Corporation of Harvard University:

> "*to propose changes for remedying the acoustical difficulties in the lecture-room of the Fogg Art Museum, a building that had just been completed.*" (Sabine 1900, p3)

It is interesting to realise, this research was prompted by the lack of intelligibility in the Fogg theatre - a speech intelligibility problem, not a music appreciation problem. Three years of research led Sabine to formulate the Reverberation Time Equation, which links room volume, frequency and absorption. (Beranek 1994)

The reverberation time equation is:

$$T_{60} = 0.163\frac{V}{A_f}\text{sec} \qquad \{\text{Eq } 2.1\}$$

where $T_{60}$ the time in seconds it takes a sound to decay by 1 millionth (60 dB) of its level

$V$ the volume in cubic metres

$A_f$ the total sound absorption at a given frequency in m² sabins

This formula has a number of limitations to its applicability and neglects room modes, the influence of the shape of the enclosure and placement of acoustic absorption within the enclosure. It is based on the theoretical assumption that the sound waves hit each of the boundary surfaces in succession (Beranek 1992); that the sound in the enclosure is reasonably reverberant; the acoustic absorption is uniformly distributed; the sound field is diffuse[2]; and that the sound can be propagated in any direction with equal probability (Ginn 1978; Northwood 1977). This is not the case in speech auditoria. The unaided voice is very directional and the source is located in only one area of the auditorium. Generally the stage or source area of the auditorium is reflective (acoustically), the rear wall is acoustically absorbent, seating/audience is absorbent and the ceiling is reflective. Additionally when reflectors are utilised to increase the overall signal level present to the listener the sound has significant directionality thus reducing the diffuseness of the sound field.

[2] A diffuse sound field, in this context, refers to a sound field in which the average levels are the same in all parts of that field. (Northwood)

With the aid of formulas such as Sabine {Eq 2.1} and others[3], acousticians are able to predict, with increasing accuracy, the expected reverberation time for spaces. Reverberation is important in the acoustic appreciation of spaces as Beranek outlines:

> *"During continuously flowing music, listeners hear the first 10 or so decibels of the sound decay. If this early reverberation time is long enough, each note is prolonged and the music takes on a singing tone. When the music stops abruptly, the listeners hear 35 or more decibels of the decay in the quiet interval. This longer reverberation adds both fullness of tone and loudness and gives the listener a sense of being enveloped by the sound."* (Beranek 1994, p4)

Reverberation also has significant effect on the intelligibility of speech. As the reverberation increases the intelligibility decreases. This is readily experienced when two conversations are conducted in spaces at the opposite ends of the reverberation spectrum, eg. an anechoic and reverberation chamber. In the anechoic chamber, the lack of reverberation is evidenced by the apparent reduced power of the voice. (Loudness is reduced in the face to face mode). In the reverberation chamber, with the abundance of reflections, reverberation, has a dramatic and obvious impact on the intelligibility of the speech making speech difficult to understand.

In the period from 1900 to 1950, there was considerable research and development activity to established optimum reverberation times, for various facilities of differing size and purpose. This research was centred on spaces used for music and concert halls. Examples (Beranek 1994) of the established reverberation times are: at mid frequencies (500-1000 Hz) the reverberation time, for Baroque music is approximately 1.6 seconds; for Classical music is approximately 1.8 seconds; for Romantic music is approximately 2 seconds.

As can be seen in Figure 2.1 (AS2107 - 1987), the optimum reverberation times for speech auditoriums differs greatly from those of churches, opera houses and concert

[3] Other reverberation time equations, such as the Eyring, Fitzroy Sabine, Fitzroy Eyring, Millington and Sette, Norris and the Arau-Puchades, have been defined to extend the scope of the original Sabine formula.

halls. The lower optimum reverberation times for the speech auditoriums demonstrate the influence of reverberation on speech intelligibility.

NB: Speech studios are a specialised space, in which the overall requirements for recording have more to do with the electronic post processing requirements than speech intelligibility. In these situations, the requirement is for 'acoustically dry', very short reverberation times. Additional reverberation is added at a later stage electronically as required.

Figure 2.1 Typical chart *(AS2107 - 1987, p8)* of optimum reverberation times for spaces with differing uses.

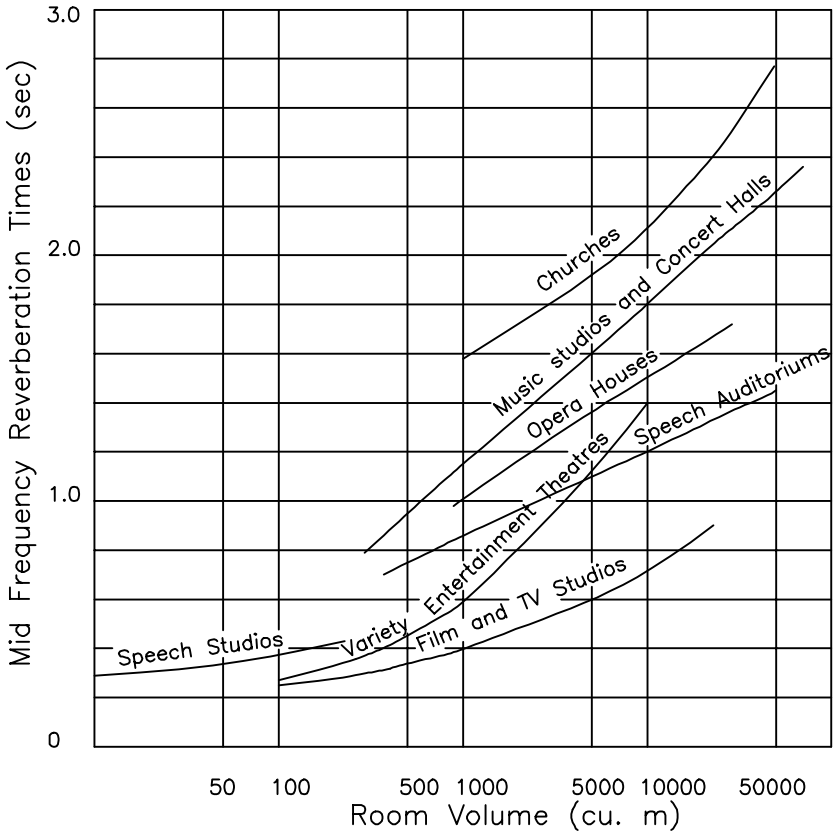


The importance of Sabine's reverberation time relationships can be seen in the almost predominance of reverberation in the acoustical design of spaces used for music and speech in period following the 1900. In 1958, Parkin and Humphreys (1958, p82) wrote:

> *"The present state of knowledge about the acoustics of rooms for music is such that major faults (such as echoes) can be avoided in design … nearly all the advice that can be given is qualitative only; at this stage of knowledge. The one important exception is the reverberation time which can be specified and … measured objectively"*

Research investigations, such as those reported in Beranek (1992), Jordan (1980), Schroeder, Gottlieb and Siebrasse (1974), with halls predominantly based on the reverberation time design revealed that other factors were important in the way people distinguish acoustic events (Beranek 1994; Jordan 1980). Research into the transient effects of very short duration sound events led to a number of criteria being established, such as Deutlichkeit, Centre Time, Early Decay Time, Articulation Index, Speech Transmission Index and RASTI. These criteria involved physical measurement of events and so are classified in the evaluation stage rather than the design stage.

Much of the speech intelligibility development can be traced back to the telephone industry. For example, Bell Telephone Laboratories have been responsible for much of the research (French and Steinberg, 1947; Knudsen 1929; Cavanaugh, Farrell, Hirtle, Watters 1962). It is largely this research that underpins our understanding of speech intelligibility and speech reinforcement systems.

> *"The most feasible scheme for such a rating [speech intelligibility testing] is probably the one used by telephone engineers for testing speech-transmission over telephone equipment, which goes by the name of articulation tests. … The writer has used this same scheme for investigating the effects of reverberation and noise upon speech reception in auditoriums."* (Knudsen 1929, p56)

In the period between 1922 to 1950, researchers, driven by the telephone industry, developed methodologies to test speech intelligibility. As these methodologies became available, development of optimum reverberation times for assembly halls were made considerably easier (Jordan 1980).

> *"It is not a simple matter to give a quantitative rating to a room which is used for music, since so much depends upon the musical tastes and disposition of the listeners. It is, however, a relatively simple matter to give a quantitative rating to a room which is to be used*

> *for speaking, since our primary concern is how well we hear spoken words of the speaker."* (Knudsen 1929, p56)

In 1947, French and Steinberg published a procedure and methodology for computing the Articulation Index. This was based on work carried out some 25 years previously by H. Fletcher (French and Steinberg 1947). Their paper examines factors which govern the intelligibility of speech by examining quantitatively the ability of the ear to distinguish sounds. The paper provides a platform to examine the influence of reverberation and masking noise on speech intelligibility.

The development of Articulation testing and the Articulation Index procedure in particular, as a quantitative measure of the intelligibility of speech in a closed system was important to the development of the optimum reverberation times as seen in Figure 2.1, page 14.

## 2.2 Design Tools

As expected, development of the scientific approach to the study of enclosure (building) acoustics followed the general approach of analysis of the completed building. Sabine used this approach in the development of reverberation time calculations used to predict acoustical performance. These calculations became the major and often only tool used to predict performance by many people in the early 1900's.

There are a variety of tools which are used in acoustic design. They vary according to the project type, type of sounds present in the facility, perceived problems, architectural style and practitioner approach. These tools can be grouped into broad classifications, namely:

a) Statistical tools which would include approaches such as reverberation time calculation and room resonance;

b) Geometrical tools such as reflection/ray tracing, sight-line analysis; and

c) Model testing.

### 2.2.1 Statistical Acoustics

The term 'statistical' acoustics is used to describe the manner in which the reverberant sound field is assessed by treating all the reflected sounds statistically to calculate an average reverberant sound pressure level (Northwood 1977).

Approaches in determining the reverberant sound pressure level in a space are reverberation and room resonance investigations.

#### *2.2.1.1 Reverberation*

The Sabine Reverberation formula, and most of its derivatives treat the enclosure as a single homogenous space. Other formula, such as the Eyring, Fitzroy and Arau-Puchades, attempt to take into account placement of a acoustic absorption on a surface pair arrangement. eg. Floor - Ceiling or End Walls or Side Walls.

These formulae provide estimates of the reverberation time as a single set of frequency dependent times for the *whole* enclosure. This simplification is useful on the global scale, especially with regular shaped spaces, but can be quite misleading when used with irregular shapes. Eg fan shaped auditoriums; balconies; stage versus audience sections.

Other simplifications in the reverberation formulas derive from the assumptions that form the basis of these formulas. For example:

- The Eyring Formula is based on the assumption of reasonably diffuse sound fields and acoustically 'dead' rooms.

$$RT = \frac{(0.07 * \text{Volume})}{(-\text{Total Surface Area} * \log_{10}(1 - \text{Mean Absorption}))} \qquad \{\text{Eq } 2.2\}$$

- The Fitzroy Sabine Formula is based on the assumption of non uniform absorption and a reasonable reverberant sound field.

$$RT = \frac{0.161 * Volume}{(S * S)} * \left( \frac{x * x}{A_x} + \frac{y * y}{A_y} + \frac{z * z}{A_z} \right) \quad \{Eq\ 2.3\}$$

- The Fitzroy Eyring Formula is based on the assumption of non uniform absorption and acoustically 'dead' rooms.

$$RT = \left(\frac{x}{S}\right) * \left( \frac{0.07 * Volume}{-S * \log_{10}(1 - Mean\ Absorption\ Side\ Walls)} \right) + \left(\frac{y}{S}\right) * \left( \frac{0.07 * Volume}{-S * \log_{10}(1 - Mean\ Absorption\ Ceiling\ Floor)} \right) + \left(\frac{z}{S}\right) * \left( \frac{0.07 * Volume}{-S * \log_{10}(1 - Mean\ Absorption\ End\ Walls)} \right) \quad \{Eq\ 2.4\}$$

- The Arau-Puchades Formula (Arau-Puchades 1988) is based on the assumption of non uniform distribution of absorption

$$RT = \frac{0.161 * Volume}{S * Geometric\ Mean\ Absorption} \quad \{Eq\ 2.5\}$$

There is always the necessity for the Acoustican to decide which formula is most appropriate to a given situation. Care must be taken when using any of these formulas for odd shaped rooms especially when there is large amounts of acoustic absorption (Gilbert 1988). Detailed calculations, using these various formulae, for Lecture Theatre (Room 412) at Curtin University, Building 201 are given in Appendix 1 Reverberation Calculations. The results are summarised in Table 2.1.

The space has a volume of 308m³ and only moderate amounts of acoustic absorption, predominantly at the rear.

Table 2.1 Summary of Reverberation Calculations

| Description | Frequency | | | | | |
|---|---|---|---|---|---|---|
| | 125 | 250 | 500 | 1 K | 2 K | 4 K |
| RT Sabine | 1.42 | 0.90 | 0.68 | 0.78 | 0.72 | 0.68 |
| RT Eyring | 1.34 | 0.82 | 0.60 | 0.71 | 0.64 | 0.60 |
| RT Arau-Puchades | 1.63 | 1.00 | 0.66 | 0.80 | 0.69 | 0.64 |
| RT Fitzroy - Sabine | 2.07 | 1.34 | 0.83 | 1.01 | 0.83 | 0.79 |
| RT Fitzroy - Eyring | 1.99 | 1.26 | 0.75 | 0.94 | 0.75 | 0.71 |

Table 2.2 below, gives a summary of physical reverberation time measurements in the space. It is quite apparent from the measurements, that the sound field is not homogenous at all frequencies. Position 1 is approximately center of row 4, while Position 2 is the first seat in the same row. (See also Chapter 4, Case Study 1)

Table 2.2 Summary of physical Reverberation Time Measurements

| | Frequency | | | | | |
|---|---|---|---|---|---|---|
| | 125 | 250 | 500 | 1 K | 2 K | 4 K |
| Position 1 | 1.77 | 1.54 | 1.52 | 1.62 | 1.67 | 1.70 |
| Position 2 | 2.04 | 1.54 | 1.53 | 1.62 | 1.67 | 1.70 |
| Average | 1.91 | 1.54 | 1.53 | 1.62 | 1.67 | 1.70 |

Mid frequency (1kHz) reverberation times range from 0.71 for the Eyring formula through to 1.01 seconds for the Fitzroy Sabine formula. As can be seen in Table 2.1 and Figure 2.2, there is significant variation in the calculated results, depending on the underlying basic assumptions. These calculated results show significant variations to the measured reverberation times shown in Table 2.2 and as the 'Averaged Measured' results in Figure 2.2.

Detailed examination of the spreadsheet presented in Appendix 1 Reverberation Calculations and the Case Study 1 details in **Appendix 7 Simulation Geometric Data** will show a number of simplifications in the spreadsheet model. For example there is no allowance for seating, the lectern or the Bio-Box. These simplifications will significantly affect the validity of the calculated results particularly in the higher frequencies. Whether the calculations could then 'track' the frequencies spectrum of the measured

reverberation times is then a function of the 'closeness' of calculation models to the physical room as measured.

Figure 2.2 Chart of Calculated Reverberation Times.

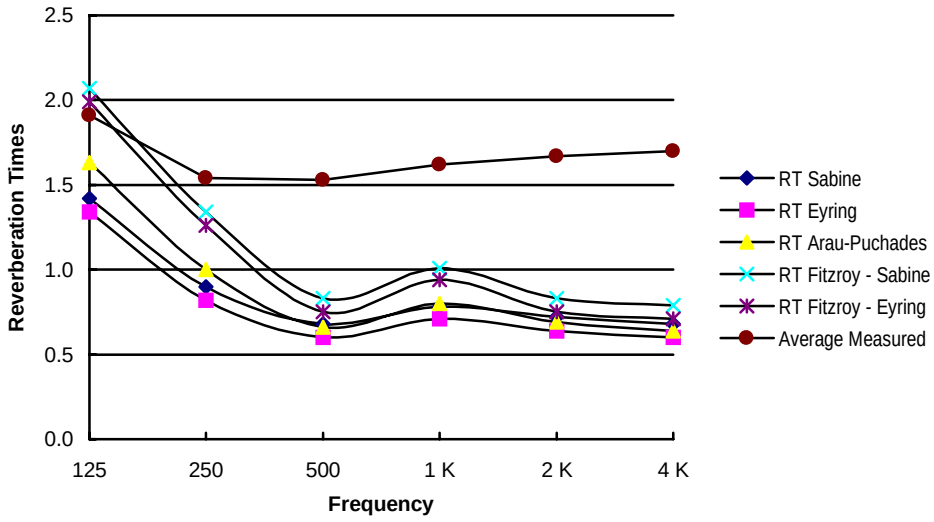


In these circumstances, it would be reasonable to use the Arau-Puchades formula as the basic assumptions are for non uniform distribution of the absorption or possibly the Fitzroy formulas depending on the interpretation of the degree or amount of reverberation in the sound field.

It is interesting that Beranek (1992) recommends the use of the Sabine formula for use in concert hall design where the largest portion of the absorption is the audience and the reverberation time is not less than 1.5 seconds. The condition of reverberation time greater than 1.5 seconds does not hold for speech auditoriums. (See Figure 2.1, page 14 for recommended reverberation times.)

### *2.2.1.2 Room Resonance*

In Table 2.2, above, the actual measurements for the two positions begin to show significant variation at 125 Hz. This is typical for spaces where the sound field is not homogenous. That is where the sound pressure level is not the same level at all points with in the space.

It is a demonstrable room characteristic that in a rectangular room the sound pressure level will vary from position to position, for the two conditions:

- when the source is stationary and the listener moves about the space; and
- when the listener is stationary and the source moves about the space.

These observable effects can be readily explained using wave acoustics. Wave acoustics is based on the motion of sound waves in a three dimensional enclosure (Ginn 1978).

Representation of the acoustic performance of spaces using 'wave acoustics' can be traced back to Rayleigh (Northwood 1977). In the 1945 book titled '*The Theory of Sound Vol II'* wave equations were published for the calculation of room modes (Rayleigh 1945). These equations aid in the detection and description of room resonances.

In essence, the three dimensional enclosure is mathematically described by defining the acoustical performance of boundary surfaces, eg. walls, floor, ceiling, etc. The application of wave acoustics is limited by the difficulty in defining the boundary conditions for irregular shapes.

> *"When employing wave theory, a room is considered as a complex resonator possessing many normal modes of vibration and each mode having a characteristic frequency of damped free vibration. These modes can be excited by introducing a sound source into the room. … The characteristic frequencies … depend principally on the room's size and shape whereas the damping of these waves depends on the boundary conditions."* (Ginn 1978, p40).

There are three types of normal modes which occur in rooms:

- Axial modes - where the waves move parallel to one axis. These waves are often characterised as flutter echoes.
- Tangential modes - where the waves are tangential to one pair of surfaces and reflected from the other surface pairs.
- Oblique modes - where the waves are at oblique angles and impact all surfaces.

As can be appreciated, with the axial, tangential and oblique modes, travelling within an enclosed space, there will be difficulty in consistently measuring the reverberation

time. Therefore to accurately measure the reverberation time, it is essential that multiple sound decays are averaged together. This is called ensemble averaging. See 2.5.1 Measurement of Reverberation Time on page 40 for further discussion.

### 2.2.2 Geometrical Acoustics

The term 'geometrical acoustics' relates to the application of the principles of optical geometrics to acoustical phenomena. Its main relevance is in the application of graphical ray tracing of a sound from the source through to the listener/receiver via reflections of the boundary surfaces of the space. (Northwood 1977)

There are obvious limitations in the use of the optical analogy, in that for specular reflections to occur from a surface, that surface must be large compared to the wavelength (frequency) of the sound wave. The surface also needs to be smooth compared to the sound wave wavelength.

The frequencies of speech are in the region of 100Hz to 2kHz, these wavelengths range from 3.4m (100Hz) to 172mm (2kHz). The limits of human hearing are approximately 20Hz to 20kHz which equate to wavelengths of 17.2m to 17mm. Small rough surfaces tend to scatter incident sound waves rather than reflect the sound as would be expected using the simple specular reflection laws.

Additionally, the problem of the straight ray path, as expected with the simple specular reflection laws, is complicated due to the size of the wavelengths of sounds we hear. As the wavelengths increase in size, the paths tend to refract around objects. This has been summarised by Frank, Bergmann and Yaspan (n.d., p34) as follows:

> *"the wavelengths of most audible sounds are not small compared to the obstacles in the path of the sound. Consequently, sounds audible to the ear do not travel straight-line or nearly straight-line paths; they bend around corners and fill almost all of any space into which they are directed."*

### 2.2.2.1 2D Ray Tracing

One of the simplest forms of determining the ray path, path length and direction of a reflection is by tracing the ray from the source via each reflecting boundary to the receiver location. Figure 2.3 illustrates a typical two dimensional ray trace. Sound rays are sprayed from the source, with each ray being traced through a number of reflections. It can be seen that some surfaces, for instance the wall behind the source, have been considered as non reflective.

> *"Sound reflections in a room naturally play a very important role in the subjective evaluation of acoustic performance of the room and favourable reflections should be provided by the walls and ceilings."* (Maekawa 1975, p181)

Figure 2.3 Typical two dimension ray trace illustrating the reflected ray paths from the source via the boundary ceiling surfaces.

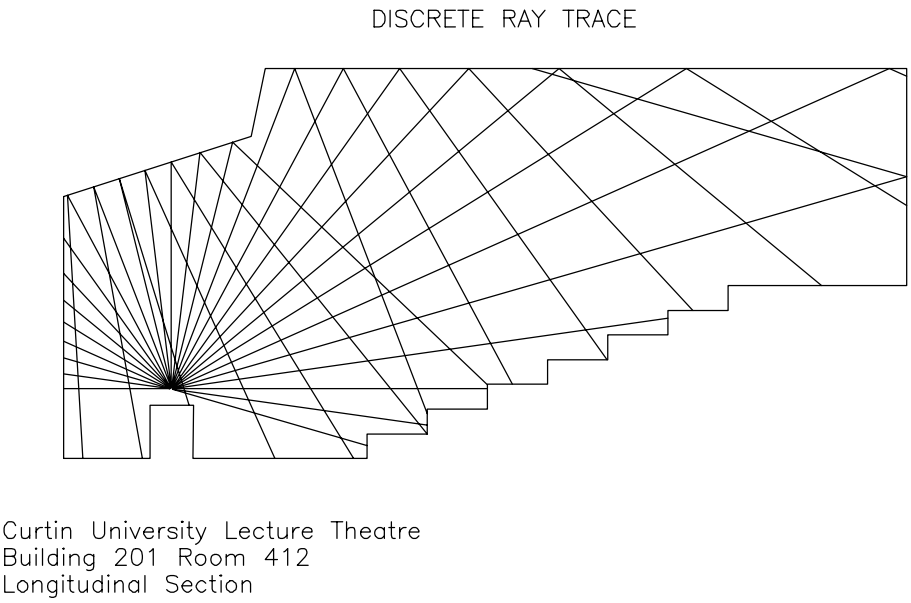


Various information can be derived from these simplified tracings such as the time delays for the reflected ray compared to the direct ray; ray angles, intersection coordinates, path lengths, path length differences and boundary surface hit. In Appendix 2 Two Dimensional Ray Trace, the Curtin University Lecture Theatre, used in the Reverberation calculations has been analysed.

The simulation summary indicates potential echo problems when considering the full 360º radiation of sound from the source. (Echoes are defined for this purpose as having time delays greater than 30ms.) The summary also shows the relative density of rays terminating at the rear of the theatre eg. 34 rays for row 8 compared to 15 for row 5. Ray path geometry along with various measures such as the difference in path lengths between the direct and reflected rays and that same difference in milliseconds are also detailed.

This form of ray tracing tends to be a gross simplification. There is no recognition of the true acoustic absorption of the various boundary surfaces, nor any accounting for the air absorption. Typically, a boundary surface is simply constrained to *n* number of reflections of the same ray. Other restrictions of this form of analysis is that the method is two dimensional only. Eg. a singular plane or cut through the model, thus eliminating analysis of the oblique modes (See section Room Resonance on page 20 for a description of oblique modes.)

Two dimension ray tracing is very effective in analysing wall, panel placement, as calculation times are almost instantaneous, as long as the problem can be defined in the two dimensions. There are very few indices that can be calculated from the geometric data available from these programs.

#### *2.2.2.2 Sight Line Analysis*

The importance of an unobstructed path between the source and the listener is illustrated by Parkin and Humphreys (1958, pp67-68):

> *"It is important that the direct sound, i.e. sound proceeding directly from the source to the listener without having been reflected from any room surface, shall be as strong as possible. … the average distance between the source and the listener should be kept as small as possible. It is also important that this direct sound path shall not be obstructed."*

The sight analysis is based on the generalisation that if the audience has a direct and unobstructed view, then they will also have an unobstructed direct sound path. Parkin

and Humphreys (1958) indicate that a minimum of 75mm and preferably 100mm clearance is required in the sightline from one row to the row below. In plan view, the directionality of speech is such that all seating should be within an angle of approximately 140º.

Figure 2.4 Typical sightline analysis

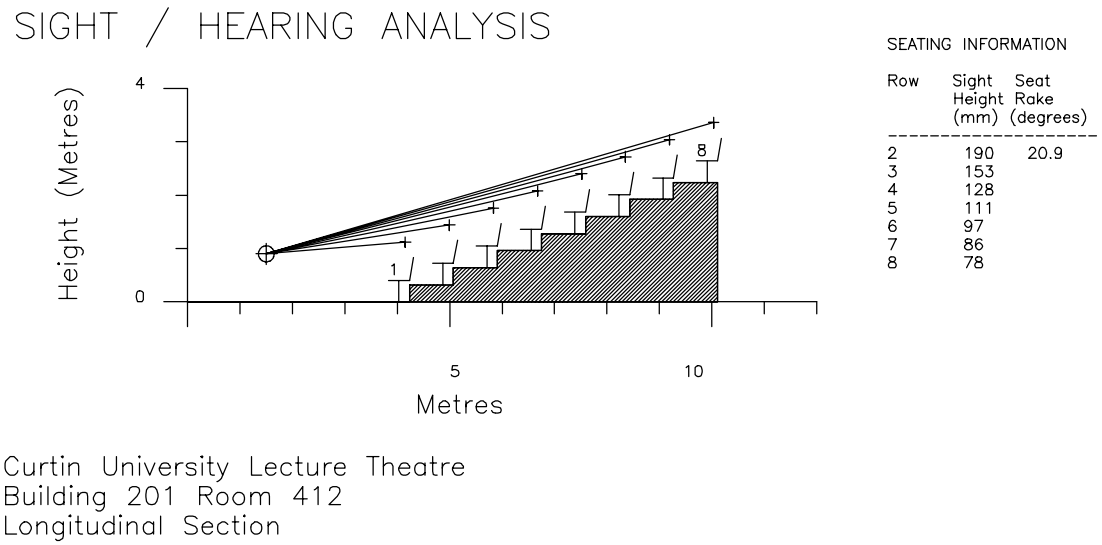


This form of analysis readily shows how for a given seating rake angle, in this case 20.9º, the sight height rapidly reduces as the audience head height increase above the sound source.

### *2.2.2.3 3D Simulations*

The history of ray tracing to determine the acoustical performance of enclosed spaces can be traced back to 1958 (Lehnert 1993). Lehnert's paper outlines some of the difficulties in using the various reverberation formulas, with their inherent assumption of a steady state nature of the sound signal and the non diffuse distribution across the audience, for prediction of the sound pressure levels within an enclosure.

The nature of ray tracing was advanced from the two dimensional form to three dimensions by Gibbs and Jones (1972). Their simulation of contrived geometry correlated better with the observed results than did the classical prediction methods.

Figure 2.5 Typical 3d simulation

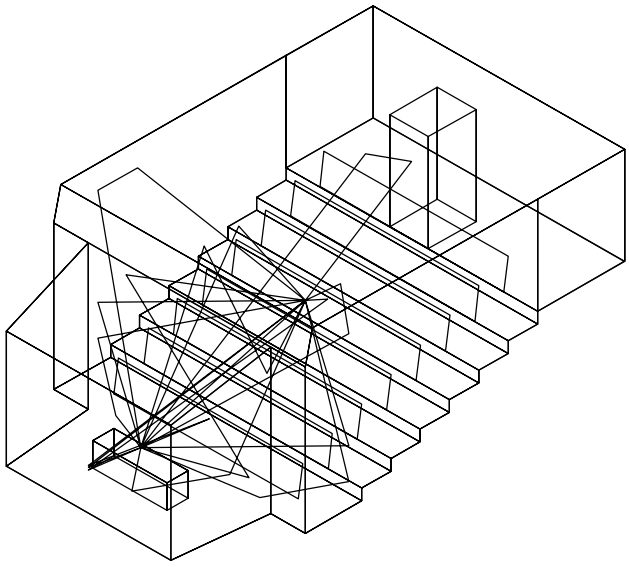


As can be seen in Figure 2.5, when the complete three dimensional geometry is available, ray paths can be computed from a source to any given receiver location.

The advantages of computer simulations can be summarised as follows:

i) There are no materials to source for the matching acoustic performance,

ii) There is no physical space or construction requirements compared to the physical modelling approach.

iii) Computer models can readily be modified and simulated without loss of the original investment in time and resources necessary to build the original model.

iv) Construction materials can be altered by the designer with possible immediate feedback of results. (This is highly dependent on the modelling implementation.)

v) Generation of unlimited orthographic views and perspective views are available through CAD programmes. With conversion of existing data files, photo-realistic images from rendering packages such as Radiance (Ward 1995) are possible. The Radiance rendering package is able to accurately and realistically render the lighting of the space. This is a potential that physical models lack.

vi) It may be possible to utilise existing computer data (CAD models) in the basic modelling.

Disadvantages of computer simulations can be summarised as follows:

i) Due to the need for huge numbers of calculations, fast computer equipment is preferred. The speed of the computer system is directly related to the simulation times.

ii) The structural and spatial aspects of the design are not as apparent as in a physical model.

iii) Difficult to simulate natural phenomena such as diffraction and scattering.

iv) The accuracy of the prediction is highly dependent on the extent of the simulations.

### 2.2.3 Model Testing

Physical models are used for a variety of reasons. Architects use models to aid visualisation (Marshall 1990). Acousticians use models to aid in the acoustic design eg. detecting reflections and echoes, articulation, reverberation, auralisation, reproduction of natural phenomena such as diffraction and scattering (Beranek 1994).

The testing of acoustic models has a history dating back at least to Sabine's use of the Toeppler-Boys-Foley method of photography of air disturbances in a model of the New Theatre (New York) (Sabine 1913). The Toeppler-Boys-Foley method utilised a

three dimensional slice of the model. Photographs were taken as the sound passed through the model. A strobe light was used to aid time series photographs.

The basic principle used in scale model testing, is frequency transformation. By this it is meant, as the scale of the model decreases, the frequency to be tested increases. Eg. 1000Hz in the full scale model equates to 10,000Hz in a 1:10 scale model. The performance range of materials, sound source and microphones in the 1:10 scale model need to cover the frequency range of 500 to 200kHz to equate to the normal hearing range of approximately 50 to 20kHz.

There are a number of fundamental difficulties involved in model testing:

i) Selection of materials having similar acoustic properties at the scaled frequencies as the full-scale materials at normal frequencies. This is discussed by Day (1975). He also outlines some the design implications of model scaled porous absorbers and Helmholtz resonators.

> *"Ideally the model boundary surface should represent at scale frequency the impedance and the variation of impedance with angle of incidence of its prototype at normal frequency."* (Day 1975, p88)

Normally the effect of incorrect impedances, as long as the overall absorption coefficient is correct, is a slight shift in the position of the boundary. The worst case would be a half wavelength shift either in or out. This can become problematic when the sound waves are in close proximity to a surface. Interference occurs when the total phase shift increases. This is the Bekesy effect - the indoor equivalent of the ground effect in external noise propagation. This is one explanation for the high attenuation rates over audiences (Day 1975).

ii) Adequate compensation of the effects of air absorption at high frequencies compared to those at normal frequencies. Day (1975) outlines how humidity, temperature and oxygen content alters the molecular absorption of air.

There are three methods of compensation used today: air dryers; air replacement (nitrogen); and numerical compensation as used by the MIDAS system (Dodd et al. 1992) and in scale modelling of the New Music Centre in Eindhoven (Boone and Braat-Eggen 1994).

iii) Selection of acceptable sensitivity and frequency response sound sources and microphones (Boone and Braat-Eggen 1994). Often due to the high frequencies used, broad band sources are not available, therefore, speech and music cannot be used. In these cases either a spark generator is used to generate an impulse (Dodd et al. 1992), or a swept sine wave can be used (Boone and Braat-Eggen 1994).

iii) Size of the microphones and sound sources must be accounted in the design so as not to introduce unintentional effects in the sound field.

iii) Time to construct the model plus any modifications.

Significant time is required to design, source suitable materials and construct these models, particularly when the acoustic properties of materials need to be identified. Burd (1975) suggest 12 to 24 weeks for a limited model dependent on available materials. For large scale models with detailed absorption, he suggests 6 months is not unreasonable.

vi) Construction skills in model making.

Some aspects of the design are practically impossible to model, particularly for concert halls, such as orchestras and the correct blend of instruments on the stage. Some measurements such as the degree that the mu-

sicians maybe able to hear one another are equally difficult to achieve (Beranek 1994).

vi) Space to store and test the model.

Many models are so large that space becomes a governing criteria in the choice of scales. For example the 1:10 model of the Sydney Opera house was so large it could only be accommodated on its side (Jordan 1980).

vi) Cost.

The models have significant costs attached to them. Burd (1975) suggest costing of £UK 1-5,000 for a small scale model and a minimum of £UK 25,000 for a large scale model. Dodd et al. (1992) estimates for a 1:50 model of the Municipal Theatre in Le Manns cost $NZ 4,000. This theatre contained 1009 seats, ground floor plus two levels of balconies. The model for the Orange County project took 4 months to build, with plant costing $US 10,000 (Marshall 1990).

ix) The accuracy of the prediction is highly dependent on the accuracy and the quality of the model.

The constructional quality, methods of fixing materials, adhesives used, the accuracy of the impedance matching and overall acoustic absorption all effect the potential accuracy of the model. Other factors discussed above, such as the air absorption compensation techniques and the quality of the sound source and microphones have a direct impact on the measurement accuracy. Finally the issue of the analysis equipment and data acquisition units, which is not discussed in this thesis, will significantly effect the overall accuracy, measurement types and applicability of the scale model.

There are many potential areas of difficulty in model testing, which require significant effort to allow quality predictions on the acoustic performance of spaces. As Hodgson (1990, p877) concludes on the applicability of scale models:

> *"Given the other limitations of small scale modelling techniques, scale models appear to constitute an inaccurate prediction method"*

The over-riding criteria regarding the applicability of scale model testing, is to what degree and accuracy is necessary for the design decision to be made. Should the model measurements attempt to duplicate in total, the response of the finished building? Or can the model allow sufficiently accurate evaluation of the performance to aid design decisions? This can only be answered on a case by case study. For some projects, simplified predictions are adequate, while on other projects a high correlation with the final building is essential.

## 2.3 Indices

With the introduction of reverberation time predictions and the subsequent recognition that there were other parameters involved in defining acoustical performance, various indices were proposed. Those related to speech performance evaluation included Early Decay Time, Deutlichkeit, Reverberant to Early Sound Ratio, Clarity, Centre Time, Initial Time Gap, Hallabstand and Room Response.

### 2.3.1 Early Decay Time

The Early Decay Time (EDT) is the reverberation time based on the first 10dB of the decay curve and extrapolated to 60dB (Beranek 1992). Its importance can be seen in the words of Kuttruff (1994, p38):

> *"The full decay process in a room is audible only after an abrupt and complete stop of sound excitation, but not during running speech or music signals. Nevertheless, reverberation affects the temporal and also the spectral structure of any sound by smoothing it and by mixing its constituents - otherwise there would be no reason to give so much weight to it. However it is rather the initial part of a decay curve which determines to which extent the signal is smoothed or blurred, or generally: how we hear the signal."*

Beranek (1994, p20) also confirms that it is the first 10 decibels of the decay curve that is the most important for understanding:

> *"In continuous music, approximately 10 decibels of the sound decay can be heard after each note. If the early decay time is short, the sound is clear; if long, but not too long, the music is said to take on the desirable attribute of fullness or singing tone. A very long reverberation time will muddle all but liturgical music."*

Jordan (1980, p52) also outlines a criteria by which deficiencies in the acoustical performance of an enclosure maybe detected:

> *"Values of EDT which are considerably lower than values of RT are regarded, generally, as signifying acoustical deficiencies."*

Early Decay Time as a measurement is an important index in the design of speech performance enclosures.

### 2.3.2 Deutlichkeit

Deutlichkeit (D) (Meyer and Thiele 1956), also known as Definition, was proposed by Thiele as a measure of clarity. Deutlichkeit is defined as the:

> *"ratio of the early sound energy in the first 50ms after the arrival of the direct sound to the total sound energy"* Bradley (1983, p2051)

$$D = \frac{\int_0^{0.05} p^2(t)dt}{\int_0^{\infty} p^2(t)dt} \qquad \{\text{Eq } 2.6\}$$

The lower limit of time $t_0$ is the arrival of the direct sound (Kuttruff 1991). This index is based on a impulse or short duration pulse sound source (Jordan 1980).

Research by Boré, has shown that there is a good correlation between Deutlichkeit and speech intelligibility (Kuttruff 1991).

### 2.3.3 Reverberant to Early Sound Ratio

Proposed by Schultz, the Reverberant to Early Sound Ratio (R) is a measure of the balance between definition and blend. It is the ratio of late arriving sound energy, between 50ms and 500ms, and the early sound energy up to 50ms. (Bradley 1983, p2051)

$$R = 10\log\left(\frac{\int_{0.05}^{0.5} p^2(t)dt}{\int_{0}^{0.05} p^2(t)dt}\right) \qquad \{\text{Eq } 2.7\}$$

This formula is essentially the same as the Hallmass formula (Jordan 1980, p158):

$$Hallmass = 10\log\left(\frac{\int_{0.05}^{\infty} p^2(t)dt}{\int_{0}^{0.05} p^2(t)dt}\right) \qquad \{\text{Eq } 2.8\}$$

The difference being the upper limit of *t* in the numerator. Reverberant to Early Sound Ratio is based on the assumption that the sound arriving after the first half second does not add much energy.

### 2.3.4 Clarity

Clarity Index ($C_{80}$), Klarheitsmass (Bradley 1986), was proposed by Reichardt as a measure suitable to music with an 80ms limit. The 80ms limit allows for reflections which are less noticeable within this time limit in music than the 50ms for speech (Kuttruff 1991). This index is not intended to indicate speech intelligibility but to rate the ease of distinguishing successive notes in rapid music passages.

$$C_{80} = 10\log\left(\frac{\int_{0}^{0.08} p^2(t)dt}{\int_{0.08}^{\infty} p^2(t)dt}\right) \qquad \{\text{Eq } 2.9\}$$

The Clarity Index includes the direct sound (Beranek 1994, p22). The lower limit of time $t_0$ is the arrival of the direct sound (Barron and Lee 1988). From Reichardt's re-

search a value of $C_{80}$ = 0dB is indicative of sufficient clarity for fast musical passages; a value of $C_{80}$ = -3dB is still acceptable (Kuttruff 1991).

### 2.3.5 Centre Time

Centre Time (seconds), also known as Centre of Gravity Time, Point of Gravity and Schwerpunktzeit (Bradley 1986), is a:

> *"measure of the balance between clarity and reverberance that was proposed to avoid the abrupt division between early and late arriving reflections"*. (Bradley and Halliwell 1989, p17)

$$TS = \frac{\int_0^\infty tp^2(t)dt}{\int_{0.}^\infty p^2(t)dt} \qquad \{\text{Eq 2.10}\}$$

The Centre Time index is very similar to the *echo criterion* proposed by Dietsch and Kraak (Kuttruff 1994, p38):

$$TS = \frac{\int_0^\tau t|p(t)|^n dt}{\int_{0.}^\tau |p(t)|^n dt} \qquad \{\text{Eq 2.11}\}$$

where $n$ = 1 for music and $n$ = 2/3 for speech. When $n$ = 2 and $\tau = \infty$ this equation agrees with the equation {Eq 2.10}.

Both Deutlichkeit and Center Time are closely related to speech intelligibility. The smaller the value of the Center Time (or higher the Deutlichkeit value) the higher is the expected speech intelligibility at the receiver position (Kuttruff 1994).

### 2.3.6 Initial Time Gap

The Initial Time Gap has been defined by Beranek (1994) as the difference in the arrival times of the first reflection and the direct sound.

$$t_1 = t_{R1} - t_D \qquad \{\text{Eq 2.12}\}$$

where $t_{R1}$ is the arrival time of the first reflection

$t_D$ is the arrival time of the direct sound.

Beranek (1994) suggests that most successful concert halls have an Initial Time Gap of 20ms, while the poorest halls the gap exceeds 70ms. The Initial Time Gap is measured at the middle of the main floor.

### 2.3.7 Hallabstand

Hallabstand has been proposed by Reichardt (Jordan 1980, p158) as a ratio of the very early sound energy (first 5ms) to the rest of the sound energy.

$$Hallabstand = 10\log\left(\frac{\int_0^{0.005} p^2(t)dt}{\int_{0.005}^{\infty} p^2(t)dt}\right) \quad \{Eq\ 2.13\}$$

### 2.3.8 Room Response

The Room Response index has been proposed by Jordan (1980, p161) as an index which is highly correlated with the subjective evaluation of the spatial effect.

$$RR = 10\log\left(\frac{\int_{0.025}^{0.08} lateral + \int_{0.08}^{0.16} total}{\int_0^{0.08} total}\right) \quad \{Eq\ 2.14\}$$

## *2.4 Simulation Methods*

Of the simulation programs reported in the literature (Hodgson 1990; Santon 1976; Stephenson 1990) the three major techniques in use are:

- Ray Method;
- Image Method; and
- Sound Particle Method

Note: Scale models, which could be thought as simulation techniques, are discussed in section 2.2.3 Model Testing, page 27.

### 2.4.1 Ray Method

In the ray method, sound particles are 'sprayed' from a single source point along sound rays (Rindel 1995). The sound particles are traced as they bounce around the enclosing space. At each reflection the particles lose energy according to the absorption coefficient of the material.

Each ray is traced to determine the first surfaces it strikes. The stream of particles are reflected, according to Snell's law, and the trace continues until the desired number of reflections have been reached. The major difficulty with this approach, is determining an adequate number and pattern of rays which will effectively strike all relevant surfaces in the simulation.

Rietschote, Houtgast and Steeneken (1981, p246) have developed a method to distribute the rays so that the *"every solid angle around the source contains approximately the same number of rays."* This methodology allows simple simulation of directivity, by altering the relative strength of each ray.

A difficulty in using the ray method is actually hitting the receiver point. The smaller the receiver, the more rays which are need to be cast (Santon 1976). A method of relaxing the exact intersection of a ray with the receiver, is to make the receiver a sphere. Rietschote, Houtgast and Steeneken (1981) suggest a radius of 1 to 1.5 metres. This 'large' sphere receiver would then be struck by many rays.

An alternative to the spherical receivers, are flat plane receptors (Ondet and Barby 1989; Santon 1976). Both receptor forms, allow the calculation of the energy impinging on the receptor as being the intersection of a cone and the receptor.

Rindel (1995) estimates for any surface of area $A$ there is a reasonably high possibility that the surface will be hit during a travel time $T$. The minimum number of rays need is given in {Eq 2.15}:

$$N \geq \frac{8\pi c^2}{A} t^2 \qquad \{Eq\ 2.15\}$$

where $c$ is the speed of sound in air (m/s)

$A$ is the surface area ($m^2$)

$t$ is the travel time (s)

### 2.4.2 Image Method

The image method uses a mathematical construct of defining 'mirror images' of the source, where the source is mirrored about the plane under consideration (see Figure 2.6). As the number of reflections increase, so does the number of mirror sources (Kristiansen, Krokstad and Follestad 1993). This method is capable of resolving ray paths and reflected ray paths through each defined surface plane.

Figure 2.6 Example of mirror source

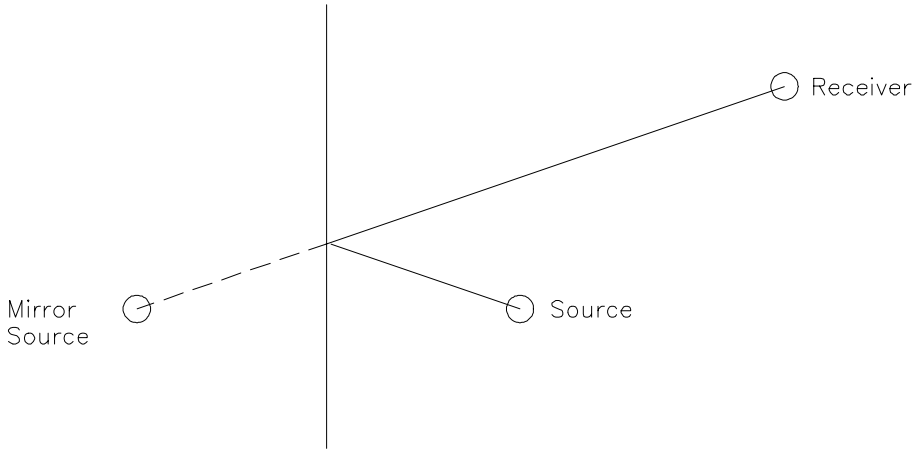


Rindel (1995) estimates the number of reflections that will arrive in time $T$ to be {Eq 2.16}. He notes that that in typical auditoriums, there is often a higher number of early reflection and a lower number of late reflections.

$$N = \frac{8\pi c^3}{3V} t^3 \qquad \{Eq\ 2.16\}$$

where $c$ is the speed of sound in air (m/s)

$V$ is the volume ($m^3$)

$t$ is the travel time (s)

The major difficulty in using this algorithm, is in detecting which rays are valid. Lee and Lee (1988) gives statistics for a small auditorium of 17 surfaces. These are summarised in Table 2.3

Table 2.3 Number of Ray Paths for a single source and receiver location.
Abstracted from (Lee and Lee 1988, table 3 p110)

| Number of Reflections | Number of valid ray paths | Number of all possible ray paths |
|---|---|---|
| Direct | 1 | 1 |
| 1 | 7 | 17 |
| 2 | 20 | 272 |
| 3 | 37 | 4,352 |
| 4 | 56 | 69,632 |
| 5 | 73 | 1,114,112 |
| 6 | 95 | 17,825,792 |
| 7 | 130 | 285,212,672 |
| Total | 419 | 304,226,850 |

Unlike the ray method, the image method does not require large receptor surfaces to 'catch' the passing rays. The image method uses a single receiver point. It would be computationally difficult and expensive to implement a large receiver receptor surface using the image method.

### 2.4.3 Sound Particle Method

This form of simulation is similar to that of the ray and image methods, in that sound particles replace rays (Kuttruff 1994). In the ray and image methods, the sound rays are reflected specularly, with the signal strength reduced by (1-α). The term α is used

to denote the acoustic absorption of a plane. With the sound particle method the signal is reflected either specularly or non-specularly, i.e. diffusely, reflected (see Figure 2.7). Kuttruff (1991, p282) describes the diffuse reflection's method of determining the direction and strength as:

> *"the computer generates two random numbers from which the azimuth angle $\varphi$ and the polar angle $\vartheta$ of the new direction".*

Figure 2.7 Principle of Sound Particle Propagation

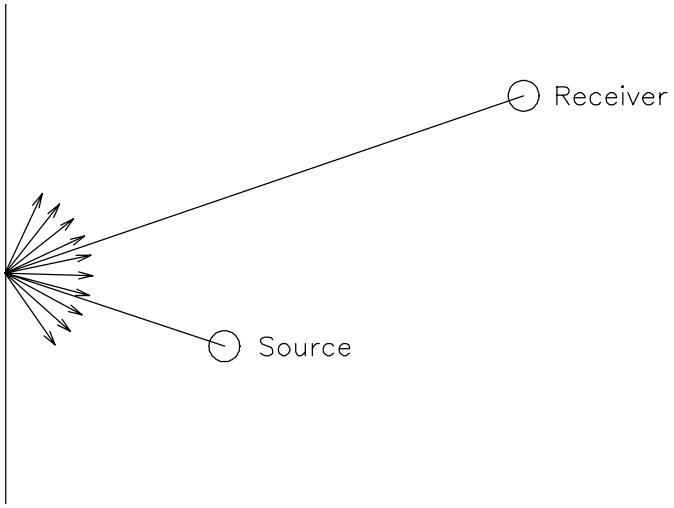


After reflection the particle is then traced to the next plane, as in the ray and image methods. As with the ray method, pre-defined counters or receptors are required to 'catch' the particles. To incorporate diffusion effects, the number of particles which replace the original sound impulse must be large. Kuttruff (1991) suggests that the number of counters required for 'sufficiently precise' calculation is in the order of $10^4$ - $10^5$ particles for a 1 metre counter.

A comparison of the image and sound particle methods has been published by Stephenson (see Table 2.4) in which he estimates the degree of difficulty in simulating various effects by the two methods.

Table 2.4 Comparison of Simulation Methods for Integration of Effects (Stephenson 1990, p70)

| Effect | Mirror Image Source Method | Sound Particle Simulation Method |
|---|---|---|
| Curved Walls | Does not work | Works with simple geometry |
| Diffuse reflections | Does not work | Works |
| Scattering | With modified propagation law | Works |
| Screening | Only low order reflection practical | Does not work |
| Diffraction in general | Does not work | Difficult approach |
| Refraction | Does not work | Works |

There have been improvements made by various researchers into the overall performance of the particle method. Vian and Van Maercke (1985) have integrated the ray tracing (cone) methods, while Vorländer (1989) uses a combined ray-tracing/image-source algorithm to define the position of the images sources. Hybrid approaches, such as these promise faster simulation timings without some of the inherent problems predicted by Stephenson in Table 2.4.

## *2.5 Physical Measurement*

### 2.5.1 Measurement of Reverberation Time

The origins of the physical measurement of reverberation can be laid at the feet of Sabine, as it was he who coined the phrase 'Reverberation' (Sabine 1900) in his article of the same name, in the American Architect and the Engineering Record of 1900. The equipment of the time, used by Sabine in his historic investigations to measure the rate of decay of the sound, or more precisely the *'duration of audibility'* consisted of an organ pipe, for a constant sound source and a chronograph to record the duration of audibility after the sound had ceased.

It is of interest to note that various approaches to determine the rate of decay were tested by Sabine. Methods included using a sensitive manometric gas flame and meas-

ured used a micrometer telescope. Photography of the flame was trialed. Both methods were abandoned due to the fluctuating decay rate. Figure 2.8 illustrates a trace of a fluctuating decay. Ultimately, Sabine returned to using the ear aided with the chronograph to record the duration of the audible sound.

Figure 2.8 Typical reverberation decay trace.

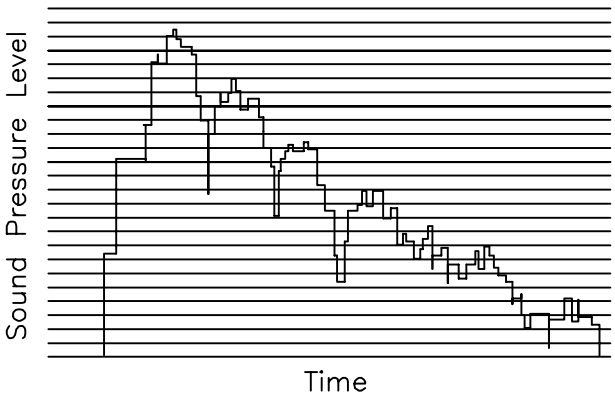


At the present time there are various methods used to determine enclosure decay rates. The traditional methods use a sound source to produce a steady state signal or an impulse source such as a pistol or gun shot. The decay is measured with a sensitive microphone and recorded via a level recorder (paper trace) or digitally using a computer. Normally the dynamic response of the sound signal above the background noise necessary to measure a 60 dB decay is rarely achieved. Therefore the reverberation time is measured in the -5 to -35 dB region of the decay (AS 1045-1988) and interpolated out to the 60 dB limit. Typically, many decays are averaged together. An explanation of the rationale behind the need to average many decays is given by Schroeder (1965, p409):

> *"The accuracy with which reverberation time can be determined from decay curves is limited by random fluctuations in the decay curves. These random fluctuations result from the mutual beating of normal modes of different natural frequencies. The exact form of the random fluctuations depends on, among other factors, the initial amplitudes and phase angles of the normal modes at the moment that the excitation signal is turned off. If the excitation signal is a bandpass-filtered noise, the initial amplitudes and phase angles are different from trial*

> *to trial. Thus, for the same enclosure, and identical transmitting and receiving positions within the enclosure, different decay curves are obtained - the differences being a result of the randomness of the* ***excitation signal****, not of any changes in the characteristics of the enclosure."*

A new technique, the *Integrating Impulse Method* developed by Schroeder (1965) is currently being incorporated into many new devices. This technique is said to equal, in one single impulse measurement, the *ensemble average* of indefinitely many decays curves.

For this measurement procedure, a tone burst or filtered pistol shot is used. The decay is measured, squared and integrated producing a smooth curve. Figure 2.9 illustrates the comparison of the two decay curves. The second curve gives a far more accurate interpolation equation for the determination of the reverberation time over 60 dB. (See Appendix 4 Calculation of the Integrating Impulse Response Method for explanation of the procedure.)

Figure 2.9 Tone Burst decay and Integrating Impulse Decay curve

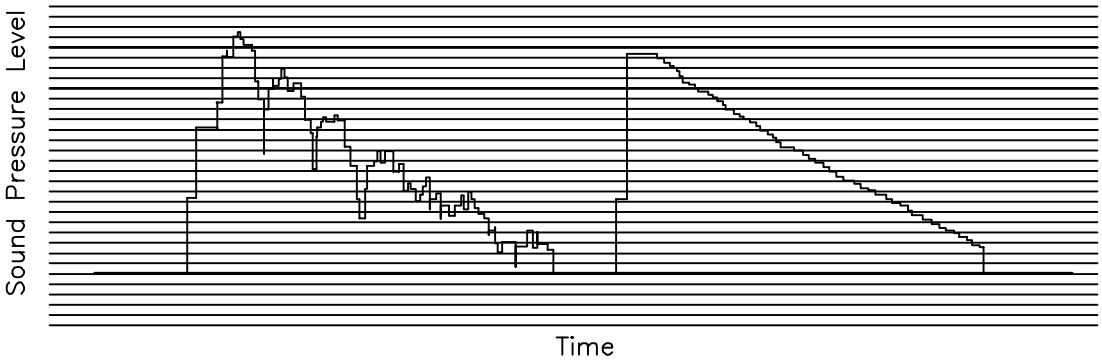


A major problem in the measurement of reverberation times is having a sufficiently powerful sound source with a flat spectrum. This is particularly problematic in conjunction with the impulse measurement procedures. Common impulse sources such as electrical sparks, popping balloons, pistols, rifles and cannon shots do not always have a flat spectrum, while loud speakers often have insufficient power to achieve an ade-

quate signal to noise ratio for the 20 or even 30dB decays, above the ambient noise levels.

There has been published an experimental procedure using a low power pseudorandom noise which is reported to be successful in noisy environments, such as during a lecture (Schroeder, 1979). There is one instrument (MELISA) on the market based on this procedure.

### 2.5.2 Articulation Index

French and Steinberg (1947, p100) characterise speech:

> *"A distinguishing characteristic of speech is movement. Conversation at the rate of 200 words per minute, corresponding to about four syllables and ten speech sounds per second, is not unusual. … The various sounds differ from each other in their build-up and decay characteristics, in length, in total intensity, and in the distribution of the intensity with frequency."*

To measure the ability to distinguish speech sounds clearly, methods have been devised where the percentage of syllables heard correctly are determined by using a team of 'speakers' and 'talkers'. These tests involve the reading of a list of syllables commonly used in conversation. The lists are known as phonetically balance (PB) word lists (Kryter, 1962a) with each list containing 50 words representing by proportion the same speech sounds as in normal conversational speech.

A major problem with these types of test is that they are dependent on the experience and skill of the 'speaker' and 'listener' team (French and Steinberg 1947). The difficulties can be partially overcome by using 'calibrated crews' and applying appropriate corrections. The syllable tests do not provide a means of assessing the contributions of the speech sounds to the overall intelligibility.

The Articulation Index is derived from these 'articulation tests'. The relationship between Articulation Index and syllables, words and sentences understood, is illustrated in Figure 2.10. French and Steinberg (1947, p101) describes Articulation Index as:

> *"The Articulation Index is based on the concept that any narrow band of speech frequencies of a given intensity carries a contribution to the total index which is independent of other bands with which it is associated and that the total contribution of all bands is the sum of the contributions of the separate bands."*

Figure 2.10 Relationship between Articulation Index and syllables, words and sentences understood.

(Cavanaugh, Farrell, Hirtle and Watters 1962, Fig 6. p480)

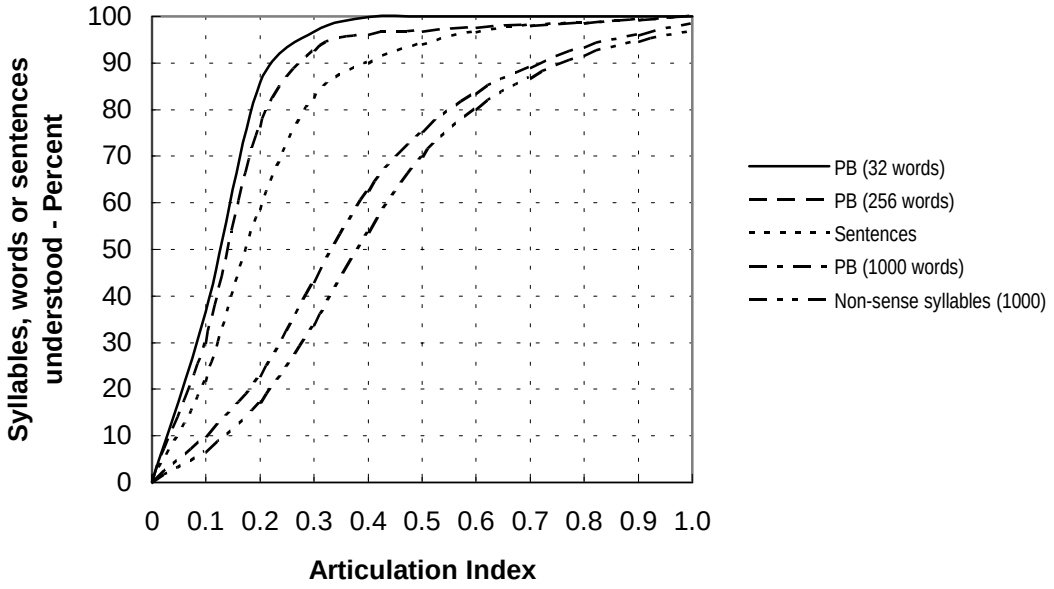


By having an index which is based on the contributions of speech sounds in various frequencies the Articulation Index provides a means of measuring the effects of reverberation and masking noise on the overall speech intelligibility.

The basic methodology developed by French and Steinberg has been expanded by Beranek, Kryter and others. The Articulation Index procedure *"is believed to be a fairly accurate way of predicting from purely physical measures of a communications system what the intelligibility of speech will be when transmitted over that system."* (Kryter 1962b, p1698)

Cavanaugh, Farrell, Hirtle and Watters (1962, p481) outline the basic aspects of this procedure:

1. *The intelligible part of speech energy lies roughly between 200 and 6000 cps.*

2. *Most of the energy of speech is in the frequency range below 800 cps; most of the contribution to intelligibility above 800 cps.*

3. *In each frequency band, speech has a dynamic range of about 30dB; the peak values lie about 12dB above the long-time rms levels.*

4. *Any frequency band in the range 200 to 6000 cps may be considered to make a contribution to intelligibility that is proportional (a) to the fraction of its 30dB dynamic range which is greater than the masking noise (or threshold of hearing), (b) to the bandwidth, and (c) to the "importance function" for that band. The importance function is a maximum at about 2000 cps.*

The Articulation Index procedure has been validated with speech intelligibility test involving male talkers (ANSI S3.5-1969). In situations involving female and children as talkers, there may be some need for correction of the importance function to take into account the different speech spectrums of those groups.

### 2.5.3 Speech Transmission Index

The Speech Transmission Index is an extension of the Articulation Index procedure. Its purpose is to be a measure of the effective signal to noise ratio in a number of octave bands (Schmidt-Nielsen 1987).

Speech Transmission Index is quantified by utilising a Modulation Transfer Function. The rationale in using the Modulation Transfer Function was described in a series of five articles on the theory and application of the Modulation Transfer Function by Houtgast, Steeneken, Plomp, Wattel and Rietschote in the period 1980 - 1983.

Houtgast and Steeneken (1985a, pg1069) summarise the need to define a methodology:

> *"Ongoing speech may be regarded as a flow of sound with a specific distribution pattern of sound intensity over frequency and time. When after transmission in an enclosure, the resulting distribution pattern is compared to that of the original speech, it will reveal a certain degree of smearing: the finer details of the temporal intensity distribution will be blurred by the combined effect of the many individual sound-paths with various time delays."*

### 2.5.4 Rapid Speech Transmission Index

The Rapid Speech Transmission Index (RASTI) is a reduced Speech Transmission Index. It was developed as a fast field implementation of the Speech Transmission Index measurement system. It uses a reduced number of frequencies and modulations. In all other particulars, RASTI and STI are the same.

> *"For the great majority of actual situations in auditoria, this set [STI] of 98 data points constitutes an unnecessarily detailed grid of analysis. Therefore, for a fast evaluation of auditorium conditions a more rapid measuring procedure was developed, based on a subset of the original 98 data points."* Steeneken and Houtgast (1985, pg 15)

### 2.5.5 Modulation Transfer Function

The application Modulation Transfer Function from the field of optics, was not an entirely new measure *"Essentially, it is the Fourier transformation of the squared pulse responses … which in turn, reflects the derivation of the reverberation curve"* Houtgast, Steeneken and Plomp (1980, pg62). The underlying principles have been described in a number of papers. Essentially:

> *"The MTF quantifies to what extent the modulations in the original signal are reduced, as a function of the modulation frequency. The modulations are defined by the* ***intensity envelope*** *of the signal: it is only in the intensity domain, that the interfering noise or reverberation will affect only the degree of modulation of a sine-wave shaped modulation* ***without*** *affecting the sine-wave shape."* (Houtgast and Steeneken 1985b, pg4)

Houtgast, Steeneken and Plomp (1980) show that for a system with a varying intensity, the input signal is:

$$\bar{I}_i\left[1+\cos\{2\pi F(t)\}\right] \qquad \{\text{Eq 2.17}\}$$

where F is the modulation frequency

and the output is equal to:

$$\bar{I}_o\left[1+m\cos\{2\pi F(t-\theta)\}\right] \qquad \{\text{Eq 2.18}\}$$

As can be seen by comparing {Eq 2.17} and {Eq 2.18}, the effects of noise and reverberation on the output signal, can be described by the *m* (modulation index) and $\theta$ (time lag). The operation of these variables can be seen in Figure 2.11. The term *m* affects the height of the output signal sine-wave (Dotted curve) while the term $\theta$ affects the offset of the output signal sine-wave (Dotted curve).

Figure 2.11 Effects of noise and reverberation on the Modulation Transfer Function

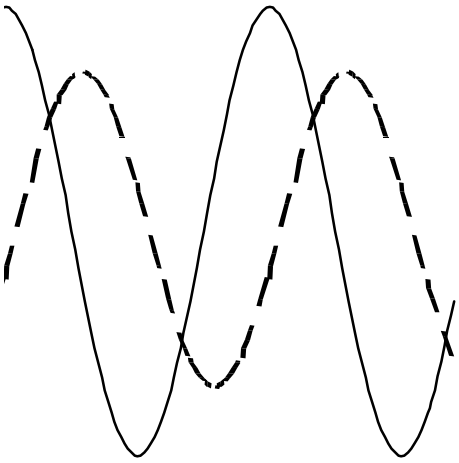

The Modulation Transfer Function is defined as

$$MTF = m(F) \qquad \{\text{Eq 2.19}\}$$

The relevant modulation frequencies *(F)* for speech are given in Table 2.5 below. For a complete analysis these 14 third octave frequencies bands are used for each octave band 125, 250, 500, 1k, 2k, 4k and 8k Hz (Steeneken and Houtgast 1985 also Houtgast, Steeneken, 1985a) resulting in a matrix of 98 *m* values. For the RASTI procedure a reduced set of frequencies are used based on the two octave bands, 500 and 2k Hz. These are given in Table 2.6 (Brüel and Kjær 1986).

NB: The theoretical model described in Houtgast, Steeneken and Plomp (1980) uses 18 *F*-values, starting at 0.4 Hz through to 20 Hz in third octave intervals to cover the whole of the audible range. With experimentation, they concluded:

> *"It has been found that the specific choice of F-range considered has no great effect on the resulting STI, providing the upper and lower limits are shifted symmetrically relative to the given values of 0.4 and 20 Hz. For instance, actual measurements may well be based on the 14 F-values from 0.63 to 12.5 Hz (at 1/3 octave intervals or, for a quick first-order estimation, even on the 6 F-values from 0.5 to 16 Hz in octave intervals."* (Houtgast, Steeneken and Plomp, 1980 pg63)

Table 2.5 Modulation Frequencies Steeneken and Houtgast 1985, pg14 also Houtgast, Steeneken, 1985a, pg1072)

| Full Analysis |
|---|
| 0.63 Hz |
| 0.8 Hz |
| 1 Hz |
| 1.25 Hz |
| 1.6 Hz |
| 2 Hz |
| 2.5 Hz |
| 3.15 Hz |
| 4 Hz |
| 5 Hz |
| 6.3 Hz |
| 8 Hz |
| 10 Hz |
| 12.5 Hz |

Table 2.6 RASTI Modulation Frequencies (Brüel and Kjær 1986, pg48)

| 500 | 2k Hz |
|---|---|
| 1.02 Hz | 0.73 Hz |
| 2.03 Hz | 1.45 Hz |
| 4.07 Hz | 2.90 Hz |
| 8.14 Hz | 5.81 Hz |
| | 11.63 Hz |

The *m(F)* can be derived by comparison of the input signal *($I_i$)* and the output signal *($I_o$)*. For the case of continuous noise and no reverberation, the *m(F)* is calculated by:

$$m(F) = \frac{1}{1+10^{(-S/N)/10}} \qquad \{\text{Eq 2.20}\}$$

Conversely, in cases of reverberation and no noise, the *m(F)* is calculated by:

$$m(F) = \frac{1}{1+\sqrt{\left[2\pi F\left(\frac{T}{13.8}\right)\right]}} \qquad \{\text{Eq 2.21}\}$$

where *T* is the reverberation time (seconds)

In cases of both noise and reverberation the *m(F)* is the product of both types of disturbances (Houtgast and Steeneken 1985b, pg7):

$$m(F) = \frac{1}{1+\sqrt{\left[2\pi F\left(\frac{T}{13.8}\right)\right]}} \bullet \frac{1}{1+10^{(-S/N)/10}} \quad \{\text{Eq 2.22}\}$$

The *m(F)* values are converted to apparent signal-to-noise ratios for each modulation frequency (Houtgast, Steeneken and Plomp, 1980 pg72):

$$\left(S/N\right)_{app,F} = 10 * \log_{10}\left(\frac{m(F)}{1-m(F)}\right) \quad \{\text{Eq 2.23}\}$$

The signal-to-noise ratio is then limited to the range between ±15 dB. The mean apparent signal-to-noise ratio is calculated for the 14 *m(F)* values:

$$\overline{\left(S/N\right)}_{app} = \frac{1}{14}\sum_{F=0.63}^{12.5}\left(S/N\right)_{app,F} \quad \{\text{Eq 2.24}\}$$

where F is in third octaves intervals.

The Speech Transmission Index is calculated from the $\overline{S/N}$ ratio:

$$STI = \frac{\left[\overline{\left(S/N\right)}_{app} + 15\right]}{30} \quad \{\text{Eq 2.25}\}$$

Speech Transmission Indexes are in the range of 0 to 1

From equations {Eq 2.23} to {Eq 2.25}, it is apparent that the Speech Transmission Index represents the average signal to noise ratio of a speech transmission system, over the frequency range relevant to the speech modulation frequencies.

The abbreviated calculation of the Speech Transmission Index, the Rapid Speech Transmission Index (RASTI), uses a reduced number of frequencies and modulation frequencies. Instead of the octave frequencies of band 125, 250, 500, 1k, 2k, 4k and 8k Hz, RASTI uses only two octaves - 500 and 2k Hz. (See Table 2.6 for the nine modulation frequencies associated with these frequencies.)

The full Speech Transmission Index procedure requires a test signal and analysis for each data point which is time synchronised. The reduced frequencies of the RASTI procedure, allow a continuous test signal and parallel measurement of both the 500 and 2k Hz octave bands (Steeneken and Houtgast 1985).

## 2.6 Summary

This chapter has discussed the three major approaches to tracking sound from the source to the receiver. For this thesis, the 'image method' will be used as it ensures every surface is examined for sound reflections. Lee and Lee's (1988) modifications to the basic method will be incorporated to improve the efficiency of the algorithm. Diffusion, diffraction and refraction is not implemented.

The Modulation Transfer Function will be used to calculate the Rapid Speech Transmission Index. Other information indices: Early Decay Time, Deutlichkeit, Reverberant to Early Sound Ratio, Clarity, Centre Time, Initial Time Gap, Hallabstand and the Room Response are calculated from the resultant 'ray trace' decay data.

# 3. Methodology

This chapter discusses the methods used to implement the Modulation Transfer Function, Rapid Speech Transmission Index, plus the other indices discussed in the previous chapter in the evaluation program. The implementation requires a geometric model, the 'ray trace' using the image method, calculations for the various statistics and indices and finally the reporting section.

The computational aspects of this thesis are considerable and reasonably complex. To explain the relevant procedures this chapter is subdivided into three major segments:

i) Geometry and Ray Tracing Algorithm

ii) Statistics and Indices

iii) Program Implementation

These segments are a natural division as the development of the indices is totally dependent on a functional ray tracing algorithm.

## *3.1 Geometry and Ray Tracing Algorithm*

The geometric model uses an object oriented approach. The use of objects improves the overall integrity of the modelling by encapsulating data and data handling within specified objects. This process enforces all references to the data to be correctly processed through the object's member functions.

The traditional programming method allows access to the global data to occur from all parts of the program. The significant advantage of the object oriented approach is that data within an object can only be accessed through an object's member functions, which only need to be written and verified once. Other advantages of object code is that once an object class has been written, it can be encapsulated into further objects without any rewriting of code or debugging. This speeds development significantly, as any modifications of the base object are automatically and immediately incorporated

into other objects derived from the base object. There is no need to re-copy the algorithm for each instance where the algorithm is used, eg. list are used repeatedly in objects such as list of points, surfaces, receiver locations and source locations.

An example of the encapsulation mechanism, is the base code for the points list. To create a list of receiver points and source points, it is only necessary to define the new objects as being a list of points.

### 3.1.1 Geometry

A building's geometric data is entered as a series of surfaces. That is, each wall, floor, ceiling panel, etc. is created as a flat surface. Each surface has specific properties:

i) Absorption Coefficients at 125, 250, 500, 1000, 2000 and 4000 hertz

ii) Number of boundary coordinates

iii) Description of the surface

iv) A list of X, Y, Z points describing the boundary coordinates.

v) Plane equation data (A, B, C, D)

vi) Derived Center point coordinates

vii) Translation Matrix *(T)*

There are some restrictions on the definition of surfaces:

i) The surface needs to be flat.

ii) The surface must be capable of description using straight boundaries, ie a curved surface needs to be segmented.

iii) A surface must comprise three or more vertices.

iv) The vertex coordinates are entered in metres.

v) The boundary coordinates must describe a closed loop. By default a check is made by comparing the first and last vertices. If they are dissimilar, then a loop is incorporated to link the first and last vertices.

vi) The surface coordinates must run in sequence in an anti-clockwise direction when looked at from in front of the surface.

NB: Provisions is made within the program to reorder the boundary coordinates (invert the directional vector of a surface). The process is one in which the order of the list of boundary coordinates are reversed. The application of the anti-clockwise ordering is problematic to visualise, thus provisions to allow viewing of the directional vector of the surface and its manipulation. This provides a far easier method to manually alter the order of the data.

v) The axes are arranged in the Right Handed Coordinate System (see Figure 3.1). To view this coordinate system, use the right hand. Hold the THUMB as the X axis pointing to the right, the FIRST FINGER as the Y axis, pointing straight up and the SECOND FINGER as the Z axis, pointing to your nose. The fingers and the thumb are mutually at right angles to each other.

Figure 3.1 Coordinate System

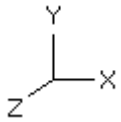


### 3.1.2 Display Views

As an aid to correctly entering the geometric data, there are six separate display projections or views. These views are ‘wire frame’ style projections, not ‘hidden line’ projections. They are intended for fast viewing of the geometric data (see Figure 3.2). Each projection is displayed in an individual child window.

Figure 3.2 Display Projections

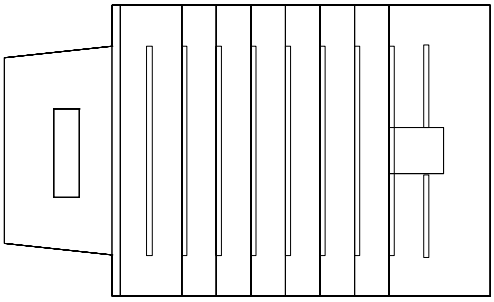

Plan

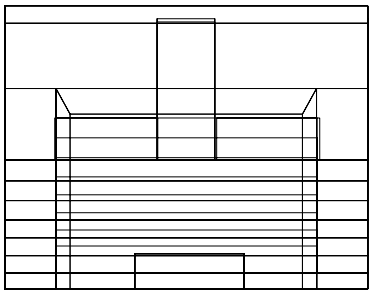

Front

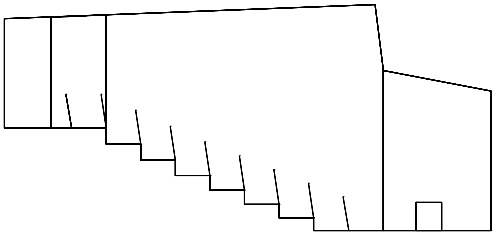

Side Right

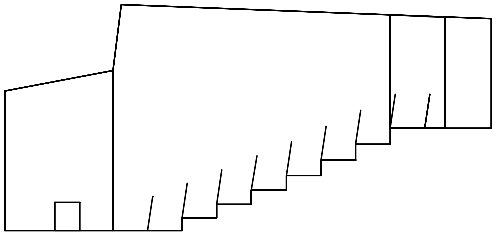

Side Left

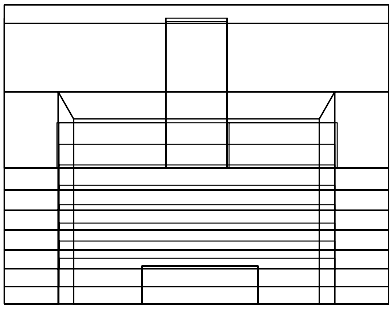

Back

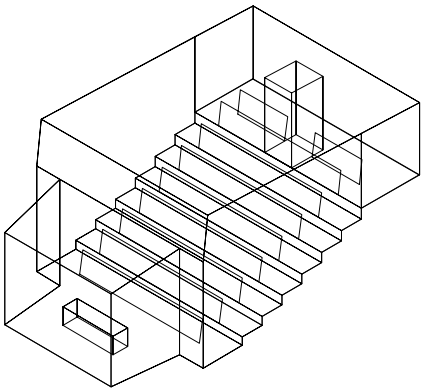

Isometric

The relationships of the various 'wire frame' projections (display views) to the xyz axis (see Figure 3.1) is as follows:

- Plan view is a projection onto the X and Z axis (looking down the Y axis);
- Front view is a projection onto the Y and Z axis (looking along the X axis);
- Side Right view is a projection onto the Y and X axis, but rotated 180° (looking back along the Z axis)
- Side Left view is a projection onto the Y and X axis (looking along the Z axis)
- Back view is a projection onto the Y and Z axis, but rotated 180°° (looking back along the X axis)
- Isometric view is a projection on the X and Y axis, with the X axis projected at 30° and the Y axis projected at 60°.

As can be appreciated from the descriptions above of the various projections, significant coordinate manipulation is required. Extensive use of 'Homogenous Coordinate

Matrices - four dimensional matrix' enable relatively straight forward matrix manipulation to calculate the various transformation of three dimensional space into a two dimensional display.

NB: Homogenous coordinates are used to represent a three dimensional coordinate [x y z] with a four dimensional vector [X Y Z H] (see Rogers and Adams 1976; Kindle 1950, Newman and Sproull 1973; Salmon and Slater 1987). The relationship between the 'normal' three dimensional format and the four dimensional vector form is given by:

$$\begin{bmatrix} X & Y & Z & H \end{bmatrix} = \begin{bmatrix} x & y & z \end{bmatrix} T \qquad \{\text{Eq } 3.1\}$$

where $T$ is a four by four transformation matrix.

The key to the flexibility of using a transformation matrix and homogenous coordinates can be seen in the subdivision of the $T$ matrix in {Eq 3.2}

$$\left[\begin{array}{ccc:c} a & b & c & p \\ d & e & f & q \\ h & i & j & r \\ \hdashline l & m & n & s \end{array}\right] \qquad \{\text{Eq } 3.2\}$$

The matrix is formed in four sections:

i) the 3 x 3 section (elements *abc def hij*) control scaling, shearing and rotation

ii) the 3 x 1 section (elements *lmn*) control translation in the xyz directions

iii) the 1 x 3 section (elements *pqr*) control perspective transformation in the xyz axis

iv) the final section (element *s*) controls overall scaling.

### 3.1.3 Ray Tracing

The method used in the program *R3d,* to trace the path of a 'sound particle' along a 'sound ray' from the source to the receiver location via any reflecting surfaces is the image method. There have been a number of researchers who have developed and improved the efficiency of the image method to allow its use in arbitrary polyhedral spaces. Allen and Berkley (1979) produced an efficient algorithm for rectangular enclosures; Borish (1984) extended the algorithm to arbitrary polyhedra with any number of sides. Lee and Lee (1988) demonstrated that the image method could be made more efficient (computationally faster and requiring less computer memory) using the 'coordinate transformation method' for the calculation of the image source and subsequent ray path.

#### *3.1.3.1 Coordinate Transformation Method*

The transformation method of Lee and Lee (1988) involves calculating the image source position (O'X'Y'Z') by transforming the original source (OXYZ) position by the transform matrix $[T_1]$. Implicit in the formation of the transformation matrix is the concept of rotation and translation. This requires the use of homogeneous coordinates, a concept commonly used in computer graphics when working with three dimensional coordinate systems. The homogeneous coordinate representation of a normal three dimensional coordinate (X,Y,Z) is (x, y, z, 1).

Figure 3.3 Geometrical relationship of the original coordinate system and the image coordinate system.

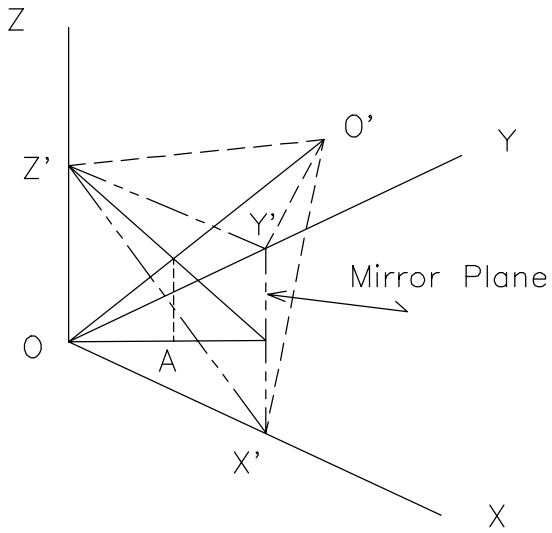


Notes

i) In Figure 3.3 the original coordinate system is OXYZ and the image coordinate system is O'X'Y'Z'.

ii) The vector $\bar{d}$ is normal to the mirror plane (X'Y'Z') from coordinate O.

iii) The OA is the projection of vector $\bar{d}$ on the X-Y plane.

iv) Angle θ describes the azimuth angle between OA and the X axis.

v) Angle ϕ describes the altitude angle of elevation of vector $\bar{d}$ from the X-Y plane.

The image coordinate system O'X'Y'Z' is obtained from the original coordinate system OXYZ through:

i) Rotation about the Z axis through angle θ

ii) Rotation about the Y axis through angle -ϕ

iii) Translation to the positive X direction through a distance of 2d, where d is defined as the distance of the source to the mirror plane

iv) Rotation about the Y axis through angle -ϕ

v) Rotation about the Z axis through angle θ

i) Reflection through the Y-Z plane.

All positive angles are in the anti-clockwise direction.

Using standard matrix equations for rotation and translation the individual matrix formulas can be written for each of the six steps outlined above. These individual matrices are then multiplied together resulting in the transformation matrix shown in {Eq 3.3} (Lee and Lee 1988, pg 93)

$$[T]=\begin{bmatrix} \sin^2\theta-\cos^2\theta\cos2\phi & -\cos\theta\sin\theta(\cos(2\phi)+1) & -\cos\theta\sin2\phi & 0 \\ -\cos\theta\sin\theta(\cos(2\phi)+1) & -\sin^2\theta\cos2\phi+\cos^2\theta & -\sin\theta\sin2\phi & 0 \\ -\cos\theta\sin2\phi & -\sin\theta\sin2\phi & \cos2\phi & 0 \\ 2d\cos\phi\cos\theta & 2d\cos\phi\sin\theta & 2d\sin\theta & 1 \end{bmatrix}$$

{Eq 3.3}

Using the transformation matrix *[T]* above, image source locations can be readily calculated. The intersection point of the mirror plane and the ray path joining the image source and the receiver can then be calculated. (Paragraphs 3.1.3.2 to 3.1.3.5 detail the process.) In this fashion, the complete ray path is readily calculated. Lee and Lee (1988) give an extensive description on the procedure including numerical examples. These examples were essential in the implementation of the transformation matrix into a working computer program.

### *3.1.3.2 Plane Equations and Transformation Equations*

Prior to calculating the altitude angle $\phi$ and the azimuth angle $\theta$, it is necessary to determine the plane equations for each mirror surface. Generally, for any flat plane, it is possible to derive the plane equation from any three xyz coordinates within the plane.

The general equation of a plane is given by Kindle (1950, pg115) as:

$$Ax + By + Cz + D = 0 \qquad \text{{Eq 3.4}}$$

There are many methods of deriving the plane equation {Eq 3.4} from coordinates on the plane. See Salmon and Slater (1987) and Bowyer and Woodwark (1983) for just two examples. The Salmon and Slater method has been used in the program.

Essentially for three coordinates within a plane $(x_1y_1z_1)$, $(x_2y_2z_2)$ and $(x_3y_3z_3)$ the plane equation can be calculated:

$$A=(y_2-y_1)*(z_3-z_1)-(z_2-z_1)*(y_3-y_1)$$
$$B=(z_2-z_1)*(x_3-x_1)-(x_2-x_1)*(z_3-z_1)$$
$$C=(x_2-x_1)*(y_3-y_1)-(y_2-y_1)*(x_3-x_1)$$
$$D=-(x_2*A+y_2*B+z_2*C) \quad \{\text{Eq } 3.5\}$$

The values of the plane equation coefficients *A,B,C,D* have been normalised, so that at least one of the values equals one. This helps to keep the floating point numbers within subsequent calculations much smaller. This reduces overflow and rounding errors.

A plane's perpendicular distance from the origin is calculated using the standard *Distance of a point from a plane (Kindle 1950, pg115)* equation:

$$d = \left| \frac{Ax_0 + By_0 + Cz_0 + D_0}{\sqrt{A^2 + B^2 + C^2}} \right| \quad \{\text{Eq } 3.6\}$$

where $X_0Y_0Z_0$ is the origin.

The altitude and azimuth angles are then generated. This proved to be a major problem, in that the proper generation of the angular sign is critical in the following calculation procedures. The program was cross checked and corrected against commercial CAD programs, EAGLE® and AutoCAD®.

The transformation matrix is calculated for particular plane. (See {Eq 3.3}). The transformation matrix is calculated once for each mirror plane, after the plane geometry has been defined, or edited or read from file.

### 3.1.3.3 Calculation of Image Source Position

The image source position is calculated for any depth of reflections by matrix multiplication of the relevant transformation matrices of each reflecting plane and the origi-

nal source coordinate. For example a third level reflection image source position can be derived from the following equation:

$$\overline{S}_{143} = \overline{S}_0 \left[ T_{143} \right] \qquad \{\text{Eq 3.7}\}$$

where $\overline{S}_0$ is the source coordinates

$T_{143}$ is the resultant from the multiplication of the transformation matrices of $T_1 * T_4 * T_3$

### 3.1.3.4 Calculation of Intersection Points

Calculation of the intersection point of the mirror plane and the straight line between the image source and the receiver locations requires a straight line equation, for the image source to the receiver locations, to be derived. There are a number of routines available to determine the intersection point of a plane and a line. The one used is from Bowyer and Woodwark 1983, pp 103, 111-112)

$$t = \frac{-(A * S_x) - (B * S_y) - (C * S_z) - D}{((A * R_x) - (A * S_x)) + ((B * R_y) - (B * S_y)) + ((C * R_z) - (C * S_z))} \qquad \{\text{Eq 3.8}\}$$

*if the divisor is equal to zero, then there is no intersection.*

$$\begin{aligned} Pt_x &= (t * (R_x - S_x)) + S_x \\ Pt_y &= (t * (R_y - S_y)) + S_y \\ Pt_z &= (t * (R_z - S_z)) + S_z \end{aligned} \qquad \{\text{Eq 3.9}\}$$

and $Pt_{xyz}$ is the intersection coordinate of the line and the plane.

This procedure is carried out for each mirror plane in the ray path.

### 3.1.3.5 Intersection Point in Plane

Every intersection point, once calculated, must then be checked to determine whether the intersection point is actually within the mirror plane. There are a number of 'point in plane' algorithms available - see (Borish 1984) and (Kulowski 1992).

The method used in these algorithms sums the angles formed by the lines joining the intersection point to each successive vertex of the mirror plane, as in Figure 3.4. The dotted lines have been drawn between the intersection point and the plane's vertices. A total of 360º means that the intersection point is inside the defined plane; 0º means it's outside (Borish 1984). This algorithm is tolerant of re-entrant angles.

Figure 3.4 Plane with re-entrant angles

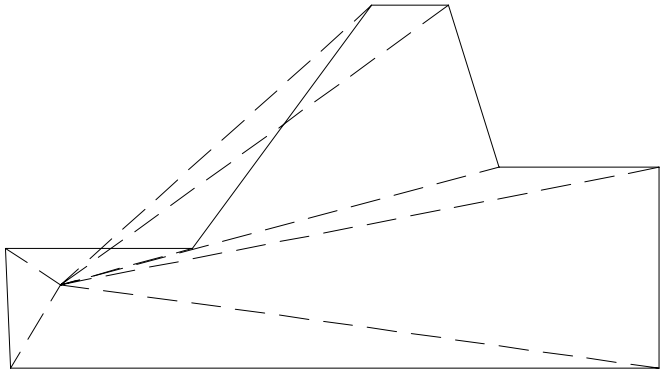

### 3.1.3.6 Obstructions in Ray Path

For every ray path constructed, the algorithm must check whether there are any obstructing surfaces. This process is carried out in two parts:

i) Pre-calculation of mutually invisible planes;
ii) Each segment of the ray path backwards from the receiver to the source is checked.

A segment is any portion of the ray path between two mirror planes, including the source to the first mirror plane and the receiver to the last mirror plane.

The purpose of the pre-calculation check, is to reduce the number of possible ray paths prior to the calculation of the image sources. For example determine whether the under balcony ceiling is visible to balcony front or the balcony audience area. Lee and Lee (1988, pp103-104) described this operation as checking for "*non-feasible combinations of reflecting walls … which are mutually invisible*".

A combination of a hidden plane algorithm and a check for parallel planes in the deduction process for determining where two planes are 'mutually invisible' is used. The result of this 'mutually invisible' check can be seen in the matrix in Table 3.1. The matrix has been calculated for the same test file *(lee10n.scr)* used in the speed comparisons of Figure 3.6 and in Appendix 5 Simulation Times (See Figure 3.5 below).

Figure 3.5 Isometric view of model lee10n.scr

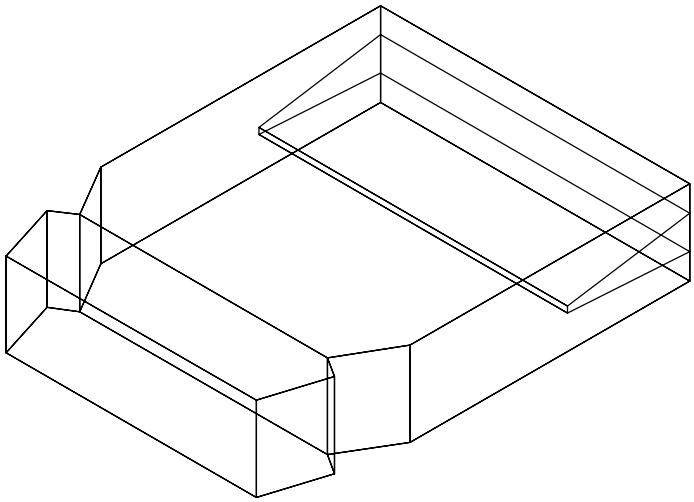

Table 3.1 Matrix of 'mutually invisible' planes

| Surface | Description | 1 | 2 | 3 | 4 | 5 | 6 | 7 | 8 | 9 | 10 | 11 | 12 | 13 | 14 | 15 | 16 | 17 |
|---|---|---|---|---|---|---|---|---|---|---|---|---|---|---|---|---|---|---|
| 1 | Audience Ceiling | ✓ | ✓ | – | – | – | – | – | – | – | – | – | – | – | – | – | – | – |
| 2 | Stage Ceiling | ✓ | ✓ | – | – | – | – | – | – | – | – | – | – | – | – | – | – | – |
| 3 | Audience Right Wall | – | – | ✓ | – | – | – | – | – | – | – | – | – | – | – | – | – | – |
| 4 | Audience Left Wall | – | – | – | ✓ | – | – | – | – | – | – | – | – | – | – | – | – | – |
| 5 | Audience Front Right | – | – | – | – | ✓ | – | – | – | ✓ | – | – | – | – | – | – | – | – |
| 6 | Audience Front Left Wall | – | – | – | – | – | ✓ | – | – | – | ✓ | – | – | – | – | – | – | – |
| 7 | Proscenium Right Wall | – | – | ✓ | – | ✓ | – | ✓ | – | – | – | – | ✓ | ✓ | ✓ | ✓ | – | – |
| 8 | Proscenium Left Wall | – | – | – | ✓ | – | ✓ | – | ✓ | – | – | – | ✓ | ✓ | ✓ | ✓ | – | – |
| 9 | Stage Right Wall | – | – | – | – | – | – | – | – | ✓ | – | – | – | – | – | – | – | – |
| 10 | Stage Left Wall | – | – | – | – | – | – | – | – | – | ✓ | – | – | – | – | – | – | – |
| 11 | Stage Floor | – | – | – | – | – | – | – | – | – | – | ✓ | – | – | – | – | – | ✓ |
| 12 | Balcony Audience | – | – | – | – | – | – | – | – | – | – | – | ✓ | ✓ | ✓ | – | – | ✓ |
| 13 | Balcony Front | – | – | – | – | – | – | – | – | – | – | – | ✓ | ✓ | ✓ | ✓ | – | – |
| 14 | Balcony - Underside | ✓ | ✓ | – | – | – | – | – | – | – | – | – | ✓ | ✓ | ✓ | – | – | – |
| 15 | Auditorium Back Wall | – | – | – | – | – | – | – | – | – | – | – | – | ✓ | – | ✓ | – | – |
| 16 | Stage Screen Wall | – | – | – | – | – | – | – | – | – | – | – | – | – | – | – | ✓ | – |
| 17 | Floor - Audience Area | – | – | – | – | – | – | – | – | – | – | ✓ | – | – | – | – | – | ✓ |

Any calculated ray path attempting to use any of the illegal combinations, identified in the 'mutually invisible' matrix, can be immediately eliminated.

The next part of the process in checking for obstructions is carried out for each individual ray segment.

Obstructions are first checked for each plane by whether the two end points of a given ray segment are the same side of the plane. If they are then, this plane is not an obstruction. If the intersection point calculated for the ray segment and the plane is not inside the plane then the plane is considered not to be obstructing.

NB: The plane equation definition, using the notation of {Eq 3.4}, results in a plane of infinite size.

### 3.1.3.7 Calculation of Ray Length

For valid ray paths, the overall path length is calculated using a three dimensional length of line formula. The length of each ray segment is calculated using:

$$d = \sqrt{(Pt_{x2} - Pt_{x1})^2 + (Pt_{y2} - Pt_{y1})^2 + (Pt_{z2} - Pt_{z1})^2} \qquad \{\text{Eq } 3.10\}$$

### 3.1.3.8 Ray Calculation Strategy

A recursive strategy is employed to calculate valid ray paths. The deduction of valid ray paths is as follows:

i) For the direct ray path between the source and the receiver, check for obstructions.
   For a valid ray path, calculate the length of the ray path:
   Output details to the ray file. (See Appendix 6 File Formats for file layout)

ii) For each level of reflection, to the specified ray depth (maximum number of reflections or mirror planes allowed in a ray path):

Loop for each plane: Check if the receiver and the plane's normal are both the same side of the mirror plane.

NB: A plane's normal axis is used to determine the direction the plane is facing. For this calculation, a point $(X_{Vertex}, Y_{Vertex}, Z_{Vertex})$ is calculated perpendicular to the plane (along the plane's normal axis) from the center of plane.

$$X_{Vertex} = A + X_{center}$$
$$Y_{Vertex} = B + Y_{center}$$
$$Z_{Vertex} = C + Z_{center} \quad \{Eq\ 3.11\}$$

For valid planes recursively call:

1) For each mirror plane multiply the current transformation matrix $T$ by the plane's $T_p$ matrix.
2) Recursively call, for the next level of the ray depth.
3) The final result is the current transformation matrix $T$ being the product of all plane's $T_p$ matrices for a particular ray path. For example, $T_{1\ 3\ 17\ 1}$ for the ray path from the source through the mirror planes 1, 3, 17, 1 to the receiver. This is effectively the $T_{143}$ in {Eq 3.7}
4) For each level of ray depth from the receiver to the source:
5) Check for any surfaces obstructing this segment.
   For valid segments calculate the intersection vertex of the ray segment to the mirror plane. (See 3.1.3.4 for the methodology)
   Check the intersection is in the mirror plane. (See 3.1.3.5 for methodology)
6) For valid rays output details to the ray file.

NB: If a ray segment is found to be in someway invalid through obstructions, or the intersection vertex not being part of the mirror plane, then the whole ray path is immediately dismissed as being invalid.

## 3.2 Statistics and Indices

The program calculates a number of statistics and indices. These are:

i) Derived directly from the ray path data file.
For example the number of reflections, or ray depth, used to produce the ray path data, duration of the calculation, etc.

ii) Calculated from the ray path data.
For example Resultant SPL, Reverberation Time, Early Decay Time, Deutlichkeit, Reverberant to Early Sound Ratio, Clarity, Center Time, Modulation Transfer Function, Speech Transmission Index, Signal to Noise Equivalent, Rapid Speech Transmission Index and Initial Time Gap.

These indices have their origins in full scale enclosure measurements not computer or physical scale modelling. The ray path data produced by the 'ray trace' is used as the vehicle to calculate these indices. It is obvious that the quality of the 'ray trace' will have an impact on the accuracy of all indices. Some will be quite adversely effected. They may not be able to be calculated when there is insufficient ray paths. This is particularly true of indices which are predominantly devoted to the tail of the decay. The 'ray trace' is more effective in determining the early portion of the decay rather than the decay tail.

### 3.2.1 Calculation of SPL at the Receiver Position

To calculate the resultant sound pressure level at the Receiver position the strategy is to allocate a voice level then to reduce the overall level by:

i) the inverse square law for the ray distance;
ii) source directivity;
iii) air absorption related to the total distance of travel for the ray;
iv) the absorption for each mirror plane in the ray path.

The voice level, shown in Table 3.2, incorporated into the program is a modified spectrum based on the Idealised Speech Spectrum from the American National Standards Institute, ANSI S3.5-1969. The Spectrum has been modified to comply with the IEC publication 268 Sound System Equipment Part 16.

Table 3.2 Voice Sound Pressure Levels at 1m from the speaker's mouth

| 125 | 250 | 500 | 1000 | 2000 | 4000 |
|---|---|---|---|---|---|
| 56.0 | 57.5 | 59.0 | 56.0 | 50.0 | 45.0 |

Source directivity is assumed to be uniform across the spectrum. The directivity model used is the Rietschote and Houtgast (1983) model. In this model, the directivity pattern is taken as being rotational symmetric with respect to the normal direction (0º) of the source. In this implementation, the source normal (0º) is taken as being the direction of the direct ray between the source and the receiver. Rietschote and Houtgast (1983) assign the range of $q_i$ between 1,0 to 0,16, which equate to 0dB to -8dB.

For each segment of a ray path, the voice level is reduced due to air absorption and surface absorption. Air absorption coefficients are shown in Table 3.3 below.

Table 3.3 Air Absorption Coefficients

| 125 | 250 | 500 | 1000 | 2000 | 4000 |
|---|---|---|---|---|---|
| 0.0 | 0.0 | 0.0 | 0.003 | 0.007 | 0.02 |

Air absorption is incorporated into the calculation by {Eq 3.12} (Rietschote and Houtgast 1983, pg74)

$$a_{air}=e^{(-air\_absorption * distance)} \qquad \{Eq\ 3.12\}$$

where the distance is the ray segment length.

Surface absorption is incorporated into the calculation by {Eq 3.13} (Rietschote and Houtgast 1983, pg74)

$$a_{surface}=(1 - \alpha) \qquad \{Eq\ 3.13\}$$

The overall sound pressure level for a particular ray path and frequency is:

$$Impulse\ Response_{ray} = 10 * log_{10}\left\{\sum_{n=1}^{\text{number of segments}}\left(10^{\left(\frac{Voice*a_{air}*a_{surface}}{10}\right)}\right)\right\} \quad \{Eq\ 3.14\}$$

## 3.2.2 Calculation of the Modulation Transfer Function

In a 'ray trace' the input signal, or sound particle, is considered to be an impulse. Therefore the Modulation Transfer Function at the receiver location is the:

> *"vectorial sum of all rays received, divided by their absolute sum"*
> (Rietschote, Houtgast and Steeneken 1981, pg247)

This translates to {Eq 3.15} and {Eq 3.16} (Rietschote, Houtgast and Steeneken 1981, pg247)

$$m(F) = \frac{\sqrt{\left(\sum_i a_i \cos(2\pi F t_i)\right)^2 + \left(\sum_i a_i \sin(2\pi F t_i)\right)^2}}{\sum_i a_i} \quad \{Eq\ 3.15\}$$

where:

$a_i$ is the ray strength at the receiver location

$F$ See Table 2.6 for the nine modulation frequencies *(F)* associated with the 500 and 2000 Hertz frequencies

$t_i$ $\dfrac{Ray\ Path\ Distance}{Speed\ of\ Sound}$ {Eq 3.16}

time (s) taken for the ray to have travelled (m) from the source to the receiver.

The *m(F)* is calculated over the total range of ray paths.

### 3.2.3 Calculation of Total Energy

The total energy is calculated from all ray paths within a defined time interval. The start and finish times (seconds) are first converted into distances by:

$$distance = \left(time_{specified} * c\right) + Ray\_distance_{Path0} \quad \{Eq\ 3.17\}$$

Where $c$ is the speed of sound *(m/s)*

If the time is infinity, then this takes on the distance of the last ray path.

NB: The ray paths are sorted in distance order, therefore the last path is the longest ray.

The resultant value is the sum of the energy levels between the start and finish ray distances, inclusive.

## *3.3 Program Implementation*

The program executes on current IBM PC (compatible) machines using WINDOWS™ 3.1 or later and MS-DOS® 5 or later. WINDOWS™ 3.1 provides better memory management facilities than the earlier WINDOWS™ versions. The program has been written and compiled using Borland C++ 3.1 and the Borland ObjectWindows for C++ (OWL) version 1.1 for the graphical user interface.

For adequate performance it is recommended that the minimum computer specification is a 486DX-66 with 8MB of memory (WINDOWS™ 3.1). For WINDOWS™ 95 machines then a minimum specification of 486DX-100 and 16MB of memory. It is quite likely that the program will work on lower specified machines, though this has not been tested.

### 3.3.1 Program Limitations and Parameters

Maximum flexibility, in the size and complexity of spaces modelled, is achieved using a methodology of dynamic memory allocation. There are no in-built limits on the number of surfaces which can be used to describe a space, nor the number of points

used to describe a surface. The dynamic memory allocation allows the model to grow. Thus the limits on complexity then become more dependent on the memory in the system and the hardware configuration, not to mention the simulation time.

The operating system and choice of compiler can have a large influence on the simulation times as does the raw performance of the central processor unit (CPU). Figure 3.6 illustrates the differences between various operating systems on the same hardware. Appendix 5 Simulation Times has more details of how the speed comparisons were made plus discussion on simulation times under different operating systems and hardware.

Figure 3.6 Speed Comparison of different Operating Systems on the same hardware.

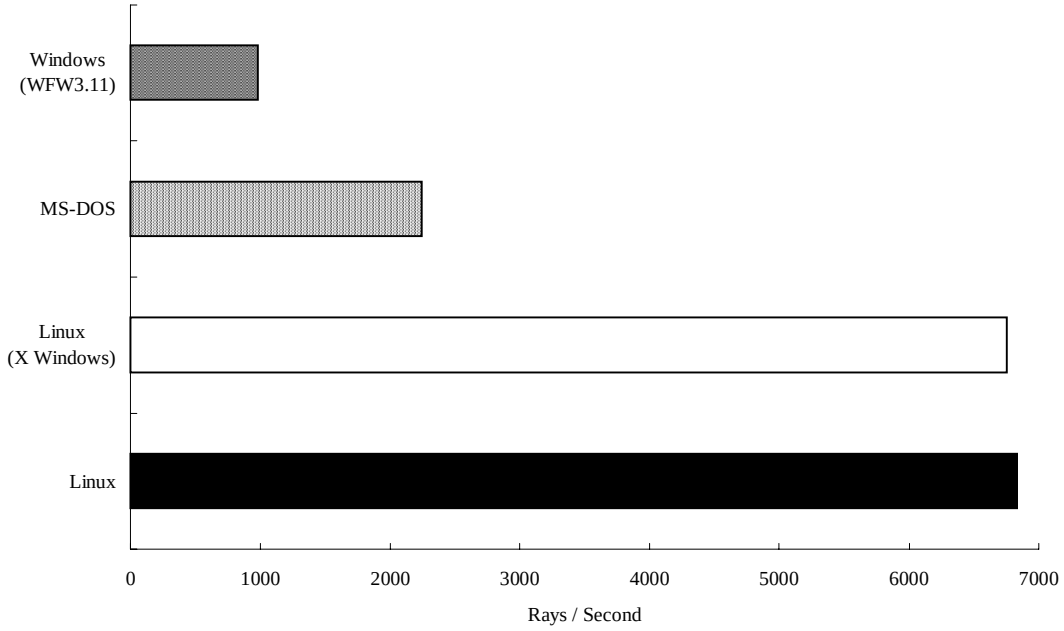


Figure 3.7 clearly shows that the raw processing power of the hardware is a major factor in the overall simulation times. Appendix 5 Simulation Times has performance information for some other Unix based multi -users systems.

Figure 3.7 Intel 486 Processor and Operating System Speed Comparisons

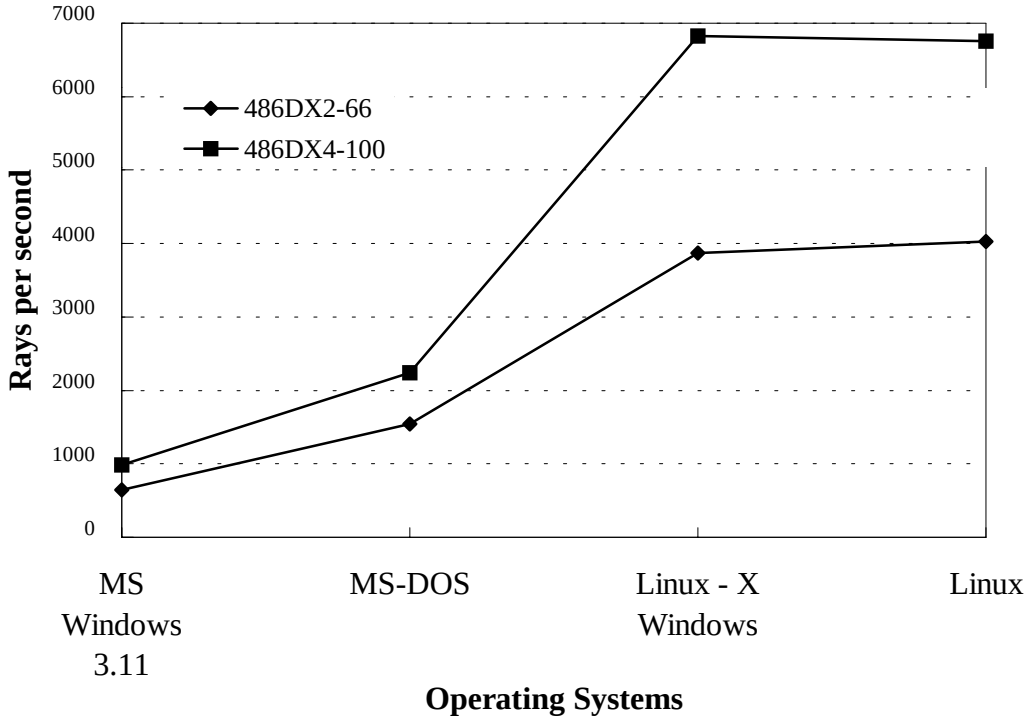


## 3.3.2 Graphical User Interface

The application uses the Multiple Document Interface (MDI) (Borland International 1991) which is an industry standard method of presenting multiple documents (children) within the (parent) application. Each child window can be resized, deleted, moved, iconised, tiled, arranged etc in the same manner as having three or four different documents open simultaneously in a word processor. Typical MDI applications WINDOWS users may be familiar with would include Microsoft Office (Word, Excel, Powerpoint), Program Manager and File Manager (WINDOWS 3 not WINDOWS 95® Explorer).

## 3.3.3 Program Operation

The program has been designed and implemented as a windows style program. This implies that once loaded, the operator controls the operation by the use of the menus. The menu structure is shown in Figure 3.8.

Figure 3.8 Main Menus

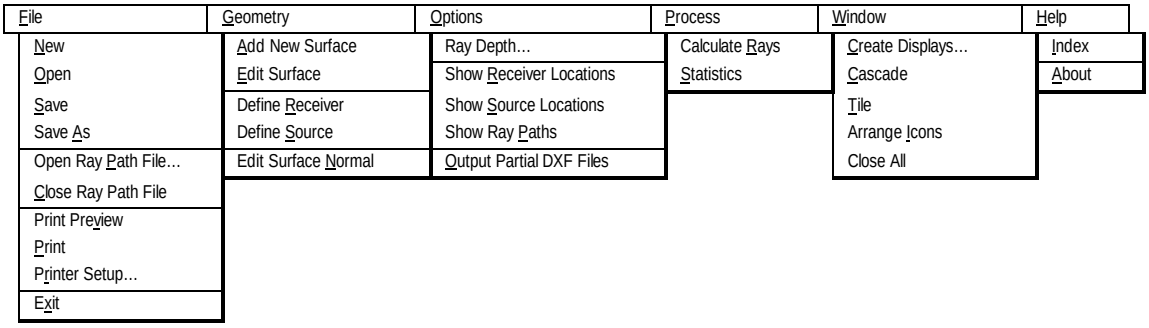


Some options are restricted. For example the Options (all the show features); Process; Geometry (all but Add New Surfaces), etc are unavailable until one or more surfaces have been defined.

### *3.3.3.1 Enclosure Geometry Definition*

The enclosure geometry is entered using the 'Add New Surfaces' option. This allows both the surface vertices to be defined (in metres) plus the material description and acoustic absorption data to be entered.

After the surface data has been entered, the option to manipulate the surface facing direction is available using the 'Edit Surface Normal' option. This option draws an arrow from the surfaces centre out in the direction that the surface is facing and allows simple reordering of the vertices to flip the surface normal's direction.

NB: The vertices should be entered in an anti-clockwise direction when looked at from in front of the surface.

At the completion of the 'Open', 'Add' and 'Edit' operations, the surface's plane equation is calculated along with the translation matrix.

### *3.3.3.2 Source and Receiver Definitions*

Multiple receiver and source locations can be entered, though only the first is used at this stage.

### 3.3.3.3 Calculation Strategy

The calculation module reads the output ray file produced by the image ray trace (see 3.1.3.8 above) and calculates the resultant sound pressure levels at the receiver location for each valid ray. It is apparent in the discussion in 3.1.3.8 above, generally ray processing is terminated at an arbitrary point - the ray depth, and not at some predetermined decibel decay. The rationale behind this strategy, is to allow alteration of the surface material's acoustic specification without the need to recalculate the ray paths. This allows extremely fast 'what-if' style experimentation with changes to the material properties only - not geometric changes. It is implicit that any changes in the geometry will require recalculation of the ray paths.

The strategy for computing the various statistics is:

i) Sort the ray file, if required. (See Appendix 6 File Formats for more information on the ray file contents plus the sorting process and flags).

ii) Various statistics from the ray file are extracted:
- start time
- finish time
- duration
- number of possible reflections
- ray depth
- number of calculated reflections
- number of rays processed
- calculation speed (rays computed / second)

This is not a complete list of statistical information contained in the ray file.

iii) The ray path information is read into memory.

iv) The following are determined:
- The resultant impulse response level at the receiver for each ray path.

- Calculate the overall sound power level at the receiver location. This is done by adding all the ray path's impulse responses.
- The time offset for each impulse response is calculated by {Eq 3.16}
- Calculation of *m(F)* for the four modulation frequencies associated with the 500 Hz octave band and the five modulation frequencies associated with the 2k Hz octave band
- Calculation of the apparent signal-to-noise ratio $(S/N)_{app,F}$
- Limit the apparent signal-to-noise ratio to $\pm 15$ dB
- Calculate $STI_{500\ Hz}$ as $\frac{1}{4}\sum_{F=1.02}^{8.14}\left\{\frac{(S/N)_{app,F}+15}{30}\right\}$ (see Table 2.6 for the 500 Hz octave *F* values) This formula is equivalent to the {Eq 2.24} and {Eq 2.25}. (Brüel and Kjær 1986, pg39)
- Calculate $STI_{2k\ Hz}$ as $\frac{1}{5}\sum_{F=0.73}^{11.63}\left\{\frac{(S/N)_{app,F}+15}{30}\right\}$ (see Table 2.6 for the 2k Hz octave *F* values)
- Calculate RASTI as $\frac{(4STI_{500Hz}+5STI_{2kHz})}{9}$
- Calculate the equivalent signal-to-noise ratios (Brüel and Kjær 1986, pg39):

  $S/N\ Equiv_{500\ Hz} = 30\ STI_{500} - 15$

  $S/N\ Equiv_{2k\ Hz} = 30\ STI_{2k} - 15$

  *"The S/N Equiv. (equivalent signal-to-noise) is defined as that value of S/N ratio which alone would result in the measured STI value. That is, it is assumed that the reverberation time is zero."* (Brüel and Kjær 1986, pg39)

  See (Eq 2.21, Eq 2.22 and Eq 2.23)

v) The following are then determined:

- The Deutlichkeit *(D)*. (See paragraph 2.3.2 on page 32)
- The Reverb to Early Sound Ratio *(R)* (See paragraph 2.3.3 on page 33)
- The Clarity *($C_{80}$)* (See paragraph 2.3.4 on page 33)

- The Centre Time *(TS)* (See paragraph 2.3.5 on page 34)
- The Early Decay Time *($EDT_{10}$)* over the first 10dB of the decay (see paragraph 2.3.1 on page 31). A linear regression is applied to the data to extrapolate out to the 60dB decay limit.
- The Reverberation Time *($T_{30}$)* over the range -5 to -35dB decay. A linear regression is applied to the data to extrapolate out to the 60dB decay limit.
- The Initial Time Gap *($t_1$)* (See paragraph 2.3.6 on page 34). This is calculated from:

$$t_1 = \left( \frac{Ray\ Path\ _{1_{distance}} - Ray\ Path\ _{0_{distance}}}{c} \right) \quad \{Eq\ 3.18\}$$

## 3.4 Summary

This chapter outlines the methods employed in the simulation program for the calculation of the Modulation Transfer Function, Rapid Speech Transmission Index and other indices. The chapter discusses:

- The method used in calculating ray paths using the 'image' method.
- Description of the validation of the ray in terms of intersection points within planes, obstructions in the ray paths and mutually invisible planes.
- Calculation of the resultant sound pressure level for each ray.
- The implemented directivity model.
- Calculation of the Modulation Transfer Function, Rapid Speech Transmission Index and other indices in the simulation tool.
- Computation speed based of a number of computer operating systems.

# 4. Results

This chapter presents the results of simulations of two case studies and compares these results with physical measurements. The case studies have been chosen of two very different rooms: one being a lecture theatre, the other a tutorial room.

The first case study space is a small lecture theatre which does not have voice amplification equipment. The theatre has a seating capacity of 62. It is reasonably intimate with the furthermost audience seat approximately 10.5 metres from the front of the room.

The second case study is an eight sided tutorial room. It is presently used by final year Architecture students as a student workspace, for small tutorial groups and group presentations. The space is small, approximately 6 by 6 metres and 2.9 metres high. It has a flat floor.

## *4.1 Case Study 1 - Lecture Theatre*

This case study is the Curtin University's Robinson Lecture Theatre, Building 201 Room 412. It is located on the main Curtin University of Technology Campus at Bentley and located within the Architecture building.

### 4.1.1 Simulation

The plan and isometric form of the lecture theatre are shown in Figure 4.1. The theatre has been modelled using 47 surfaces and 7 different materials.

Figure 4.1 Plan and Isometric View of Lecture Theatre 201:412

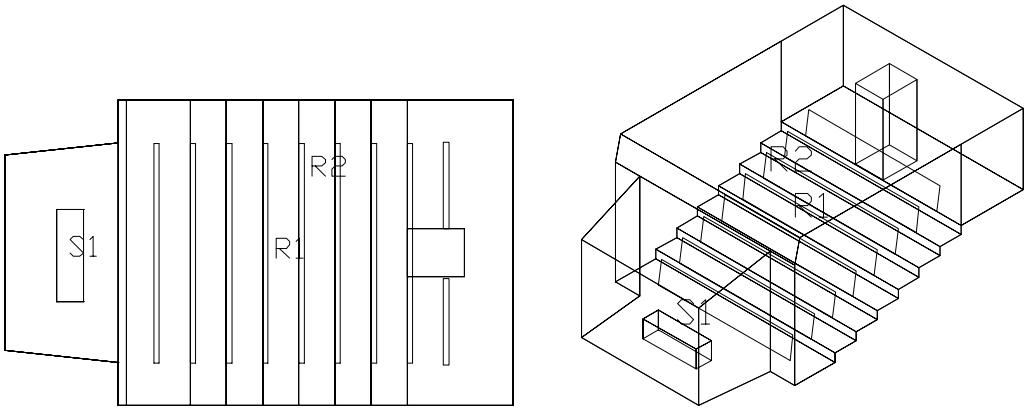


NB: R1 and R2 in Figure 4.1, show the locations of the two receiver locations. S1 is the source location.

### *4.1.1.1 Description*

For the purpose of the simulation, the geometry of this lecture theatre has been simplified. A number of constructional elements have been left out or simplified. For example, the stair tread recesses in the two aisles have not been modelled; likewise the chair seats (up position) and the table tops (down position). The exact details of the chalk board - 2 independent halves with two sliding panels to each half have been ignored. The exact shape of the seat back panel is approximated with one face, facing the front of the room.

The input data is presented below in the same format as the simulation's printed report. Firstly the geometric data is presented in XYZ coordinates for each surface. The order of the vertices have been entered so that the surface face's in the correct direction.

The complete geometric and absorption data is listed in Appendix 7 Simulation Geometric Data.

### 4.1.1.2 Input Geometric Data

The geometric information for each surface takes the form of X, Y, Z coordinates. The description for surface number one is reproduced below.

Surface 1: Screen Wall - Chalkboard

| Vertex data | X | Y | Z |
|---|---|---|---|
| | 0.000 | 0.000 | 1.271 |
| | 0.000 | 3.391 | 1.271 |
| | 0.000 | 3.391 | 5.774 |
| | 0.000 | 0.000 | 5.774 |

### 4.1.1.3 Source Location

| Vertex data | X | Y | Z |
|---|---|---|---|
| | 1.500 | 0.900 | 3.600 |

### 4.1.1.4 Receiver Locations

| Vertex data | X | Y | Z |
|---|---|---|---|
| | 6.277 | 2.131 | 3.650 |
| | 7.104 | 2.487 | 1.751 |

### 4.1.1.5 Results - Receiver Location 1

#### Ray Calculation Statistics -

| | |
|---|---|
| Number of Calculated Rays | 84 |
| Number of Rays Processed | 687431879 |

#### Statistics

| | Frequency | | | | | |
|---|---|---|---|---|---|---|
| Description | 125 | 250 | 500 | 1000 | 2000 | 4000 |
| Voice Level | 56.0 | 57.5 | 59.0 | 56.0 | 50.0 | 45.0 |
| Resultant SPL | 53.4 | 52.2 | 52.9 | 52.7 | 45.2 | 38.4 |
| RT | 0.16 | 0.15 | 0.15 | 0.18 | 0.18 | 0.20 |
| EDT | 0.12 | 0.10 | 0.10 | 0.11 | 0.12 | 0.13 |
| Deutlichkeit (D) | 0.98 | 0.99 | 0.99 | 0.98 | 0.98 | 0.97 |
| R | -17.83 | -20.21 | -20.95 | -16.97 | -16.20 | -14.51 |
| C80 | 45.44 | 48.19 | 48.10 | 39.12 | 38.91 | 37.20 |
| Center Time (TS) | 1047.32 | 1768.84 | 1659.67 | 239.82 | 233.20 | 166.30 |

Initial Time Gap 8.51

### *Modulation Transfer Function*

| | | 500 | | | 2K | |
|---|---|---|---|---|---|---|
| | F | mtf | S/N app. | F | mtf | S/N. app |
| 1 | 1.02 | 0.99 | 15.00 | 0.73 | 0.99 | 15.00 |
| 2 | 2.03 | 0.97 | 14.65 | 1.45 | 0.98 | 15.00 |
| 3 | 4.07 | 0.87 | 8.39 | 2.90 | 0.92 | 10.55 |
| 4 | 8.14 | 0.59 | 1.56 | 5.81 | 0.71 | 3.87 |
| 5 | | | | 11.63 | 0.31 | -3.46 |
| STI | | 0.83 | | | 0.77 | |
| S/N equiv. | | 9.90 | | | 8.19 | |
| RASTI | | 0.80 | | | | |

## *4.1.1.6 Results - Receiver Location 2*

### *Ray Calculation Statistics*

Number of Calculated Rays 112

### *Statistics*

| | Frequency | | | | | |
|---|---|---|---|---|---|---|
| Description | 125 | 250 | 500 | 1000 | 2000 | 4000 |
| Voice Level | 56.0 | 57.5 | 59.0 | 56.0 | 50.0 | 45.0 |
| Resultant SPL | 50.6 | 46.7 | 47.9 | 52.4 | 44.5 | 37.5 |
| RT | 0.23 | 0.26 | 0.27 | 0.22 | 0.26 | 0.29 |
| EDT | 0.12 | 0.12 | 0.07 | 0.09 | 0.08 | 0.09 |
| Deutlichkeit (D) | 0.97 | 0.94 | 0.95 | 0.98 | 0.96 | 0.93 |
| R | -15.15 | -12.18 | -13.07 | -16.72 | -13.97 | -11.06 |
| C80 | 27.18 | 23.95 | 24.86 | 29.22 | 25.85 | 22.55 |
| Center Time (TS) | 17.35 | 8.59 | 9.63 | 24.21 | 12.01 | 6.43 |

Initial Time Gap 5.23

### *Modulation Transfer Function*

| | | 500 | | | 2K | |
|---|---|---|---|---|---|---|
| | F | mtf | S/N app. | F | mtf | S/N. app |
| 1 | 1.02 | 0.98 | 15.00 | 0.73 | 0.99 | 15.00 |
| 2 | 2.03 | 0.94 | 11.78 | 1.45 | 0.97 | 15.00 |
| 3 | 4.07 | 0.78 | 5.39 | 2.90 | 0.89 | 9.03 |
| 4 | 8.14 | 0.45 | -0.93 | 5.81 | 0.64 | 2.44 |
| 5 | | | | 11.63 | 0.32 | -3.30 |
| STI | | 0.76 | | | 0.75 | |
| S/N equiv. | | 7.81 | | | 7.63 | |
| RASTI | | 0.76 | | | | |

## 4.1.2 Physical Measurement Results

All measurements were carried out on February 16, 1995. There was no audience, only the equipment operator. Ambient noise levels were very low and had no effect on the measurements. (See also: Notes on the physical measurements of Speech Transmission Index page 80)

### *4.1.2.1 RASTI*

The results in Table 4.1 and Table 4.2 were obtained using the Brüel and Kjær Speech Transmission Meter Type 3361: Consisting of Transmitter Type 4225 and Receiver Type 4419.

Table 4.1 Case Study 1 - Receiver Location 1

| Volume Ref | Rasti | STI | | Level (dB) | | S/N Equivalent | | EDT Equivalent | |
|---|---|---|---|---|---|---|---|---|---|
| | | 500 Hz | 2 kHz | 500 Hz | 2 kHz | 500 Hz | 2 kHz | 500 Hz | 2 kHz |
| +0 dB | 0.74 | 0.73 | 0.76 | 55.50 | 47.30 | 6.80 | 7.80 | 0.54 | 0.42 |
| +10 dB | 0.72 | 0.68 | 0.74 | 65.50 | 57.30 | 5.40 | 7.30 | 0.66 | 0.46 |

Table 4.2 Case Study 1 - Receiver Location 2

| Volume Ref | Rasti | STI | | Level (dB) | | S/N Equivalent | | EDT Equivalent | |
|---|---|---|---|---|---|---|---|---|---|
| | | 500 Hz | 2 kHz | 500 Hz | 2 kHz | 500 Hz | 2 kHz | 500 Hz | 2 kHz |
| +0 dB | 0.75 | 0.72 | 0.77 | 56.40 | 46.10 | 6.70 | 8.20 | 0.55 | 0.39 |
| +10 dB | 0.71 | 0.67 | 0.74 | 66.10 | 55.90 | 5.00 | 7.20 | 0.69 | 0.47 |

Notes on the physical measurements of Speech Transmission Index:

- The Transmitter has two volume settings. Ref +0 dB and Ref +10 dB.
- By testing with both Ref settings, the effects of ambient noise levels can be assessed in terms of the overall Rapid Speech Transmission Index. An increase in the RASTI result by 0.33 (limited to a maximum RASTI of 1.00), can occur with the additional 10 dB source level if the ambient noise is effecting the RASTI result (Brüel and Kjær, 1986 pg 24). This did not occur, thus it can be assumed that there was little to no effect from ambient noise on the RASTI results.
- The Equivalent Early Decay Times given are not measured but calculated back from the Speech Transmission Index. (See Appendix D in Brüel and Kjær, 1986)

- Measurement period was set for 8 seconds.

#### *4.1.2.2 Decays*

The results in Table 4.3 were obtained using the HP 3569A Real Time Frequency Analyzer with an Impulse Sound triggered from the Analyser. The signal was fed into a Brüel & Kjær HP 1001 sound source.

Table 4.3 Case Study 1 - Reverberation Time ($RT_{60}$)

| Location | Frequency | | | | | |
|---|---|---|---|---|---|---|
| | 125 | 250 | 500 | 1K | 2K | 4K |
| 1 | 1.77 | 1.54 | 1.52 | 1.62 | 1.67 | 1.70 |
| 2 | 2.04 | 1.54 | 1.53 | 1.62 | 1.67 | 1.70 |

Notes on the physical measurements of Reverberation Time:

- There are difficulties in using a speaker for broad band impulse noise. In many cases the sound levels in the lower frequencies were insufficient for the measurement procedure.
- The analyser when conditions permitted, automatically used the Schroeder 'Integrating Impulse Method'.

- The HP 3569A Analyzer is capable of measuring EDT (over 20, 30 and 60 dB decays). The results obtained during measurements were not repeatable from instant to instant thus are not included.

### 4.1.3 Case Study 1 Discussion

This simulation was carried out to a ray depth of six reflections for receiver location 1 and seven reflections for receiver location 2. As can be seen in Table 4.4 below, the predicted RASTI values are very close to the measured values.

Table 4.4 Case Study 1 - STI and RASTI Comparisons

| | Simulation | | | RASTI Machine | | |
|---|---|---|---|---|---|---|
| | STI | | | STI | | |
| Location | 500 | 2000 | RASTI | 500 | 2000 | RASTI |
| Receiver Location 1 | 0.83 | 0.77 | 0.80 | 0.73 | 0.76 | 0.74 |
| Receiver Location 2 | 0.76 | 0.75 | 0.76 | 0.72 | 0.77 | 0.75 |

The RASTI discrepancies represent +6% for receiver location 1 and +1% for location 2. On the scale of Speech Intelligibility (see Figure 4.2) this represents an over estimation of “Excellent” to “Very Good” for receiver location 1 and from “Just under Excellent” to “Excellent” for receiver location 2. This over estimation would tend to reduce with greater ray depth in the simulations.

Figure 4.2 RASTI Scale for Speech Intelligibility

(Brüel and Kjær, n.d.)

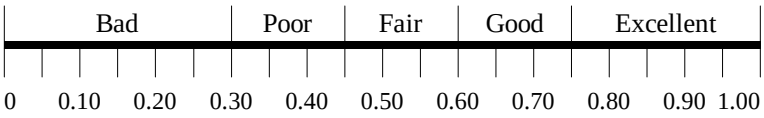


The STI at 500 Hz, Receiver Location 1 (see Table 4.4), indicates where the simulation calculations differ from the physical measurements. Speech Transmission Index has a valid range of 0 to 1, therefore a difference of 10% will effect the overall calculation of the RASTI value, to a greater of lesser extent, depending on the octave band. This is implicit in the RASTI equation (see {Eq 4.1}, also section 3.3.3.3 Calculation Strategy, page 73) which is derived from the octave band STI equations ({Eq 4.2} and {Eq 4.3})

$$\text{RASTI} = \frac{\left(4STI_{500Hz} + 5STI_{2kHz}\right)}{9} \qquad \{\text{Eq 4.1}\}$$

$$\text{STI}_{500\text{ Hz}} = \frac{1}{4}\sum_{F=1.02}^{8.14}\left\{\frac{\left(S/N\right)_{app,F} + 15}{30}\right\} \qquad \{\text{Eq 4.2}\}$$

$$STI_{2k\ Hz} = \frac{1}{5}\sum_{F=0.73}^{11.63}\left\{\frac{(S/N)_{app,F}+15}{30}\right\} \quad \{Eq\ 4.3\}$$

As can be appreciated from the above calculations, a variation in the $STI_{2k}$ value will have a greater impact than a variation in the $STI_{500}$ on the overall RASTI value. This is determined by the signal to noise ratios $(S/N)_{app,F}$ being calculated over four MTF frequencies for the 500 hertz octave band and 5 MTF frequencies for the 2k hertz octave band.

The equivalent signal-to-noise ratio is the measure of the impact the reverberation has on the overall Speech Transmission Index value. As defined in Brüel and Kjær (1986) the Equivalent S/N is the resultant signal-to-noise ratio that would produce an equivalent STI if the reverberation time was zero.

Table 4.5 clearly shows the variation between the simulations and the physical measurements. This is a very good indicator that the simulations do not have adequate time domain detail. There is insufficient decay information to accurately predict the Equivalent Signal-to-Noise Ratio.

Table 4.5 Case Study 1 - Equivalent Signal-to-Noise Ratio Comparisons

| | Simulation | | RASTI Machine | |
|---|---|---|---|---|
| Location | 500 | 2000 | 500 | 2000 |
| Receiver Location 1 | 9.90 | 8.19 | 6.80 | 7.80 |
| Receiver Location 2 | 7.81 | 7.63 | 6.70 | 8.20 |

The individual contributions from each ray reflection, to the overall sound pressure level and the reverberant decay is illustrated in Figure 4.3 to Figure 4.6.

Figure 4.3 Case Study 1: Receiver Location 1 - Individual Ray Sound Pressure Levels by Time (500 Hertz)

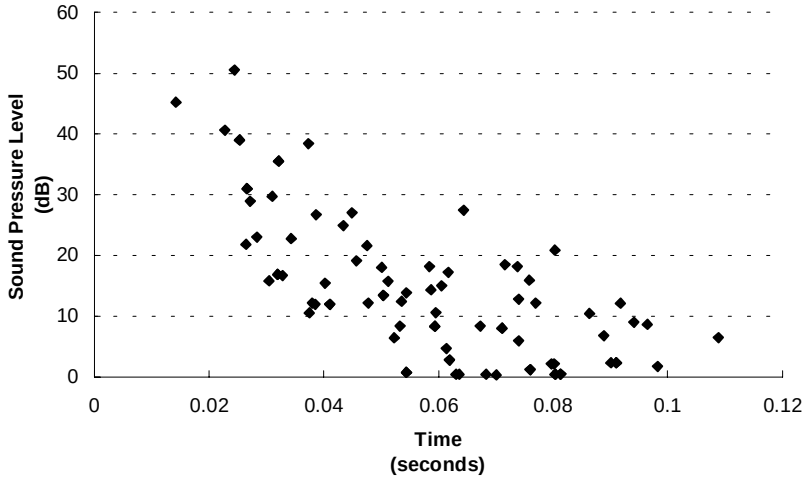


Figure 4.4 Case Study 1: Receiver Location 1 - Individual Ray Sound Pressure Levels by Time (2k Hertz)

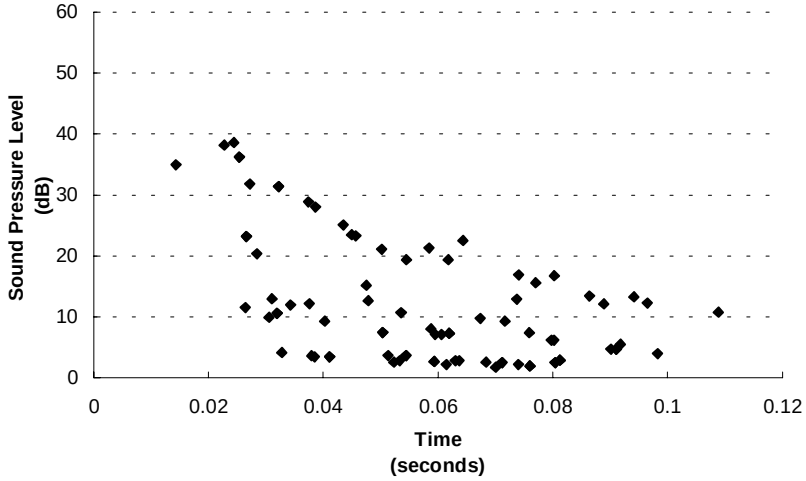

Figure 4.5 Case Study 1: Receiver Location 2 - Individual Ray Sound Pressure Levels by Time (500 Hertz)

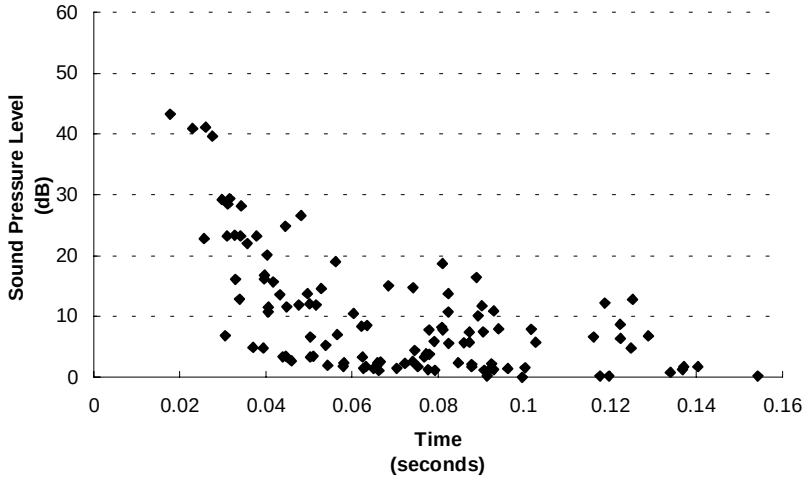


Figure 4.6 Case Study 1: Receiver Location 2 - Individual Ray Sound Pressure Levels by Time (2k Hertz)

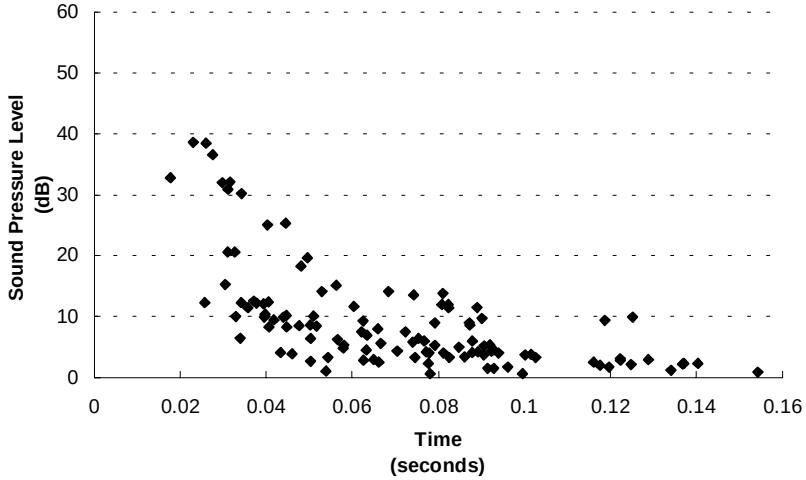


There are no distinctive echoes apparent in Figure 4.3 to Figure 4.6. The lack of a reverberant decay tail can be seen in the reduced number of rays after approximately 0.080 seconds. This area should be densely packed with late reflections.

To improve the interpolation accuracy of the decay curves, the Schroeder Impulse Response is extracted from the time domain sound pressure levels (illustrated in Figure 4.3 to Figure 4.6). The impulse response are reproduced in Figure 4.7 to Figure 4.10.

Figure 4.7 Case Study 1: Receiver Location 1 - Impulse Response (500 Hertz)

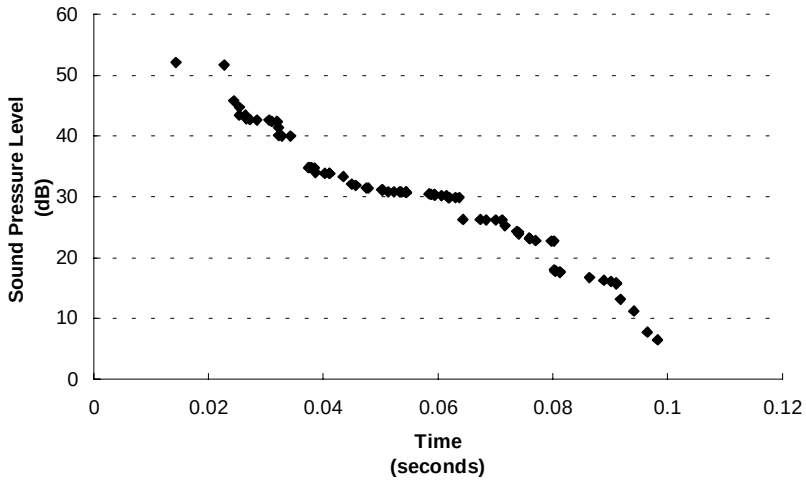


Figure 4.8 Case Study 1: Receiver Location 1 - Impulse Response (2k Hertz)

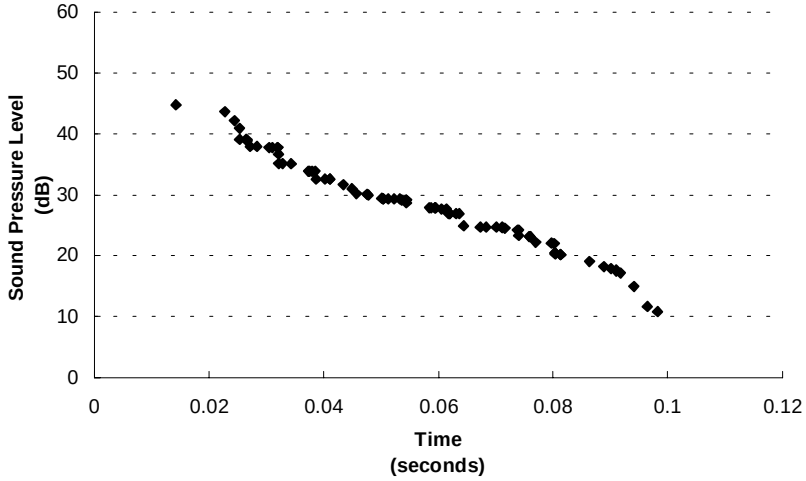

Figure 4.9 Case Study 1: Receiver Location 2 - Impulse Response (500 Hertz)

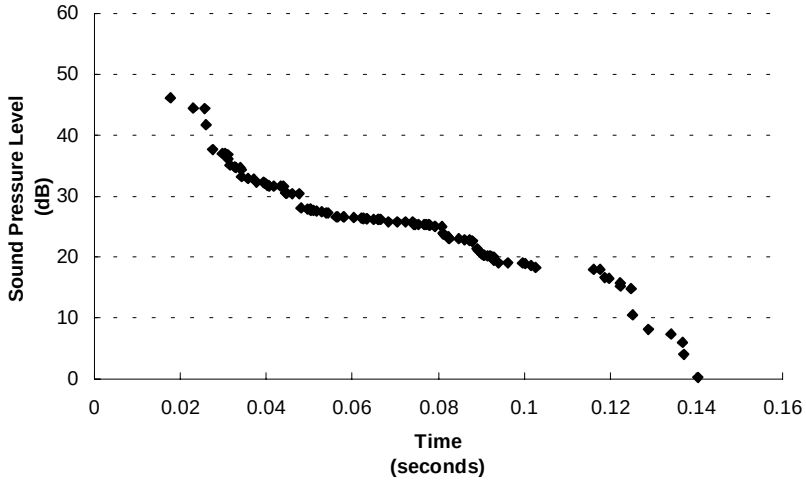


Figure 4.10 Case Study 1: Receiver Location 2 - Impulse Response (2k Hertz)

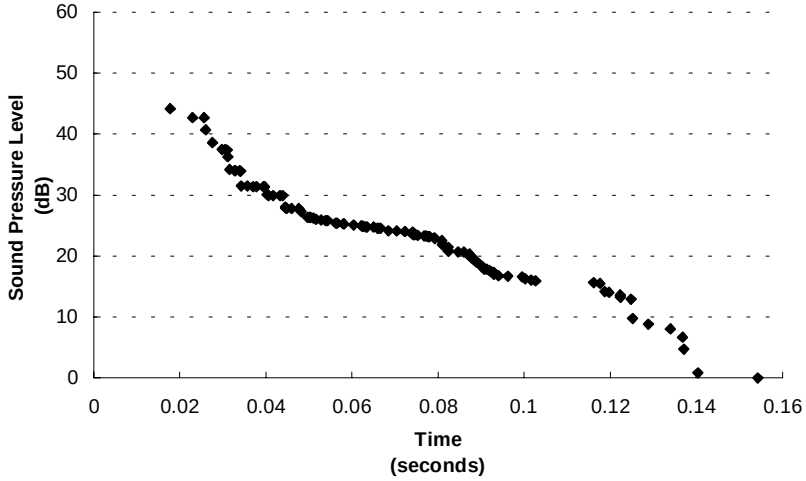


Comparison of the individual ray sound pressure levels to the impulse response clearly show the Impulse Response curves provide far greater accuracy for linear interpolation purposes. What is still apparent in the later part of the Impulse Response curves, is the lack information past 0.100 seconds. This will have a dramatic effect when the curve is extrapolated.

Table 4.6 summarises the numeric data from the simulations and the RASTI measurements. The limited scope of the simulations clearly show that the Early Decay

Times (first 10 dB of the decay curve) are widely variant to those derived from the physical measurements.

Table 4.6 Case Study 1 - EDT Equivalent Value Comparisons

| | Simulation EDT | | Lookup | | RASTI Machine | |
|---|---|---|---|---|---|---|
| Location | 500 | 2000 | 500 | 2000 | 500 | 2000 |
| Receiver Location 1 | 0.11 | 0.12 | 0.31 | 0.40 | 0.54 | 0.42 |
| Receiver Location 2 | 0.07 | 0.09 | 0.45 | 0.44 | 0.55 | 0.39 |

The RASTI machine uses a “look-up” table based on the calculated STI values to derive the Equivalent Early Decay Time. Table 4.6 shows the Equivalent EDT values from the look-up for the simulated STI results. There is no indication in the Brüel and Kjær, 1986, Instruction Manual as to the equivalence of the Equivalent EDT measure to the Early Decay Time decay based measure.

The resultant simulation sound pressure levels, shown in Table 4.7, are lower than the reported levels from the RASTI machine device. Generally the differences are in the order of 1.6 to 2.6 dB. An increased reverberant decay tail could be expected to increase the simulation levels by this order.

Table 4.7 Case Study 1 - Resultant Sound Pressure Levels

| | Simulation | | RASTI Machine | |
|---|---|---|---|---|
| Location | 500 | 2000 | 500 | 2000 |
| Receiver Location 1 | 52.9 | 45.2 | 55.50 | 47.30 |
| Receiver Location 2 | 47.9 | 44.5 | 56.40 | 46.10 |

An 8.5 dB difference at 500 hertz (receiver location 2) could result from:

- one or more major early reflections have not been resolved in the simulation. This could well be dependent on the accuracy of the geometric positioning of the source and receivers for both the simulation and the physical measurement.

  This is unlikely as the 2k hertz octave band has a difference of only 1.6 dB.
- over estimation of the surface acoustic absorption at 500 hertz.

- major differences in the directivity of the physical source and the simulated source. The directivity model used in the simulation assumes a rotational symmetric directivity pattern. The directivity of the RASTI Transmitter Type 4225 is not rotational symmetric. (see the Brüel and Kjær, 1986)

As can be seen in Table 4.8 and in the discussion of the Early Decay Time above, the lack of adequate detail in the reverberant decay tail has a dramatic effect on the interpolation of any decay dependent indices. An expected reverberation time of 1.6 seconds equates to a ray path length of approximately 544 metres over a full 60 dB decay. On the basis of a 30 dB decay, this would reduce to 272 metres, or 181 metres for 20 dB decay.

Table 4.8 Case Study 1 - $RT_{60}$

| | Simulation | | RASTI Machine | |
|---|---|---|---|---|
| Location | 500 | 2000 | 500 | 2000 |
| Receiver Location 1 | 0.15 | 0.18 | 1.52 | 1.67 |
| Receiver Location 2 | 0.27 | 0.26 | 1.53 | 1.67 |

The longest ray distance in the first simulation, Receiver location 1, is 37.5 m (after 6 reflections). This equates to 0.108 seconds (Receiver location 2 simulation - 53.1 m or 0.156 seconds). For an adequate decay trace, you need some 20 dB decay. This may take 10 to 20 plus reflections, which for this number of surfaces is impractical unless the task can the split and 'farmed' out to a number of fast computers. The current limited simulation gives a decay of only 11.1 dB at 500 hertz and 5.5 dB at 2k hertz.

## 4.2 Case Study 2 - Tutorial Room

This case study is of a hexagonal room with a large plasterboard duct across one end. The room 228, is in Building 201, the same building as the Robinson Lecture Theatre used in case study one.

The room is used as student workspace, small tutorial groups and for group presentations. There is no fixed seating or layout, though there is a white board fixed on the wall opposite one set of doors and adjacent to another set. (Large wall next to S1 in Figure 4.11)

## 4.2.1 Simulation

The plan and isometric form of the tutorial room are shown in Figure 4.11. This room has been modelled using 16 surfaces and 4 different materials.

Figure 4.11 Plan and Isometric View of Tutorial Room 201:228

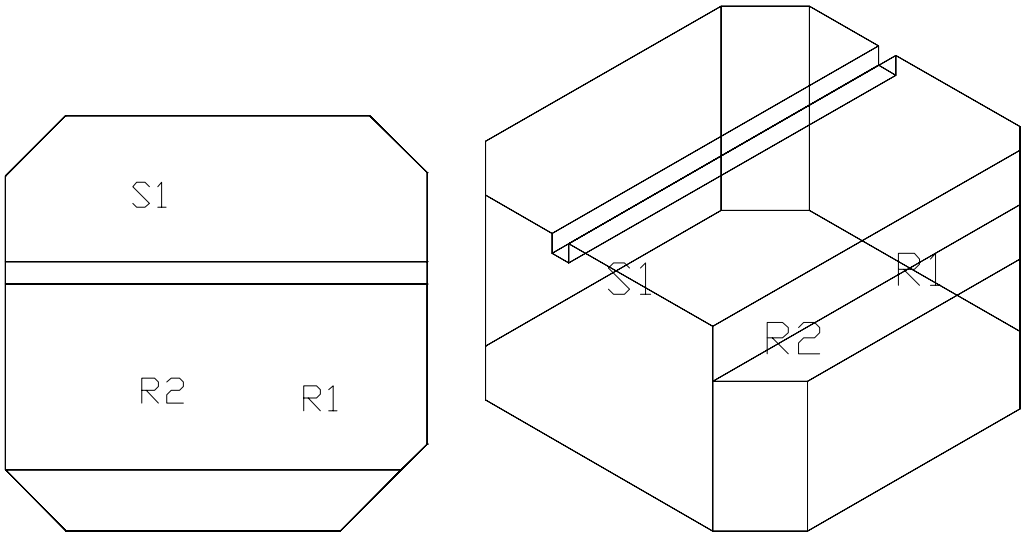


NB: R1 and R2 in Figure 4.11, show the locations of the two receiver locations. S1 is the source location.

### *4.2.1.1 Description*

This tutorial room is a simple space to model. The overall volume is a third of that of case study one. There was some furniture in the room (2 tables, the equipment trolley and 2 people) which were not modelled. The doors and small view window were also not modelled.

The data is presented in the same order and format as used in case study one above.

### 4.2.1.2 Input Geometric Data

The complete geometric and absorption data is listed in Appendix 7 Simulation Geometric Data.

### 4.2.1.3 Source Location

| Vertex data | X | Y | Z |
|---|---|---|---|
| | 1.800 | 1.000 | 1.300 |

### 4.2.1.4 Receiver Locations

| Vertex data | X | Y | Z |
|---|---|---|---|
| | 4.219 | 1.370 | 4.169 |
| | 1.930 | 1.370 | 4.059 |

### 4.2.1.5 Results - Receiver Location 1

#### Ray Calculation Statistics

Number of Calculated Rays 1183

#### Statistics

| | Frequency | | | | | |
|---|---|---|---|---|---|---|
| Description | 125 | 250 | 500 | 1000 | 2000 | 4000 |
| Voice Level | 56.0 | 57.5 | 59.0 | 56.0 | 50.0 | 45.0 |
| Resultant SPL | 64.6 | 64.1 | 62.6 | 56.6 | 50.2 | 44.5 |
| RT | 0.29 | 0.30 | 0.33 | 0.32 | 0.34 | 0.34 |
| EDT | 0.43 | 0.43 | 0.44 | 0.37 | 0.41 | 0.46 |
| Deutlichkeit (D) | 0.66 | 0.66 | 0.66 | 0.70 | 0.67 | 0.65 |
| R | -2.83 | -2.97 | -2.93 | -3.60 | -3.14 | -2.70 |
| C80 | 14.32 | 14.33 | 13.91 | 14.55 | 14.02 | 13.77 |
| Center Time (TS) | 1.47 | 1.46 | 1.33 | 1.46 | 1.33 | 1.30 |

Initial Time Gap 1.94

### *Modulation Transfer Function*

| | | 500 | | | 2K | |
|---|---|---|---|---|---|---|
| | F | mtf | S/N app. | F | mtf | S/N. app |
| 1 | 1.02 | 0.98 | 15.00 | 0.73 | 0.99 | 15.00 |
| 2 | 2.03 | 0.92 | 10.86 | 1.45 | 0.96 | 13.42 |
| 3 | 4.07 | 0.73 | 4.22 | 2.90 | 0.84 | 7.05 |
| 4 | 8.14 | 0.28 | -4.06 | 5.81 | 0.47 | -0.51 |
| 5 | | | | 11.63 | 0.09 | -9.86 |
| STI | | 0.72 | | | 0.67 | |
| S/N equiv. | | 6.50 | | | 5.02 | |
| RASTI | | 0.69 | | | | |

## *4.2.1.6 Results - Receiver Location 2*

### *Ray Calculation Statistics*

Number of Calculated Rays 773

### *Statistics*

| | Frequency | | | | | |
|---|---|---|---|---|---|---|
| Description | 125 | 250 | 500 | 1000 | 2000 | 4000 |
| Voice Level | 56.0 | 57.5 | 59.0 | 56.0 | 50.0 | 45.0 |
| Resultant SPL | 61.9 | 61.6 | 60.3 | 54.7 | 48.3 | 42.9 |
| RT | 0.25 | 0.26 | 0.28 | 0.28 | 0.28 | 0.28 |
| EDT | 0.42 | 0.42 | 0.42 | 0.36 | 0.41 | 0.45 |
| Deutlichkeit (D) | 0.68 | 0.69 | 0.68 | 0.71 | 0.69 | 0.67 |
| R | -3.35 | -3.44 | -3.31 | -3.84 | -3.43 | -3.06 |
| C80 | 16.16 | 16.16 | 15.74 | 16.26 | 15.80 | 15.59 |
| Center Time (TS) | 2.05 | 2.03 | 1.85 | 2.00 | 1.85 | 1.81 |

Initial Time Gap 2.48

### *Modulation Transfer Function*

| | | 500 | | | 2K | |
|---|---|---|---|---|---|---|
| | F | mtf | S/N app. | F | mtf | S/N. app |
| 1 | 1.02 | 0.99 | 15.00 | 0.73 | 0.99 | 15.00 |
| 2 | 2.03 | 0.94 | 12.23 | 1.45 | 0.97 | 14.80 |
| 3 | 4.07 | 0.79 | 5.74 | 2.90 | 0.88 | 8.53 |
| 4 | 8.14 | 0.37 | -2.33 | 5.81 | 0.58 | 1.36 |
| 5 | | | | 11.63 | 0.04 | -13.56 |
| STI | | 0.76 | | | 0.67 | |
| S/N equiv. | | 7.66 | | | 5.23 | |
| RASTI | | 0.71 | | | | |

## 4.2.2 Physical Measurement Results

All measurements were carried out on February 16, 1995. There were two people including the equipment operator in the room. Ambient noise levels were very low and had no effect on the measurements.

### *4.2.2.1 RASTI*

The results in Table 4.9 and Table 4.10 were obtained using the same equipment as in case study one.

Table 4.9 Case Study 2 - Receiver Location 1

| Volume Ref | Rasti | STI | | Level (dB) | | S/N Equivalent | | EDT Equivalent | |
|---|---|---|---|---|---|---|---|---|---|
| | | 500 Hz | 2 kHz | 500 Hz | 2 kHz | 500 Hz | 2 kHz | 500 Hz | 2 kHz |
| +0 dB | 0.60 | 0.51 | 0.68 | 60.20 | 51.40 | 0.20 | 5.40 | ---- | 0.64 |
| +10 dB | 0.58 | 0.51 | 0.63 | 70.00 | 61.30 | 0.30 | 3.90 | 1.40 | 0.82 |

Table 4.10 Case Study 2 - Receiver Location 2

| Volume Ref | Rasti | STI | | Level (dB) | | S/N Equivalent | | EDT Equivalent | |
|---|---|---|---|---|---|---|---|---|---|
| | | 500 Hz | 2 kHz | 500 Hz | 2 kHz | 500 Hz | 2 kHz | 500 Hz | 2 kHz |
| +0 dB | 0.58 | 0.58 | 0.57 | 61.50 | 50.90 | 2.50 | 2.10 | 0.99 | 1.10 |
| +10 dB | 0.56 | 0.54 | 0.58 | 71.40 | 61.00 | 1.30 | 2.30 | 1.20 | 1.00 |

Notes on the physical measurements of Speech Transmission Index:

- The measurement notes are similar to that for case study one. (See section 4.1.2.1 RASTI on page 80).

### *4.2.2.2 Decays*

The results in Table 4.11 were obtained using the same equipment as in case study one.

Table 4.11 Case Study 2 - Reverberation Time ($RT_{60}$)

| Location | Frequency | | | | | |
|---|---|---|---|---|---|---|
| | 125 | 250 | 500 | 1K | 2K | 4K |
| 1 | 0.70 | 0.54 | 0.91 | 1.07 | 0.82 | 0.77 |
| 2 | 1.07 | 1.02 | 0.89 | 1.09 | 0.83 | 0.82 |

Notes on the physical measurements of Reverberation Time:

- The measurement notes are similar to that for case study one. (See section 4.1.2.2 Decays on page 81).

### 4.2.3 Case Study 2 Discussion

This simulation was carried out to a ray depth of nine reflections for receiver location 1 and eight reflections for receiver location 2. As can be seen in Table 4.12 below, the predicted RASTI values are very close to the measured values.

Table 4.12 Case Study 2 - STI and RASTI Comparisons

| | Simulation | | | RASTI Machine | | |
|---|---|---|---|---|---|---|
| | STI | | | STI | | |
| Location | 500 | 2000 | RASTI | 500 | 2000 | RASTI |
| Receiver Location 1 | 0.72 | 0.67 | 0.69 | 0.51 | 0.68 | 0.60 |
| Receiver Location 2 | 0.76 | 0.67 | 0.71 | 0.58 | 0.57 | 0.58 |

The RASTI discrepancies are +9% for receiver location 1 and +13% for receiver location 2. On the scale of Speech Intelligibility (see Figure 4.2 on page 82) this represents an over estimation of “Just Good” to “Quite Good” for receiver location 1 and from “Just under Good” to “Quite Good” for receiver location 2. This over estimation would tend to reduce with greater ray depth in the simulations.

The STI values indicate where the discrepancies lie. For receiver location 1, the simulated $STI_{500}$ is 21% high. In receiver location 2, the simulated $STI_{2k}$ is 18% high. These figures suggest that the absorption rates at 500 hertz used in the simulation are possibly lower that the actual material’s absorption rates. The simulation program confirms that by increasing the 500 hertz absorption values, the computed $STI_{500}$ values reduces as does the RASTI value.

At 2k hertz, the simulation’s $STI_{2k}$ is 10% high for receiver location 2. As the simulation’s $STI_{2k}$ for receiver location 1 is 1% lower, there is confidence in the amount of absorption used in the simulation is representative of the material’s absorption present in the space.

Table 4.13 clearly shows a wide variation in values. This is indicative of a lack of ray depth in the simulation. An increase in absorption reduces the calculated Equivalent Signal-to-Noise Ratio.

Table 4.13 Case Study 2 - Equivalent Signal-to-Noise Ratio Comparisons

| | Simulation | | RASTI Machine | |
|---|---|---|---|---|
| Location | 500 | 2000 | 500 | 2000 |
| Receiver Location 1 | 6.50 | 5.02 | 0.20 | 5.40 |
| Receiver Location 2 | 7.66 | 5.23 | 2.50 | 2.10 |

The individual contributions from each ray reflection, to the overall sound pressure level and the reverberant decay is illustrated in Figure 4.12 to Table 4.15.

Figure 4.12 Case Study 2: Receiver Location 1 - Individual Ray Sound Pressure Levels by Time (500 Hertz)

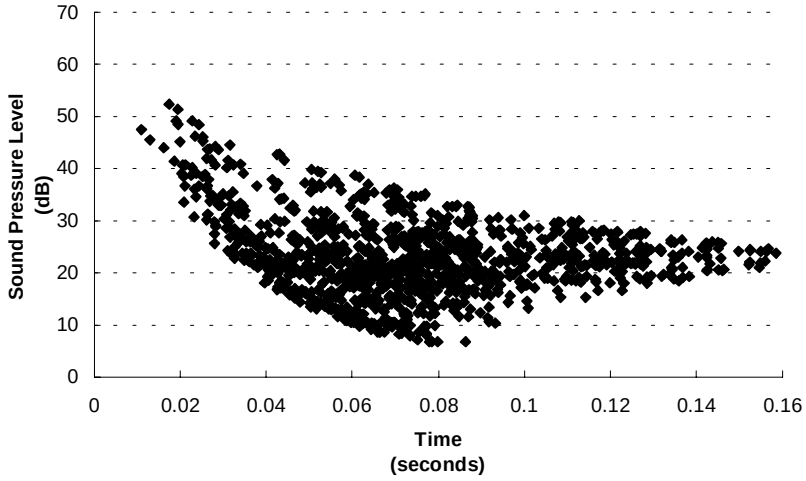

Figure 4.13 Case Study 2: Receiver Location 1 - Individual Ray Sound Pressure Levels by Time (2k Hertz)

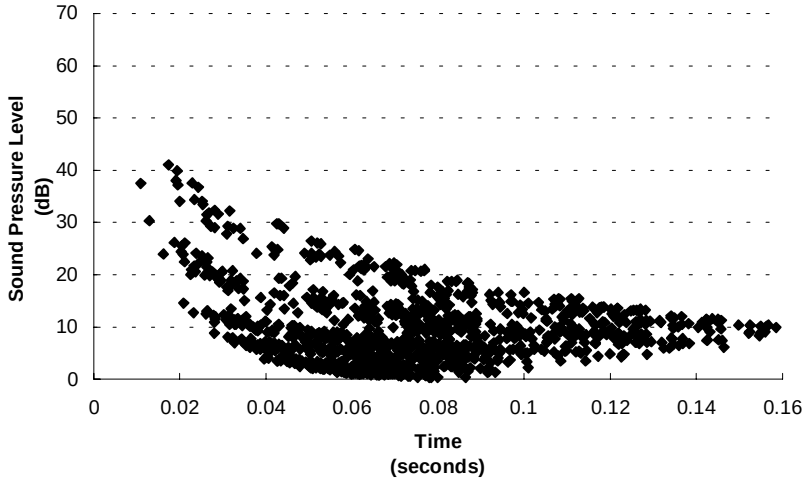


Figure 4.14 Case Study 2: Receiver Location 2 - Individual Ray Sound Pressure Levels by Time (500 Hertz)

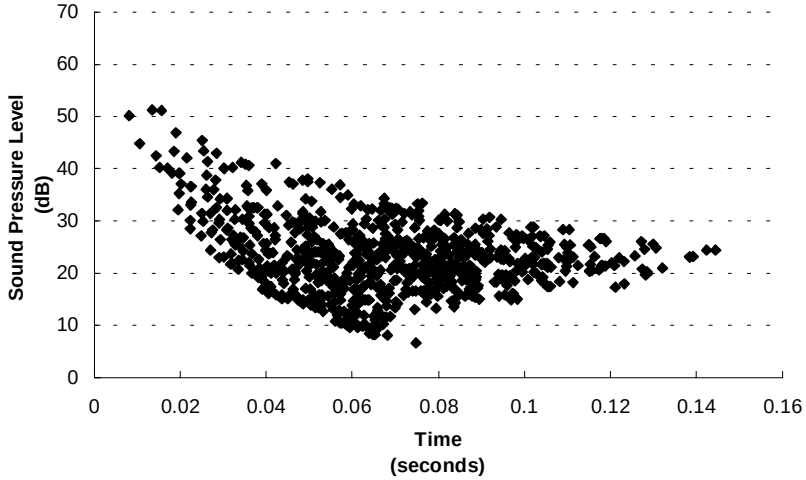

Figure 4.15 Case Study 2: Receiver Location 2 - Individual Ray Sound Pressure Levels by Time (2k Hertz)

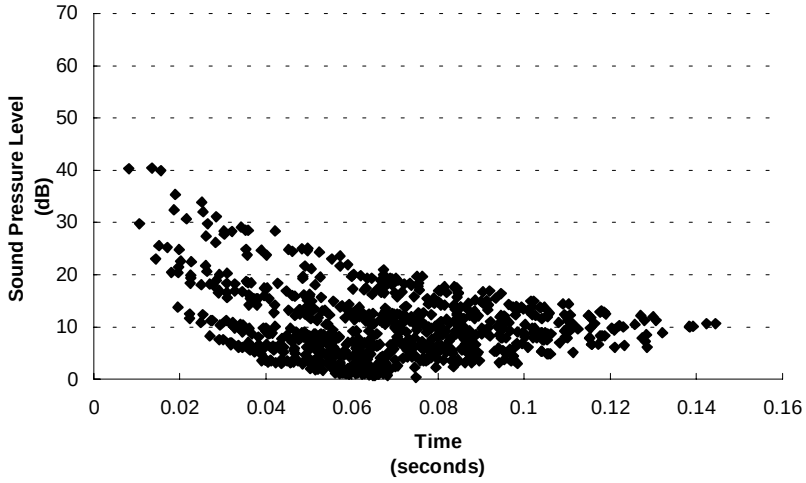


There are no distinctive echoes apparent in Figure 4.12 to Figure 4.15. The lack of a reverberant decay tail can be seen in the reduced number of rays above 0.08 seconds. This area should be densely packed with late reflections.

The impulse response are reproduced in Figure 4.16 and Figure 4.19.

Figure 4.16 Case Study 2: Receiver Location 1 - Impulse Response (500 Hertz)

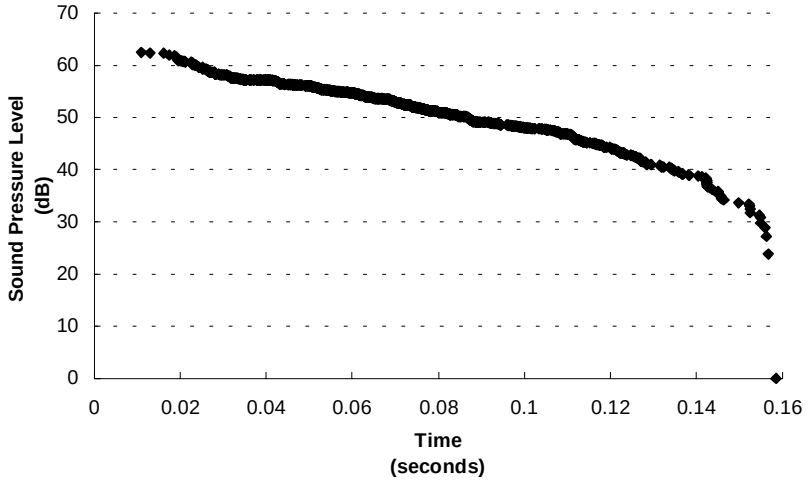

Figure 4.17 Case Study 2: Receiver Location 1 - Impulse Response (2k Hertz)

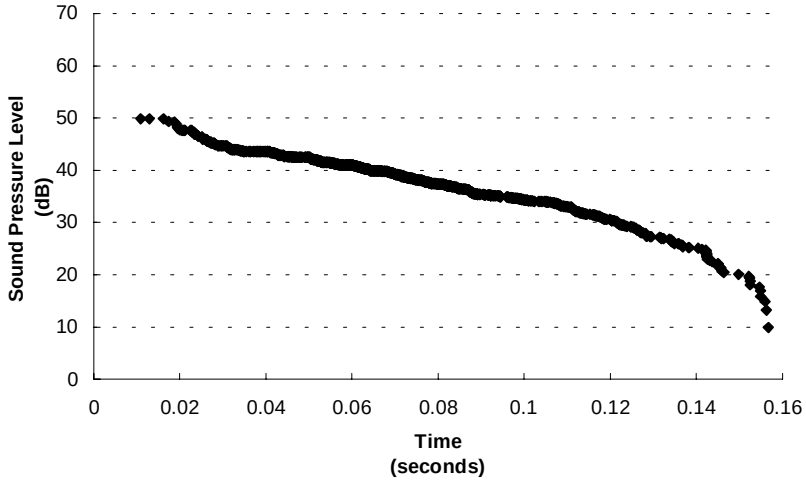


Figure 4.18 Case Study 2: Receiver Location 2 - Impulse Response (500 Hertz)

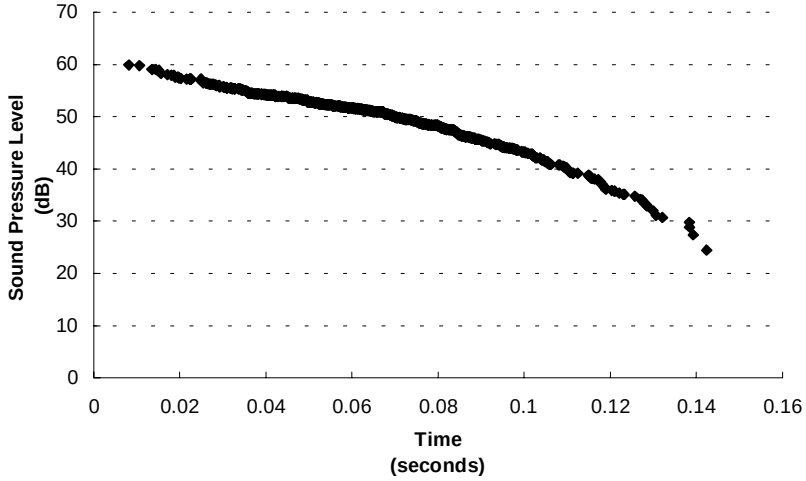

Figure 4.19 Case Study 2: Receiver Location 2 - Impulse Response (2k Hertz)

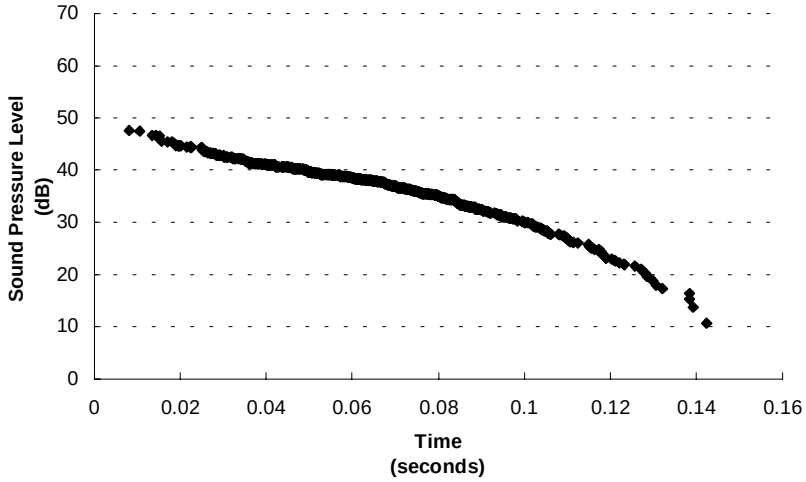


The nature of the Impulse Response curves show the lack of decay tail after 0.130 seconds. The downward curve is particularly obvious in the curves in Figure 4.16 and Figure 4.17. Linear interpolation of the curve will be adversely affected for all decay dependent indices.

Table 4.14 summarises the numeric data from the simulations and the RASTI measurements. The limited scope of the simulations clearly show that the Early Decay Times (first 10 dB of the decay curve) are widely variant to those derived from the physical measurements.

Table 4.14 Case Study 2 - EDT Equivalent Value Comparisons

| | Simulation Early Decay Time | | Lookup | | RASTI Machine | |
|---|---|---|---|---|---|---|
| Location | 500 | 2000 | 500 | 2000 | 500 | 2000 |
| Receiver Location 1 | 0.44 | 0.41 | 0.56 | 0.67 | ---- | 0.64 |
| Receiver Location 2 | 0.42 | 0.41 | 0.45 | 0.67 | 0.99 | 1.10 |

The RASTI machine was unable to determine an Equivalent EDT value for receiver location 1 - 500 hertz. According to Brüel and Kjær (1986, pg40) this occurs where *"… it is unlikely that the reduction of the speech intelligibility is due to pure exponential reverberation decay"*.

The resultant simulated sound pressure levels, shown in Table 4.15, are lower than reported levels from the RASTI machine. Generally the differences are between 1.2 to 2.6 dB

Table 4.15 Case Study 2 - Resultant Sound Pressure Levels

| | Simulation | | RASTI Machine | |
|---|---|---|---|---|
| Location | 500 | 2000 | 500 | 2000 |
| Receiver Location 1 | 62.6 | 50.2 | 60.2 | 51.4 |
| Receiver Location 2 | 60.3 | 48.3 | 61.5 | 50.9 |

A +2.4 dB difference at 500 hertz (receiver location 1) could result from:

- under estimation of the surface acoustic absorption at 500 hertz.
- major differences in the directivity of the physical source and the simulated source.

As mentioned previously and can be seen in the simulation results shown in Table 4.16, the lack of adequate detail in the reverberant decay tail, adversely effects all time domain and decay dependent indices.

Table 4.16 Case Study 2 - $RT_{60}$

| | Simulation | | RASTI Machine | |
|---|---|---|---|---|
| Location | 500 | 2000 | 500 | 2000 |
| Receiver Location 1 | 0.33 | 0.34 | 0.91 | 0.82 |
| Receiver Location 2 | 0.28 | 0.28 | 0.89 | 0.83 |

An expected $RT_{60}$ of 0.85 seconds equates to a ray path of approximately 290 metres. The maximum path length from our simulation is 54.5 metres after 9 reflections. On the basis of a 20 dB decay, this reduces to approximately 96 metres. The current limited simulations results in a 1.7 dB best case decay which is insufficient for accurate extrapolation.

## 4.3 General Conclusions

The investigation has shown that the RASTI and Speech Transmission Index values derived in the simulations are reasonably close to the measured results. This is in stark contrast to the time domain and decay dependent indices. Though this seems to be a contradiction, it has been observed by other researchers.

Steeneken and Houtgast (1985) investigated this phenomena by carrying out a number of experiments in which they examined the impact of the reverberation time on the overall RASTI value. Their experimental results indicated that the Early Decay Time and not the full Reverberation Time had the most impact on the RASTI values.

The two case studies presented in this thesis are characterised by lack of 'late reflection' data which comprises the decay tail needed to predict reverberation time. This does not indicate that the simulation is faulty or has a lack of rigour. Simply, that the 'ray trace' was not pursued to a great enough depth to provide reasonable prediction of the decay dependent variables.

The simulations were carried out over an extended number of days. In the case of case study two the simulation used the 'farm' version to split the task out to 15 Sun Sparc IPC workstations. The 'farmed' simulations were left to run in the background for approximately one week before a forced termination. The Sun's were also used during the day for general CAD classes. Case study one, used Linux on both the 486DX2-66 PC for one receiver location and the 486DX4-100 PC for the other receiver location. There were no Pentium's running Linux available for faster simulation times. Using a Pentium 120 under MS-DOS 7 is slower than using the 486DX4-100 under Linux.

The simulation program enables quick and cost effective exploration of the impact of 'late reflections' on the Speech Transmission Index. Generation of 'late reflections' is controlled by the settings for ray depth. This limits the number of mirror surfaces examined for every ray path (the major computational time factor).

The impact of ray depth on the calculated RASTI values used in simulations can be seen in Table 4.17. This is a comparison of the effect of ray depth to both the computed and measured RASTI and STI values. In case study 2, a ray depth of 9 has reasonable accuracy. This gives a maximum ray duration of 0.138 seconds. The physical measure had a duration of 8 seconds.

Table 4.17 Case Study 2 - Ray Depth Analysis

| Reflections Ray Depth | Duration (seconds) | RASTI | STI | |
|---|---|---|---|---|
| | | | 500 | 2000 |
| 1 | 0.024 | 1.00 | 1.00 | 0.99 |
| 2 | 0.043 | 0.97 | 0.98 | 0.96 |
| 3 | 0.062 | 0.91 | 0.93 | 0.90 |
| 4 | 0.078 | 0.85 | 0.87 | 0.83 |
| 5 | 0.088 | 0.82 | 0.85 | 0.80 |
| … | | … | … | … |
| 9 | 0.138 | 0.69 | 0.72 | 0.67 |
| Physical Measurement | 8.000 | 0.60 | 0.51 | 0.68 |

The ability to explore the impact of ‘late reflections’ with the simulation program is of major benefit to acousticians. It enables rapid experimentation with differing absorbent materials and surfaces to improve speech intelligibility whilst tracking the effects in the decay domain.

Whilst a reasonably low number for the ray depth can produce results approaching measured results for Speech Transmission Index, it is apparent that there is a need for a greater number of reflections if reasonable results are to be achieved for the various time domain decay dependent indices. Recent work by a number of researchers including Rindel, Naylor and Vorländer, in the field of hybrid ray tracing algorithms have enabled greater ray depth analysis with much shorter computation times.

The results presented in this chapter highlight the differences in the directives of the simulated source and the source used with the Brüel and Kjær Speech Transmission Meter. The implemented directivity model does not exactly duplicate the Brüel and

Kjær Speech Transmission Meter. This has an immediate effect on the calculated sound levels for each ray. The overall sound level may not be significantly altered, though the impulse response curve will be, thus all indices based on the decay will be effected.

The simulation program provides a unique tool to examine the relationship between material absorption and source and receiver pair geometric locations by way of Speech Transmission Index and RASTI indices. The ability to quickly experiment with surface absorption coefficients and track the changes in the STI and RASTI values is a major benefit in using the simulation program. For existing enclosures, the simulation, backed by physical RASTI measurements, allows cost effective experimentation of surface finishes along with a greater understanding of the interaction of individual surfaces on the overall Speech Transmission Index.

The discussion in this chapter has focused on only two octave bands, 500 and 2k hertz. This was due to the RASTI dependence on these frequencies. With greater ray depth analysis, the simulation program's ability to perform calculations over a range of octaves from 125 to 4k hertz produces a broad range of results of use to the acoustician.

# 5. Conclusions

This chapter compares the aims with the achievements and suggests some areas for future research. In the introduction chapter, five objectives of the research to produce a simulation tool for use at the design stage of auditoria for unassisted speech reinforcement were listed. They were:

1. To produce a simulation tool which is capable of predicting the expected Speech Transmission Index, or Rapid Speech Transmission Index, from Architect's sketch design concepts drawings;

2. To maximise design applicability, the simulation tool must be capable of using the gross sketch design parameters, eg. room shape, approximate geometry and suggested surface finishes;

3. Prediction of traditional decay dependent measures such as Reverberation Time (RT), Early Decay Time (EDT) and Center Time (C);

4. To provide the mechanism for basic assessment of various design concepts on critical speech performance of the space by way of alteration of material properties, speaker and receiver locations and surface geometry manipulation; and

5. Provide the mechanism to investigate the way in which the speech signal is modified and transmitted to the receiver and how that impacts on the speech intelligibility.

To achieve these objectives, a review of the literature identified that a three dimensional ray trace was necessary in order to develop the required sound ray path information. The Speech Transmission Index is calculated, using the Modulation Transfer Function from the ray path data.

The literature identified three predominant ray trace methods. These being the 'ray method' of "spraying" rays from a source and hopefully hitting a receiver location.

Typically the receiver is a sphere of approximate one metre diameter - considerably larger than the human head. The second was the ‘image method’ where the image source locations are computed allowing direct computation of the reflected ray to the receiver. This method does not use the receiver sphere, as the receiver is a fixed mathematical point. The third method or ‘particle method’ uses sound particles instead of rays in the propagation.

Of the three methods, the ‘image’ method was chosen primarily as it examines every surface as possible mirror surfaces. It was felt that this justification was important for the purposes of examining material properties on the overall Speech Transmission Index. The literature review identified a number of improvements to the basic ‘image’ method algorithm. The most important being those by Lee and Lee (1988). These improvements were implemented in the simulation tool to improve the overall speed of the ray tracing algorithm.

The literature review identified problems in physically measuring reverberation decays. The Schroeder ‘Integrating Impulse Method’ was implemented to improve the accuracy when extrapolating the reverberant decay based on an impulse source. This is in line with current practice for physical measurement of decay dependent indices using impulse sound sources.

To establish the accuracy of the prediction model, measurements of two case studies were undertaken. These were a small lecture theatre with a seating capacity of 62, and a seminar room. Neither space has been designed or equipped with voice amplification equipment. The theatre is reasonable intimate with the furthermost audience seat approximately 10.5 metres from the front of the room.

The second case study was an eight sided seminar room. It is presently used for student workspace, small tutorial groups and group presentations. The space is described in section 4.2.

To improve the simulation speed, some details of the actual spaces were simplified or not modelled. The results form the simulations were compared to the physical measurements.

Comparison of the results indicate that the RASTI and Speech Transmission Index values derived in the simulations are reasonably close to the measured results. This is not the case with the decay dependent indices.

The decay dependent indices suffered from a lack of depth in the ray trace. This is not a reflection of the simulation algorithm, but the run time factor for the simulations. The depth or number of reflections specified for the simulation was limited to reduce the time taken for the computation. Unfortunately this did not produce many late reflections (after say 80~100 milliseconds). Therefore, the late decay indices were not able to be correlated with the physical measurements.

Research by Steeneken and Houtgast (1985) show that the Early Decay Time and not the full Reverberation Time have the most impact on the RASTI values. Therefore a limited ray depth simulation such as these, can have adequate accuracy in the calculation of RASTI and the Speech Transmission Index. This is demonstrated in the high correlation of the speech indices.

The two case studies presented in this thesis are characterised by lack of ‘late reflection’ data which comprises the decay tail needed to predict reverberation time. This does not indicate that the simulation is faulty or has a lack of rigour. Simply, that the ‘ray trace’ was not pursued to a great enough depth to provide reasonable prediction of the decay dependent variables. The simulation program does enable a quick and cost effective exploration of the impact of ‘late reflections’ on the Speech Transmission Index.

The case study results highlight the differences in the directives of the simulated source model and the source used with the physical measurements. The implemented directivity model does not exactly duplicate the instrumentation used in the physical

measurement. This has an immediate effect on the calculated sound levels for each ray. The overall sound level may not be significantly altered, though the impulse response curve will be, thus all indices based on the decay will be effected.

In view of the inherent time limitations of the image method, even with various improvements such as tree pruning and coordinate transformation, further research into and implementation of hybrid techniques utilising both the image method and more traditional ray-tracing algorithms to improve the quality of the calculated decay data are required. Investigation of techniques used in photo-realism 'ray-tracing' may result in far more realistic and 'timely' data which is the basic input to the Speech Transmission Index calculations.

The simulation program provides a very useful tool by which both the geometric and surface material parameters can be quickly examined to determine their impact on overall speech intelligibility. Rapid RASTI assessment, by way of material acoustical property changes, are easily performed. Examination of distribution of the sound rays in the time domain provides valuable information on how a space is performing and which surfaces are producing abnormal reflections. This information is important for proper design, yet is very difficult to obtain with the current range of tools available to the profession.

The alternative method available for predicting Speech Transmission Index is scale model testing which has significant limitations. These include cost (materials, labour and testing equipment), storage space, low flexibility in altering surface finishes. At present, there is little reported research on the implementation of RASTI as a scale model technique. Certainly, the current commercial RASTI equipment is not suitable for scale model measurements.

The simulation program, whilst computationally relatively slow, is a viable alternative for predicting the Speech Transmission Index in acoustically significant projects. The model geometry can be entered quickly and the ray trace can begin immediately, before the surface materials have been chosen. This simply can not be done with scale

models! For scale model construction, the surface material must be decided prior to starting construction. Often the geometry has been established well before the material surfaces have been decided. In acoustically significant projects, the costs for scale modelling would easily exceed that of purchasing a very fast PC computer; the construction time would also exceed the ray trace time.

At the time this thesis began, there were no commercially available simulation programs for the prediction of Speech Transmission Index. There were a number of simulations available for the prediction of the reverberation time. In the time it has taken to complete this study part time, a number of commercial programs such as ODEON have been released or upgraded to provide Speech Transmission Index.

This thesis has achieved the primary objective of developing a simulation tool designed specifically to investigate the way in which the speech signal is modified and transmitted to the receiver and how that impacts on the speech intelligibility.

## 5.1 Further Work

The simulation has been designed to allow multiple source and receiver locations to be entered. Presently only the first source and receiver locations are utilised in the ray trace algorithm. Further enhancements to take into account multiple receivers and multiple sources are necessary. This would expand the utility of the simulation to take into account speech reinforcement systems. For these systems, it would be necessary to be able to alter the voice level and the directivity of the sources.

Improvements in the rate of absorption of the ‘sound ray’ above an audience is necessary. The literature suggests this can be readily modelled using a grazing absorption. That is, when the ray travels above the audience and closer than a given distance then a grazing absorption of 0.65dB/m is applied rather than the normal air absorption rates.

To improve the real life accuracy of the decay model, it would be necessary to implement diffusion in the model. At this stage the typical diffusion model is not applicable

to the ‘image method’. Therefore implementation of a hybrid system of ‘ray trace’ and ‘image methods’ should be investigated.

The literature suggests implementation of some form of statistical approach is viable to improve the detail of the decay tail. It is debateable whether this method or the hybrid methods mentioned above would provide adequate decay tail for the decay dependent indices to be computed with the required accuracy. Further research and correlation of physical measurements and simulation measurements is required to resolve this question.

For informed decision making, such as which surfaces are best candidates for experimentation with different absorptive materials, additional charts and tables of the percentage of hits each surface received, plus breakdowns of the percentages for levels of ray depth are necessary. The raw data for this analysis is in the ray path files.

The range of indices calculated should be increased to include the binaural indices such as the IACC (Interaural Cross-Correlation Coefficient). The calculation for binaural ray paths could start with a single ear main ray trace, with a check to determine whether the ray path offset for the other ear is valid. Further paths could then be investigated with a check against these combinations. This strategy should force the ‘ray trace’ times to be under a factor of twice the time of a single ‘ray trace’.

The simulation program provides a unique tool to examine the relationship between material absorption, source and receiver geometric locations by the use of the Speech Transmission Index and RASTI indices. The ability to quickly experiment with surface absorption coefficients and track the changes in the STI and RASTI indices is a major benefit of the simulation program. For existing enclosures, the simulation, backed by physical RASTI measurements, allows cost effective experimentation of surface finishes along with a greater understanding of the interaction of individual surfaces to the overall Speech Transmission Index.

## 5.2 Summary

This thesis is in two parts. This report and the simulation program on the accompanying diskette for IBM compatible PC's. The diskette contains the Microsoft Windows 3.x executable, windows help file and sample data files as used in this report.

Chapter 1 Introduction; set out the nature, scope and limitations of the work. The hypothesis as stated was to develop a simulation tool designed specifically to investigate the way in which the speech signal is modified and transmitted to the receiver and how that impacts on the speech intelligibility. This outcome has been achieved and validated.

Chapter 2 Literature Review; reviewed the literature establishing the procedures for the calculation of the 'ray trace' and Speech Transmission Index from the Modulation Transfer Function.

Chapter 3 Methodology; described the procedures employed in the 'ray trace' and the theories necessary for the calculation of the Speech Transmission Index, Modulation Transfer Function and other indices from the 'ray trace'.

Chapter 4 Results; compared the simulation results to physical measurements for two case studies. The case studies were chosen as they were two widely varying spaces in terms of usage, materials, volume, geometry and modelling complexity. The correlation of the simulation's ability to predict the Rapid Speech Transmission Index is very high though dependent on sufficient depth of the ray trace.

Chapter 5 Conclusions; compares the aim with the achievements and suggests a number of future developments and directions.

Additionally:

Glossary of Terms; provides a brief description of some of the key terms and abbreviations used in the thesis report.

References lists all material cited in this report.

Appendices, contain supplementary information, tables and data.

# 6. Glossary of Terms

Key terms used in this thesis include:

Articulation Index (AI)

A computed measure of speech intelligibility, based on speech perception tests.

Centre Time

Centre Time (seconds), also known as Centre of Gravity Time, Point of Gravity and Schwerpunktzeit is a:

> *"measure of the balance between clarity and reverberance that was proposed to avoid the abrupt division between early and late arriving reflections"*. (Bradley and Halliwell 1989, p17)

Both Deutlichkeit and Center Time are closely related to speech intelligibility. The smaller the value of the Center Time (or higher the Deutlichkeit value) the higher is the expected speech intelligibility at the receiver position (Kuttruff 1994, p36).

Clarity

A measure suitable to music with an 80ms limit. The 80ms limit allows for reflections which are less noticeable within this time limit in music than the 50ms for speech (Kuttruff 1991, p191). This index is not intended to indicate speech intelligibility but to rate the ease of distinguishing successive notes in rapid music passages.

Deutlichkeit

Deutlichkeit (D), also known as Definition, was proposed by Thiele as a measure of clarity. Deutlichkeit is defined as the:

> *"ratio of the early sound energy in the first 50ms after the arrival of the direct sound to the total sound energy"* Bradley (1983, p2051)

Early Decay Time (EDT)

The reverberation time based on the first 10dB decay and extrapolated to 60dB.

Hallabstand

The ratio of the very early sound energy (first 5ms) to the rest of the sound energy.

Initial Time Gap

The Initial Time Gap is the difference in the arrival times of the first reflection and the direct sound.

Modulation Transfer Function (MTF)

The transfer function allows differences between the original signal and the received signal to be detected by using a carrier frequency on which a special signal is modulated

Reverberant to Early Sound Ratio

R is a measure of the balance between definition and blend. It is the ratio of late arriving sound energy, between 50ms and 500ms, and the early sound energy up to 50ms.

Rapid Speech Transmission Index (RASTI)

A simplified (reduced number of frequencies) Speech Transmission Index.

Reverberation Time (also known as $RT_{60}$ and $T_{60}$)

The time required for the sound energy density to decrease by $10^{-6}$ of the initial value (60dB).

Room Response

An index which is highly correlated with the subjective evaluation of the spatial effect.

Speech Transmission Index (STI)

A method allowing quantification of speech intelligibility of a transmitted signal. STI provides an objective measure, with respect of speech intelligibility, of the acoustic communication between a source and a receiver. Its basis is the measurement of the reduction in modulation between source and receiver. (Brüel and Kjær, 1986.)

# 7. References


Allen, J.B, Berkley, D.A, 1979, 'Image method for efficiently simulating small-room acoustics', *Journal Acoustic Society America*, vol. 65, no. 4, pp943-950

Allison, C, 1993, 'File processing: An external sort program', [Computer program], *C Users Journal*, vol. 11, no. 5, pp105-107

American National Standards Institute (Inc), 1969, *American National Standard Methods for the Calculation of the Articulation Index*, ANSI S3.5-1969

Barron, M. and Lee, L.J, 1988, 'Energy Relations in Concert Auditoriums. I', *Journal Acoustic Society America*, vol. 84, no. 2 August, pp618-628

Beranek, L.L, 1992, 'Concert Hall Acoustics - 1992', *Journal Acoustic Society America* vol. 92. no. 1, pp1-40

Beranek, L.L, 1994, 'The acoustical Design of Concert Halls', *Building Acoustics*, vol. 1, no. 1, pp3-25

Boone, M.M and Braat-Eggen, E, 1994, 'Room acoustic parameters in a physical scale model of the New Music Centre in Eindhoven: Measurement method and results', *Applied Acoustics*, vol. 42, pp13-28

Borish, J, 1984, 'Extension of the image model to arbitrary polyhedra', *Journal Acoustic Society America*, vol. 75, no. 6, pp1827-1836

Borland International, 1989, *Turbo Pascal®: Object-Oriented Programming Guide*, Scotts Valley, CA

Borland International, 1990, *Turbo C++*, (DOS version 1.0) [Computer Program], Scotts Valley, CA

Borland International, 1991, *Objectwindows for C++*, (WINDOWS version 1.1) [Computer Program], Scotts Valley, CA

Borland International, 1992, *Borland C++*, (DOS and WINDOWS version 3.1) [Computer Program], Scotts Valley, CA

Bowyer, Adrian and Woodwark, J, 1983, *A Programmer's Geometry*. Butterworths, London, England, pp114-115.

Bradley, J.S, 1983, 'Experience with new auditorium acoustic measurements', *Journal Acoustic Society America*, vol. 73, no. 6 June, pp2051-2058

Bradley, J.S, 1986, 'Auditorium acoustics measures from pistol shots', *Journal Acoustic Society America*, vol. 80, no. 1 July, pp199-205

Bradley, J.S. and Halliwell, R.E, 1989, 'Making auditorium acoustics more quantitative', *Journal Sound and Vibration*, February, pp16-23

Brüel and Kjær, 1986, *Instruction Manual: Speech Transmission Meter Type 3361: Consisting of Transmitter Type 4225 and Receiver Type 4419*, Brüel and Kjær, Denmark

Brüel and Kjær, n.d., *Using RASTI to Determine Speech Privacy*, (Application Note) Brüel and Kjær, Denmark

Burd, A, 1975, 'Acoustic modelling - Design tool or research project?', in *Auditorium acoustics*, Ed. Mackenzie, R, Applied Science Publishers, London, pp73-85

Cavanaugh, W.L, Farrell, W.R, Hirtle, P.W, Watters, B.G, 1962, 'Speech Privacy in Buildings', *Journal Acoustic Society America*, vol. 34, no. 4, pp475-492

Davern, W.A, 1977, 'Perforated facings backed with porous materials as sound absorbers - An experimental study', *Applied Acoustics*, vol. 10, pp86-112

Davis, D. and Davis, C, 1989, 'Application of speech intelligibility to sound reinforcement', *Journal of the Audio Engineering Society*, vol. 37, no. 12, pp1002-1019

Day, B, 1975, 'Acoustic scale modelling materials', in *Auditorium acoustics*, Ed. Mackenzie, R, Applied Science Publishers, London, pp87-99

Dodd, G, Marshall, A.H, Polack, J.D. and Meynial, X, 1992, The MIDAS system for all-scale room acoustics measurements, *Proceedings of the 26th Australian and New Zealand Architectural Science Association*, Perth, pp73-81

Frank, P.G, Bergmann, P.G and Yaspan, A, n.d., 'Ray Acoustics', *Summary Technical Report*, Division 6, NDRC in *Benchmark papers in acoustics Vol. 4: Physical Acoustics*, Ed. Lindsay, R.B Dowden, Hutchinson and Ross, Stroudsburg, pp34-56

French, N.R, Steinberg, J.C. 1947, 'Factors Governing the Intelligibility of Speech Sounds', *Journal Acoustic Society America*, vol. 19, no. 1, pp90-119

Gibbs, B.M, Jones, D.K, 1972, 'A simple image method for calculating the distribution of sound pressure levels within an enclosure', *Acustica*, vol. 26, pp24-32

Ginn, K.B, 1978, *Architectural Acoustics*, Brüel & Kjær, Denmark, 2nd edition

Hassall, J.R. and Zaveri, K, 1979, *Acoustic Noise Measurements*, Brüel & Kjær, Denmark, 4th edition

Hodgson, M, 1990, 'On the accuracy of models for predicting sound propagation in fitted rooms', *Journal Acoustic Society America*, vol. 88, no. 2, pp871-8

Houtgast, T, Steeneken, H.J.M, 1973, 'The Modulation Transfer Function in Room Acoustics as a Predictor of Speech Intelligibility', *Acustica*, vol. 28, pp66-73

Houtgast, T, Steeneken, H.J.M, 1984, 'A Multi-Language Evaluation of the RASTI-Method for Estimating Speech Intelligibility in Auditoria', *Acustica*, vol. 54, pp185-199

Houtgast, T, Steeneken, H.J.M, 1985a, 'A review of the MTF concept in room acoustics and its use for estimating speech intelligibility in auditoria', *Journal Acoustic Society America*, vol. 77, pp1069-1077

Houtgast, T, Steeneken, H.J.M, 1985b, The Modulation Transfer Function in Room Acoustics, *Technical Review* No. 3, Brüel and Kjær, Denmark, pp3-12

Houtgast, T, Steeneken, H.J.M. and Plomp, R, 1980, 'Predicting Speech Intelligibility in Rooms from the Modulation Transfer Function. I. General Room Acoustics', *Acustica*, vol. 46, pp60-72

Hunt, F.V, 1978, *Origins in Acoustics: The science of sound from Antiquity to the age of Newton*, Yale University Press, New Haven

International Electrotechnical Commission publication 268: *Sound System Equipment Part 16: The objective rating of speech intelligibility in auditoria by the "RASTI" method*

Jackson, I, 1995, Linux Frequently Asked Questions With Answers, [CDROM] InfoMagic, *Developer's resource*, August 1995] from: disc1/docs/faqs/linux-faq/linux-faq.ascii

Jordan, V.L, 1970, 'Acoustical criteria for auditoriums and their relation to model techniques', *Journal Acoustic Society America*, vol. 47, no. 2, pp408-412

Jordan, V.L, 1975, 'Model studies with particular reference to the Sydney Opera house - Evaluation of objective tests of 'Acoustics' of models and halls' in *Auditorium acoustics*, Ed. Mackenzie, R, Applied Science Publishers, London, pp55-72

Jordan, V.L, 1980, *Acoustical design of Concert Halls and Theatres*, Applied Science Publishers, London

Kindle, J.H, 1950, *Schaum's Outline of Theory and Problems of Plane and Solid Analytic Geometry*, McGraw-Hill, New York

Kristiansen, U.R, Krokstad, A and Follestad, T, 1993, Extending the image method to higher-order reflections, *Applied Acoustics*, vol. 38, pp195-206

Knudsen, V.O, 1929, 'The hearing of speech in auditoriums', *Journal Acoustic Society America*, vol. 1 October, pp56-78 in *Benchmark Papers in Acoustics: Architectural Acoustics*, Ed. Northwood, T.D, 1977, Dowden, Hutchinson and Ross, Stroudsburg, pp26-41

Kryter, K.D, 1962a, 'Methods for the calculation and use of the articulation index', *Journal Acoustic Society America*, vol. 34, no. 11, pp1689-1697

Kryter, K.D, 1962b, 'Validation of the Articulation Index', *Journal Acoustic Society America*, vol. 34, no. 11, pp1698-1702

Kulowski, A, 1992, 'Optimization of a point-in-polygon algorithm for computer models of sound field in rooms', *Acoustics*, vol. 35, pp63-74

Kuttruff, H, 1991 *Room Acoustics*, Elsevier Applied Science, London 3rd edition

Kuttruff, H, 1994, 'On the Acoustics of Auditoria', *Building Acoustics*, vol. 1, no. 1, pp27-48

Lee, H and Lee, B-H, 1988, 'An efficient algorithm for the image model technique', *Applied Acoustics*, vol. 24, pp87-115

Lehnert, H, 1993, 'Systematic errors of the ray-tracing algorithm', *Applied Acoustics*, vol. 38 pp207-221

Maekawa, Z, 1975, 'Problems of sound reflection in rooms', in *Auditorium acoustics*, Ed. Mackenzie, R, Applied Science Publishers, London, pp181-196

Marsh, A.J. and Carruthers, D.D, 1992, The predictive capacity of ray traced acoustic models, *Proceedings of the 26th Australian and New Zealand Architectural Science Association*, Perth, pp82-91

Marshall, A.H, 1990, Recent developments in acoustical design process, *Applied Acoustics*, vol. 31 pp7-28

Meyer, E and Thiele, R, 1956, Raumakustische untersuchungen in zahlreichen konzertsälen und rundfunkstudios unter anwendung neuerer messverfahren, *Acustica,* vol. 6 pp425-444 in *Benchmark Papers in Acoustics: Architectural Acoustics*, Ed. Northwood, T.D, 1977, Dowden, Hutchinson and Ross, Stroudsburg, pp181-199 plus English summary 'Acoustical investigations in numerous concert halls and broadcast studios using new measurement techniques, pp200-205

Newman, W.M. and Sproull, R.F, 1973, *Principles of Interactive Computer Graphics,* McGraw-Hill Kogakusha, Limited, Tokyo.

Northwood, T.D (Ed.), 1977, *Benchmark Papers in Acoustics Vol. 10: Architectural acoustics,* Dowden, Hutchinson and Ross, Stroudsburg

Parkin, P.H. and Humphreys, H.R, 1958, *Acoustics, Noise and Buildings,* Faber and Faber, London

Plomp, R, Steeneken, H.J.M. and Houtgast, T, 1980, 'Predicting Speech Intelligibility in Rooms from the Modulation Transfer Function. II. Mirror Image Computer Model Applied to Rectangular Rooms', *Acustica,* vol. 46, pp73-81

Rayleigh, 1945, *The Theory of Sound Vol. II,* Dover, New York

Rietschote, H.F. Van, Houtgast, T, Steeneken, H.J.M, 1981, 'Predicting Speech Intelligibility in Rooms from the Modulation Transfer Function. IV. A Ray-Tracing Computer Model', *Acustica*, vol. 49, pp245-252

Rietschote, H.F. Van, Houtgast, T, 1983, 'Predicting Speech Intelligibility in Rooms from the Modulation Transfer Function. V, The Merits of the Ray-tracing Model Versus General Room Acoustics', *Acustica,* vol. 53, pp72-78

Rindel, J.H. 1995, 'Computer simulation techniques for acoustical design of rooms', *Australian Acoustical Society*; vol. 23, no. 3, pp81-6

Rogers, D.F. and Adams, J. A, 1976, *Mathematical Elements for Computer Graphics,* McGraw-Hill Book Company, New York.

Sabine, W.C, 1900, Reverberation, *The American Architect*, in *Collected Papers on Acoustics,* 1964, Dover, New York, pp.3-68

Sabine, W.C, 1913, Theatre Acoustics, *The American Architect*, vol. CIV, p. 257, in *Collected papers on acoustics*, 1964, Dover, New York, pp.163-198

Salmon, R. and Slater, M, 1987, *Computer Graphics: Systems and Concepts,* Addison-Wesley, Wokingham, England.

Schroeder, M.R, 1965, 'New method of measuring reverberation time', *Journal Acoustic Society America,* vol. 37, pp409-412

Schroeder, M.R, 1979, 'Integrated-impulse method measuring sound decay without using impulses', *Journal Acoustic Society America,* vol. 66, no. 2, pp497-500

Schroeder, M.R, Gottlieb, D. And Siebrasse, K.F, 1974, 'Comparative study of European concert halls: Correlation of subjective preference with geometric and acoustic parameters', *Journal Acoustic Society America,* vol. 56, pp1195

Schmidt-Nielsen, A, 1987, 'Comments on the use of physical measures to assess speech intelligibility', *Journal Acoustic Society America,* vol. 81, no. 6, pp1985-1987

Standards Association of Australian, 1987, *AS 2107 - 1987: Acoustics - Recommended design sound levels and reverberation times for Building Interiors,* Standards Association of Australia

Standards Association of Australian, 1988, *AS 1045-1988: Acoustics: Measurement of Sound Absorption in a Reverberation Room,* Standards Association of Australia

Steeneken, H.J.M, Agterhuis, E, 1982, 'Device for measuring the Speech Transmission Index', *Journal Acoustic Society America,* vol. 71, no. 6, pp1612

Steeneken, H.J.M, Houtgast, T, 1980, 'A physical method for measuring speech-transmission quality', *Journal Acoustic Society America,* vol. 67, no. 1, pp318-326

Steeneken, H.J.M, Houtgast, T, 1985, 'RASTI: A tool for evaluating Auditoria', *Technical Review* No. 3, Brüel and Kjær, Denmark, pp13-30

Stephenson, U, 1990, 'Comparison of the mirror image source method and the sound particle simulation method', *Applied Acoustics,* vol. 29, pp35-72

*TesSeRact TCXL User Interface Development System,* 1991, (DOS version 5.52) [Computer Program], Innovative Data Concepts, Hatboro, PA

Vian, J.P and Van Maercke, D, 1985, 'Computer simulation of auditorium acoustics', *Proceedings of the Institute of Acoustics,* Cambridge

Vorländer, M, 1989, 'Simulation of the transient and steady-state sound propagation in rooms using a new combined ray-tracing/image-source algorithm', *Journal Acoustic Society America,* vol. 86, no. 1, p172

Ward, G, 1995, *Radiance*, (Version 2.5) [Computer Program], Lawrence Berkeley National Laboratory, Berkeley

Wattel, E, Plomp, R, Rietschote, H.F. van and Steeneken, H.J.M, 1981, 'Predicting Speech Intelligibility in Rooms from the Modulation Transfer Function. III. Mirror Image Computer Model Applied to Pyramidal Rooms', *Acustica*, vol. 48, pp320-324

Welsh, M, 1995, The Linux XFree86 HOWTO, [CDROM] InfoMagic, *Developer's resource*, August 1995] from: disc1/HOWTO/XFree86-HOWTO

# Appendices

# *Appendix 1 Reverberation Calculations*

Curtin University Lecture Theatre Building 201 Room 412

| Description | Other | 125 | 250 | 500 | 1 K | 2 K | 4 K |
|---|---|---|---|---|---|---|---|
| Volume | 308.0 | | | | | | |
| ***SIDE WALL PAIR*** Surface Area (sq. m) | 97.85 | | | | | | |
| Dist. between surfaces | 7.20 | | | | | | |
| Ply Panel | 83.83 | 0.20 | 0.28 | 0.26 | 0.09 | 0.12 | 0.11 |
| Perforated Ply Panel | 14.02 | 0.20 | 0.28 | 0.26 | 0.09 | 0.12 | 0.11 |
| *Air absorption* | *96.25* | | | | *0.003* | *0.007* | *0.020* |
| | | | | | | | |
| ***FLOOR CEILING PAIR*** Surface Area (sq. m) | 162.9 | | | | | | |
| Dist. between surfaces | 4.09 | | | | | | |
| Floor - carpet | 78.88 | 0.05 | 0.08 | 0.20 | 0.30 | 0.35 | 0.40 |
| Ceiling - plaster | 64.48 | 0.02 | 0.03 | 0.04 | 0.06 | 0.06 | 0.03 |
| Ceiling - Ply | 13.57 | 0.20 | 0.28 | 0.26 | 0.09 | 0.12 | 0.11 |
| *Air absorption* | *54.67* | | | | *0.003* | *0.007* | *0.020* |
| | | | | | | | |
| ***END WALL PAIR*** Surface Area (sq. m) | 61.13 | | | | | | |
| Dist. between surfaces | 11.75 | | | | | | |
| Chalkboard | 16.00 | 0.20 | 0.28 | 0.26 | 0.09 | 0.12 | 0.11 |
| Upper screen - plaster | 6.46 | 0.02 | 0.03 | 0.04 | 0.06 | 0.06 | 0.03 |
| Rear wall - Perf. ply | 20.23 | 0.16 | 0.47 | 0.87 | 0.86 | 0.63 | 0.58 |
| Stair Risers - carpet | 18.43 | 0.05 | 0.08 | 0.20 | 0.30 | 0.35 | 0.40 |
| *Air absorption* | *157.0* | | | | *0.003* | *0.007* | *0.020* |
| ***REVERBERATION RESULTS*** | | | | | | | |
| RT Sabine | | 1.42 | 0.90 | 0.68 | 0.78 | 0.72 | 0.68 |
| RT Eyring | | 1.34 | 0.82 | 0.60 | 0.71 | 0.64 | 0.60 |
| RT Arau-Puchades | | 1.63 | 1.00 | 0.66 | 0.80 | 0.69 | 0.64 |
| RT Fitzroy - Sabine | | 2.07 | 1.34 | 0.83 | 1.01 | 0.83 | 0.79 |
| RT Fitzroy - Eyring | | 1.99 | 1.26 | 0.75 | 0.94 | 0.75 | 0.71 |
| Side Wall | | 0.21 | 0.14 | 0.16 | 0.48 | 0.35 | 0.34 |
| Floor/Ceiling | | 1.56 | 1.02 | 0.54 | 0.40 | 0.34 | 0.31 |
| End Wall | | 0.22 | 0.10 | 0.05 | 0.06 | 0.06 | 0.06 |
| ***MEAN ABSORPTION:UNIFORM*** | | 0.11 | 0.17 | 0.23 | 0.20 | 0.21 | 0.23 |
| Abs. Side Walls + | 97.85 | 19.57 | 27.40 | 25.44 | 9.10 | 12.42 | 12.69 |
| Abs. Floor/Ceiling + | 162.9 | 7.95 | 12.04 | 21.88 | 28.92 | 33.49 | 36.07 |
| Abs. Front/Rear walls + | 61.13 | 7.49 | 15.66 | 25.70 | 25.23 | 22.60 | 24.20 |
| Abs. all surfaces | 321.8 | 35.01 | 55.10 | 73.03 | 63.24 | 68.51 | 72.96 |
| ***MEAN ABS.:NON UNIFORM*** | | 0.09 | 0.15 | 0.23 | 0.19 | 0.22 | 0.24 |
| Abs. Side Walls x | | 0.63 | 0.71 | 0.69 | 0.49 | 0.54 | 0.55 |
| Abs. Floor/Ceiling x | | 0.22 | 0.27 | 0.38 | 0.44 | 0.48 | 0.50 |
| Abs. Front/Rear walls x | | 0.68 | 0.79 | 0.89 | 0.89 | 0.86 | 0.88 |

# *Appendix 2 Two Dimensional Ray Trace*

Jobname : Curtin University Lecture Theatre Building 201 Room 412
Comment : Longitudinal Section

STATISTICAL SIMULATION SUMMARY

Useful rays over the audience surfaces [5 to 17] = 140 of 360 rays

Useful Energy Ratio = 0.3889

| Rows | 1 | 2 | 3 | 4 | 5 | 6 | 7 | 8 |
|---|---|---|---|---|---|---|---|---|
| No. of Rays | 9 | 9 | 11 | 12 | 15 | 20 | 30 | 34 |
| No. of Rays > 30ms | | 1 | | | 1 | 1 | 1 | 2 |

Number of faces = 24
Source X coordinates = 1.5000 and Y coordinates 0.9000

| X | Y | Number of Reflections | Length | Face Angle | Source Angle |
|---|---|---|---|---|---|
| 0.0000 | 3.3900 | 1 | 2.7255 | 16.7395 | 121.0652 |
| 2.6100 | 4.1750 | 1 | 0.8976 | 77.1250 | 71.2769 |
| 2.8100 | 5.0500 | 1 | 8.9500 | 0.0000 | 72.4810 |
| 11.7600 | 5.0500 | 1 | 2.8100 | 270.0000 | 22.0225 |
| 11.7600 | 2.2400 | | 2.4900 | 180.0000 | 7.4410 |
| 9.2700 | 2.2400 | | 0.3200 | 270.0000 | 9.7849 |
| 9.2700 | 1.9200 | | 0.8400 | 180.0000 | 7.4787 |
| 8.4300 | 1.9200 | | 0.3200 | 270.0000 | 8.3730 |
| 8.4300 | 1.6000 | | 0.8400 | 180.0000 | 5.7679 |
| 7.5900 | 1.6000 | | 0.3200 | 270.0000 | 6.5569 |
| 7.5900 | 1.2800 | | 0.8400 | 180.0000 | 3.5705 |
| 6.7500 | 1.2800 | | 0.3200 | 270.0000 | 4.1399 |
| 6.7500 | 0.9600 | | 0.8400 | 180.0000 | 0.6548 |
| 5.9100 | 0.9600 | | 0.3200 | 270.0000 | 0.7795 |
| 5.9100 | 0.6400 | | 0.8400 | 180.0000 | 356.6259 |
| 5.0700 | 0.6400 | | 0.3200 | 270.0000 | 355.8346 |
| 5.0700 | 0.3200 | | 0.8400 | 180.0000 | 350.7721 |
| 4.2300 | 0.3200 | | 0.3200 | 270.0000 | 348.0056 |
| 4.2300 | 0.0000 | | 2.4300 | 180.0000 | 341.7541 |
| 1.8000 | 0.0000 | 1 | 0.6901 | 89.1697 | 288.4349 |
| 1.8100 | 0.6900 | 1 | 0.6100 | 180.0000 | 325.8855 |
| 1.2000 | 0.6900 | 1 | 0.6900 | 270.0000 | 214.9920 |
| 1.2000 | 0.0000 | 1 | 1.2000 | 180.0000 | 251.5651 |
| 0.0000 | 0.0000 | | 3.3900 | 90.0000 | 210.9638 |

DISCRETE RAY TRACE

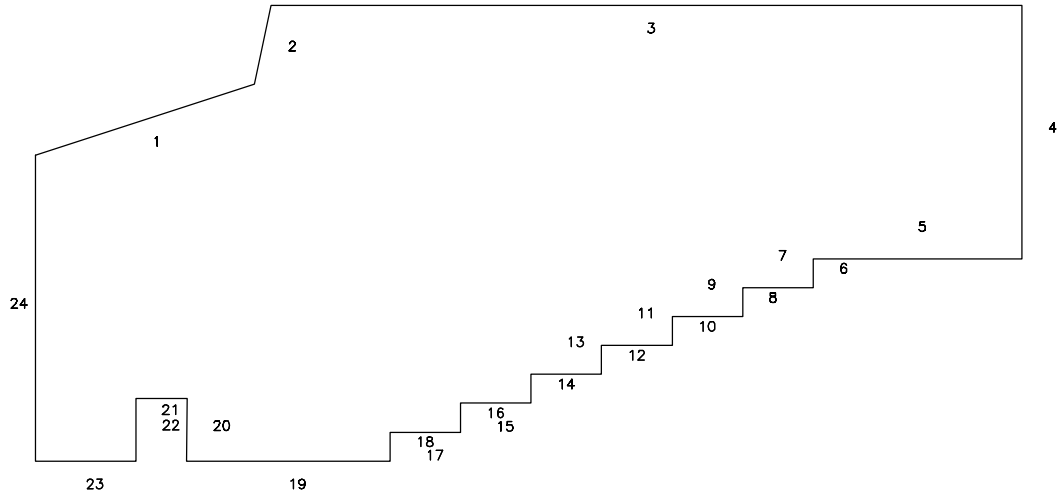


Curtin University Lecture Theatre
Building 201 Room 412
Longitudinal Section

Start End angles and Number of angles
-15.0000 180.0000 26

Offset for start of ray = 0.0200
Maximum number of hits = 1

| Ray No. | Angle Deg. | Co-ords of Point X | Y | Dir.Path Metres | Refl. Path Metres | Diff. Metres | Time Delay Milli-secs | Surfaces Hit During Path |
|---|---|---|---|---|---|---|---|---|
| 1 | -13.0 | 4.23 | 0.17 | 2.83 | 2.83 | 0.00 | 0.00 | 18 |
| 2 | -7.5 | 5.07 | 0.43 | 3.60 | 3.60 | 0.00 | 0.00 | 16 |
| 3 | 0.0 | 5.91 | 0.90 | 4.41 | 4.41 | | | 14 |
| 4 | 7.5 | 8.43 | 1.81 | 6.99 | 6.99 | 0.00 | 0.00 | 8 |
| 5 | 15.0 | 6.53 | 5.05 | 6.52 | 16.03 | 9.51 | 27.57 | 4,3 |
| 6 | 22.5 | 11.76 | 4.95 | 11.03 | 11.11 | 0.07 | 0.22 | 3,4 |
| 7 | 30.0 | 11.76 | 3.28 | 10.53 | 11.85 | 1.32 | 3.81 | 3,4 |
| 8 | 37.5 | 10.57 | 2.24 | 9.17 | 11.43 | 2.26 | 6.56 | 3,5 |
| 9 | 45.0 | 8.78 | 1.92 | 7.35 | 10.30 | 2.94 | 8.53 | 3,7 |
| 10 | 52.5 | 7.58 | 1.28 | 6.09 | 9.98 | 3.89 | 11.29 | 3,11 |
| 11 | 60.0 | 6.26 | 0.96 | 4.76 | 9.51 | 4.76 | 13.79 | 3,13 |
| 12 | 67.5 | 5.07 | 0.58 | 3.58 | 9.33 | 5.74 | 16.65 | 3,16 |
| 13 | 75.0 | 5.91 | 0.95 | 4.41 | 8.06 | 3.65 | 10.57 | 1,14 |
| 14 | 82.5 | 5.07 | 0.32 | 3.61 | 7.91 | 4.30 | 12.46 | 1,17 |
| 15 | 90.0 | 4.04 | 0.00 | 2.70 | 7.55 | 4.85 | 14.06 | 1,19 |
| 16 | 97.5 | 2.94 | 0.00 | 1.70 | 7.00 | 5.30 | 15.36 | 1,19 |
| 17 | 105.0 | 1.75 | 0.69 | 0.33 | 5.91 | 5.58 | 16.18 | 1,21 |
| 18 | 112.5 | 1.10 | 0.00 | 0.99 | 6.41 | 5.43 | 15.73 | 1,23 |
| 19 | 120.0 | 0.26 | 0.00 | 1.53 | 6.31 | 4.77 | 13.84 | 1,23 |
| 20 | 127.5 | 0.00 | 2.85 | 2.46 | 2.46 | 0.00 | 0.00 | 24 |
| 21 | 135.0 | 0.00 | 2.40 | 2.12 | 2.12 | | | 24 |
| 22 | 142.5 | 0.00 | 2.05 | 1.89 | 1.89 | | | 24 |
| 23 | 150.0 | 0.00 | 1.77 | 1.73 | 1.73 | 0.00 | 0.00 | 24 |
| 24 | 157.5 | 0.00 | 1.52 | 1.62 | 1.62 | 0.00 | 0.00 | 24 |
| 25 | 165.0 | 0.00 | 1.30 | 1.55 | 1.55 | 0.00 | 0.00 | 24 |
| 26 | 172.5 | 0.00 | 1.10 | 1.51 | 1.51 | 0.00 | 0.00 | 24 |
| 27 | 180.0 | 0.00 | 0.90 | 1.50 | 1.50 | 0.00 | 0.00 | 24 |

DISCRETE RAY TRACE

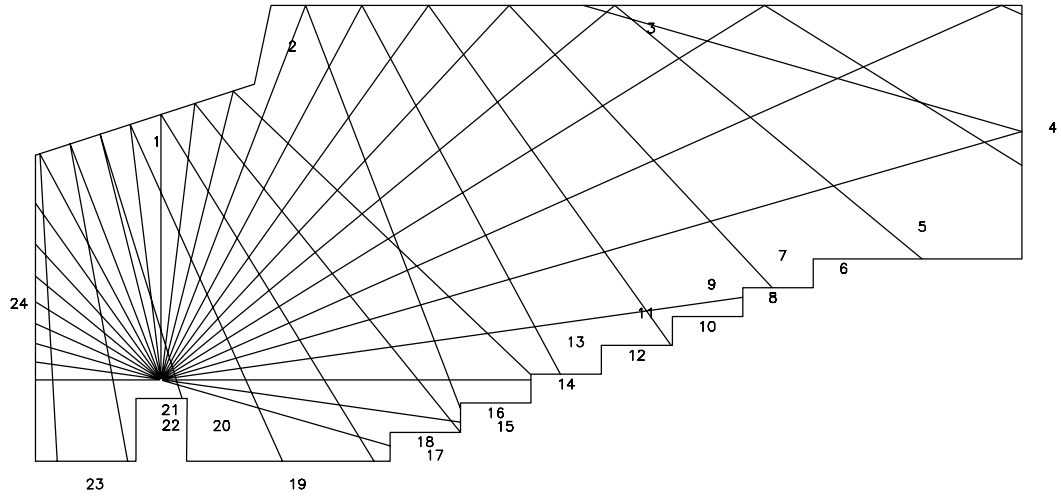


Curtin University Lecture Theatre
Building 201 Room 412
Longitudinal Section

# *Appendix 3 Sight Lines*

PROJECT : Curtin University Lecture Theatre Building 201 Room 412
Longitudinal Section

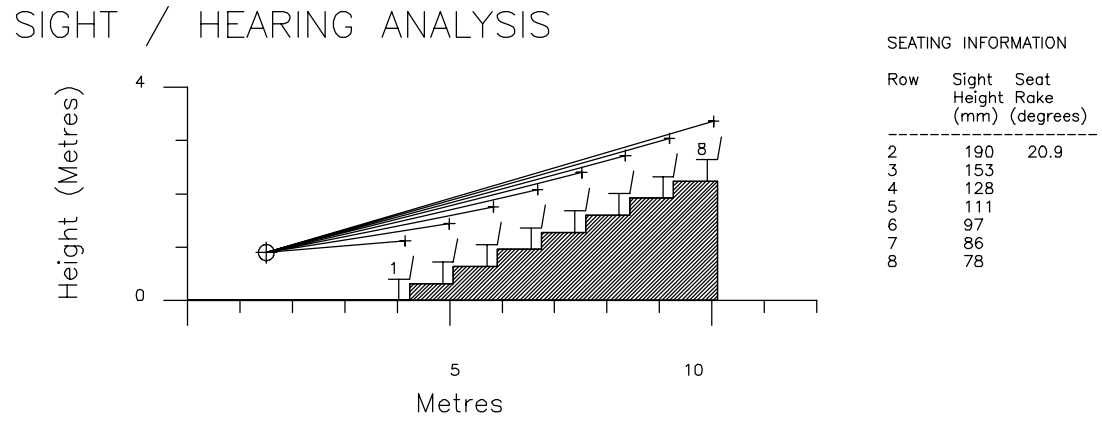


Curtin University Lecture Theatre
Building 201 Room 412
Longitudinal Section

| Desc. | Row | Coordinate data X (M) | Y (M) | Sight Height (mm) | Seat Rake (Degrees) |
|---|---|---|---|---|---|
| Focus | | 1.500 | 0.900 | | |
| Chair | 1 | 4.155 | 1.120 | | |
| | 2 | 4.995 | 1.440 | 190 | 20.9 |
| | 3 | 5.835 | 1.760 | 153 | |
| | 4 | 6.675 | 2.080 | 128 | |
| | 5 | 7.515 | 2.400 | 110 | |
| | 6 | 8.355 | 2.720 | 96 | |
| | 7 | 9.195 | 3.040 | 86 | |
| | 8 | 10.035 | 3.360 | 77 | |

| Description | Rows | Tread | Riser | Number | Nosing Coordinates | |
|---|---|---|---|---|---|---|
| | | | | | X | Y |
| Chair | 1 - 7 | 0.840 | 0.320 | 7 | 3.390 | |
| Chair | 8 | 0.840 | 0.320 | 1 | 9.270 | 2.240 |

# *Appendix 4 Calculation of the Integrating Impulse Response Method*

The methodology involved in computing the Schroeder (1965) Integrating Impulse Method is as follows:

i) Sum all the sound pressure levels from time 0 to infinity (normally several seconds is sufficient (Schroeder 1965, p410).

$$P_0 = \sum_{t=0}^{\infty} 10^{\left(P_t/10\right)} \qquad \{\text{Eq Appendix 4.1}\}$$

ii) For each value of $P_t$ from 1 to ∞ assign $P_t$ the result of the $P_{t-1}$ less the pressure $P_t$

$$P_t = P_{t-1} - 10^{\left(P_t/10\right)} \qquad \{\text{Eq Appendix 4.2}\}$$

iii) The decay pressure curve can be converted back to a logarithmic amplitude scale only when the reverberation signal exceeds the background noise (Schroeder 1965, p411).

$$P_t = 10Log_{10}\left(P_t\right) \qquad \{\text{Eq Appendix 4.3}\}$$

# *Appendix 5 Simulation Times*

To provide longer duration for the ray simulations (larger number of reflections), a sub program omitting the graphical interface and implementing parameters to control the execution of the program was developed. This program (r3dc the 'c' being for crunching) utilises the same source code files as the main application (R3d).

To cater for the different computing environments (non MS-DOS, non Microsoft Windows and non Borland C++ compiler) the source files have been modified using compiler directives. (See Example Appendix 5.1). This allows the same code to be used in all cases.

Example Appendix 5.1 Compiler Directives

```
#ifdef __BORLANDC__
#include   <alloc.h>
#endif
```

Where the directive *__BORLANDC__* is predefined by the compiler. In this example, if the code was compiled using the Borland C++ compiler, then the *#include* line would be included. For other compilers, where *__BORLANDC__* is undefined, then the *#include* line of code is dropped or treated as simply a comment.

The advantage of using pre-defined compiler directives, is that the code files can be compiled for different systems without change. The compilation is controlled by embedded statements specific to that system. The major differences between systems and compilers can be generally limited to the graphic sub system (all graphics is restricted to the Microsoft Windows environment) and minor changes due to memory handling under various compilers and operating systems. The major code, data and file handling is common on all platforms.

Both the Unix and Linux systems used the Gnu C++ compiler, which, like Linux is freely available and runs on most flavours of Unix. This compiler was chosen for these environments as it provided a more consistent platform for comparison purposes, than the propriety brand compilers.

## *Speed Comparisons*

The following tests were conducted to determine the relative processing speeds of computer hardware and operating system environments.

Test one and two used specific PC machines to compare different environments. Test three uses graphic workstations, which had a number of processes running:

i) Microsoft Windows / Windows For Workgroups (WFW version 3.11).
i) MS-DOS with no DOS memory extenders.
i) Linux and X Windows.
i) Linux with no graphical Windows.

Linux is another operating system (in place of MS-DOS) which runs on the PC yet functions like Unix.

> *"Linux is a Unix clone written from scratch by Linus Torvalds with assistance from a loosely-knit team of hackers across the Net. It aims towards POSIX compliance.*
>
> *It has all the features you would expect in a modern fully-fledged Unix, including true multitasking, virtual memory, shared libraries, demand loading, shared copy-on-write executables, proper memory management and TCP/IP networking.*
>
> *It runs mainly on 386/486/586-based PCs, using the hardware facilities of the 386 processor family (TSS segments et al) to implement these features.*
>
> *Ports to other architectures are underway…*
>
> *The Linux kernel is distributed under the GNU General Public License"* (Jackson, 1995)

X Windows is a graphical user interface used in conjunction with the Unix operating system.

> *"The X Window System is a large and powerful (and somewhat complex) graphics environment for UNIX systems. The original X Window System code was developed at MIT; commercial vendors have since made X the industry standard for UNIX platforms. Virtually every UNIX workstation in the world runs some variant of the X Window system."* (Welsh, 1995)

Data file lee10n.scr
Ray Depth 5
Machine PC - Dalcon DX2-66 486 with 8mb of memory.
Swap files were not required.
Hard Disk Disk Utilisation Not considered a bottleneck as there is very limited access - sequential reading of the data file and limited output of the rays data - common to all processes.

Table Appendix 5.1 DX2-66 486

| Platform | Windows | MS-DOS | Linux | Linux |
|---|---|---|---|---|
| Options | (WFW3.11) | | X Windows | |
| Compiler | Borlandc 3.1 | Borlandc 3.1 | GCC 2.0 | GCC 2.6.3 |
| Program | r3d.exe | r3dc.exe | r3dc_ol | r3dc_ol |
| Duration (hh:mm:ss) | 00:30:32 | 00:12:50 | 00:04:55 | 00:05:07 |
| Rays Processed | 1091362 | 1091362 | 1091362 | 1091362 |
| Rays/Second | 648 | 1543 | 4028 | 3870 |

Machine PC - Dalcon DX4-100 486 with 8mb of memory.
Swap files were not required.
Hard Disk Disk Utilisation Not considered a bottleneck as there is very limited access - sequential reading of the data file and limited output of the rays data - common to all processes.

Table Appendix 5.2 DX4-100 486

| Platform | Windows | MS-DOS | Linux | Linux |
|---|---|---|---|---|
| Options | (WFW3.11) | | X Windows | |
| Compiler | Borlandc 3.1 | Borlandc 3.1 | GCC 2.6.3 | GCC 2.6.3 |
| Program | r3d.exe | r3dc.exe | r3dc_ol | r3dc_ol |
| Duration (hh:mm:ss) | 00:20:10 | 08:50 | 02:56 | 02:54 |
| Rays Processed | 1091362 | 1091362 | 1091362 | 1091362 |
| Rays/Second | 982 | 2242 | 6752 | 6829 |

Table Appendix 5.3 Unix Work Stations

| Machine | Sun Sparc Stations | Sun Sparc | Silicon Graphics IRIS (MIPS) |
|---|---|---|---|
| Compiler | GCC 1 | GCC 2.6.3 | GCC |
| Machine / Platform | gull IPC | gannet IPX | Ambrose MIPS R4400 |
| Program | r3dc_ol | r3dc_ol | r3dc_ol |
| Duration (hh:mm:ss) | 09:36:31 | 00:20:17 | 00:02:10 |
| Rays Processed | 33658412 | 1188386 | 1188386 |
| Rays/Second | 973 | 976 | 9141 |

One rationale for the apparent efficiencies of X Windows compared to the MSDOS Windows environment is that X Windows uses less operating system overheads. It sends less messages to the software applications. This in turn allows more processing for a given application.

# Appendix 6 File Formats

The program *R3d* has two major file types:

i) The Geometry file *(scr)* and

ii) The ray path file *(ray)*

## Geometry File Format

The Geometry data file follows the AutoCAD© script format using the "PFACE" command to describe each surface's coordinates. "LAYER" commands are used to allow further description of the surfaces absorption data.

As can be seen in Table Appendix 6.2, all data is stored in AutoCAD© layers. Each plane is a separate layer. All absorption data is stored as text, at the plane's first vertex position. All absorption data is contained within the one layer *ABSORB_DATA*.

NB: Layer names within AutoCAD© cannot contain spaces, there *R3d* substitutes a '_' character.

Unfortunately, with AutoCAD© script files, they can only be read. Therefore the geometry file can be considered as a one way path to AutoCAD©.

## Ray File Format

The Ray file format is a simple ASCII text file. Each data line consists of a variable number of fields separated by commas.

i) Ray distance

ii) Number of surface intersected by the ray (integer). Also known as the ray depth

iii) If the ray depth is greater than zero:

A list of surface numbers intersected, inside a pair of square braces (space separated).

iv) The X, Y, Z location of the Receiver

v) All surface intersection X, Y, Z points
vi) The X, Y, Z location of the Source

The file layout can be seen in Table Appendix 6.3. When the statistics module has been run this file is sorted. An addition line *#00Sorted* is added at the beginning of the file.

The sorting algorithm *sort_file*, modified from Allison's (1993) program *esort.c*, is a file based sort process. If the number of lines of data are less than 1000, or there is limited memory, then the sort is done in memory, otherwise the sort module sub-divides the file into a maximum of 15 sub files; which it then sorts and finally merges into a single file. The *C Users* original algorithm has been altered in the following manner:

i) Converted to use files for input and output rather than the stdin and stdout
ii) Use data structures
iii) Sort on numeric fields rather than a line of text
iv) Add sort indicator to output file
v) Make temporary sort file the same name as the original data file

Sorting of the ray file may take place in two different places. In the *R3d* the sort takes place as the first step in statistics module, if there is no line *#00Sorted* as the first line of the data file. In the *R3dc* program, the sorting takes place immediately after normal calculation of the rays. The sorted file is in ray length order.

NB: The ray file must have read/write attributes, as the sorting process creates a temporary file (on the current disk/directory) to store the sorted data, deletes the original file (after finishing the sort) and then renames the sorted file to the same name as the original ray file.

There are a number of comments which may appear in the ray file. Comments are included by using the '#' symbol in column 1. These are not critical, but are intended to

Table Appendix 6.1 Ray File Comment Codes

| | |
|---|---|
| #01 | Ray Path start time |
| #02 | Ray Path finish time |
| #03 | Calculation Duration |
| #04 | Number of Possible Reflections |
| #05 | Ray Depth |
| #06 | Number of Calculated Reflections |
| #07 | Number of Rays Processed |
| #08 | Calculation Speed (Rays/Second) |
| #09 | User Aborted Ray Trace or<br>System Aborted Ray Trace |
| #10 | Farm process<br>When the ray path calculations are spread over a number of computers, then the process is divided into sub tasks by surface number. This is intended to be implemented in a *UNIX* type network. |

Table Appendix 6.2 Sample of a partial geometry file layout

```
LAYER
MAKE
ABSORB_DATA

TEXT
0.000000,20.000000,30.000000


ABSORB 125 HZ: 0.10, 250 HZ: 0.20, 500 HZ: 0.30, 1K HZ: 0.40, 2K HZ: 0.50, 4K HZ: 0.60
LAYER
MAKE
Side_Wall_2

pface
0.000000,20.000000,30.000000
40.000000,20.000000,25.000000
40.000000,20.000000,0.000000
0.000000,20.000000,0.000000

1
2
3
4


LAYER
MAKE
RECEIVER_LOCATIONS

POINT
10.00,34.00,1.00
POINT
10.00,15.00,1.00
LAYER
MAKE
SOURCE_LOCATIONS

POINT
10.00,34.00,1.00
POINT
10.00,15.00,1.00
```

NB: The blank lines are critical.

Table Appendix 6.3 Sample of a partial ray file layout

| | |
|---|---|
| #01Start Time: | Thu Oct 10 15:49:58 1996 |
| #04Number of Possible Reflections: | 1188386 |
| #05Ray Depth: | 5 |
| #10Farm Process: Surface Number | 1 |
| 28.5,0,28.7,5,8.2,1.6,2.1,0 | |
| 29.0,1,[1],28.7,5,8.2,21.6,6.6,6.1,1.6,2.1,0 | |
| 31.7,1,[3],28.7,5,8.2,22.1,4.2,12.1,1.6,2.1,0 | |
| . | |
| . | |
| . | |
| 24.3,4,[1 3 17 1],28.7,5,8.2,26.5,6.6,9.5,22.1,3.5,12.1,17.2,0,9.2,7.9,6.6,3.7,1.6,2.1,0 | |
| #02Finish Time: | Mon Oct 10 15:50:19 1994 |
| #03Duration: | 00:00:21 |
| #06Number of Calculated Reflections: | 69 |
| #07Number of Rays Processed: | 8738 |
| #08User Aborted Ray Trace | |

# *Appendix 7 Simulation Geometric Data*

## Case Study 1

### *Input Geometric Data*

Note: The volume and surface areas are computed by the program.

The dimensional data is in metres.

Surface 1: Screen Wall - Chalkboard

| Vertex data | X | Y | Z |
|---|---|---|---|
| | 0.000 | 0.000 | 1.271 |
| | 0.000 | 3.391 | 1.271 |
| | 0.000 | 3.391 | 5.774 |
| | 0.000 | 0.000 | 5.774 |

Surface 2: Screen Left - Ply

| Vertex data | X | Y | Z |
|---|---|---|---|
| | 0.000 | 0.000 | 1.271 |
| | 2.610 | 0.000 | 0.990 |
| | 2.610 | 3.886 | 0.990 |
| | 0.000 | 3.391 | 1.271 |

Surface 3: Screen Right - Ply

| Vertex data | X | Y | Z |
|---|---|---|---|
| | 0.000 | 0.000 | 5.774 |
| | 0.000 | 3.391 | 5.774 |
| | 2.610 | 3.886 | 6.055 |
| | 2.610 | 0.000 | 6.055 |

Surface 4: Screen Ceiling - Ply

| Vertex data | X | Y | Z |
|---|---|---|---|
| | 0.000 | 3.391 | 1.271 |
| | 2.610 | 3.886 | 0.990 |
| | 2.610 | 3.886 | 6.055 |
| | 0.000 | 3.391 | 5.774 |

Surface 5: Upper Screen - Plaster

| Vertex data | X | Y | Z |
|---|---|---|---|
| | 2.610 | 3.886 | 0.000 |
| | 2.810 | 5.486 | 0.000 |
| | 2.810 | 5.486 | 7.045 |
| | 2.610 | 3.886 | 7.045 |

Surface 6: Ceiling - Plaster

| Vertex data | X | Y | Z |
|---|---|---|---|
| | 2.810 | 5.486 | 0.000 |
| | 11.765 | 5.144 | 0.000 |
| | 11.765 | 5.144 | 7.045 |
| | 2.810 | 5.486 | 7.045 |

Surface 7: Front Left Screen - Ply

| Vertex data | X | Y | Z |
|---|---|---|---|
| | 2.610 | 0.000 | 0.000 |
| | 2.610 | 3.886 | 0.000 |
| | 2.610 | 3.886 | 0.990 |
| | 2.610 | 0.000 | 0.990 |

Surface 8: Front Right Screen - Ply

| Vertex data | X | Y | Z |
|---|---|---|---|
| | 2.610 | 0.000 | 7.045 |
| | 2.610 | 0.000 | 6.055 |
| | 2.610 | 3.886 | 6.055 |
| | 2.610 | 3.886 | 7.045 |

Surface 9: Wall - Left Ply

| Vertex data | X | Y | Z |
|---|---|---|---|
| | 2.610 | 0.000 | 0.000 |
| | 4.286 | 0.000 | 0.000 |
| | 4.286 | 0.318 | 0.000 |
| | 5.124 | 0.318 | 0.000 |
| | 5.124 | 0.648 | 0.000 |
| | 5.962 | 0.648 | 0.000 |
| | 5.962 | 0.991 | 0.000 |
| | 6.800 | 0.991 | 0.000 |
| | 6.800 | 1.347 | 0.000 |
| | 7.638 | 1.347 | 0.000 |
| | 7.638 | 1.715 | 0.000 |
| | 8.476 | 1.715 | 0.000 |
| | 8.476 | 2.096 | 0.000 |
| | 9.314 | 2.096 | 0.000 |
| | 9.314 | 5.241 | 0.000 |
| | 2.810 | 5.486 | 0.000 |
| | 2.610 | 3.886 | 0.000 |

Surface 10: Wall - Right Ply

| Vertex data | X | Y | Z |
|---|---|---|---|
| | 2.610 | 0.000 | 7.045 |
| | 2.610 | 3.886 | 7.045 |
| | 2.810 | 5.486 | 7.045 |
| | 9.314 | 5.241 | 7.045 |
| | 9.314 | 2.096 | 7.045 |
| | 8.476 | 2.096 | 7.045 |
| | 8.476 | 1.715 | 7.045 |
| | 7.638 | 1.715 | 7.045 |
| | 7.638 | 1.347 | 7.045 |
| | 6.800 | 1.347 | 7.045 |
| | 6.800 | 0.991 | 7.045 |
| | 5.962 | 0.991 | 7.045 |
| | 5.962 | 0.648 | 7.045 |
| | 5.124 | 0.648 | 7.045 |
| | 5.124 | 0.318 | 7.045 |
| | 4.286 | 0.318 | 7.045 |
| | 4.286 | 0.000 | 7.045 |

Surface 11: Rear Left - Perforated Ply

| Vertex data | X | Y | Z |
|---|---|---|---|
| | 9.314 | 2.490 | 0.000 |
| | 11.765 | 2.490 | 0.000 |
| | 11.765 | 5.144 | 0.000 |
| | 9.314 | 5.241 | 0.000 |

Surface 12: Rear Right - Perforated Ply

| Vertex data | X | Y | Z |
|---|---|---|---|
| | 9.314 | 2.490 | 7.045 |
| | 9.314 | 5.241 | 7.045 |
| | 11.765 | 5.144 | 7.045 |
| | 11.765 | 2.490 | 7.045 |

Surface 13: Rear Wall - Perforated Ply

| Vertex data | X | Y | Z |
|---|---|---|---|
| | 11.765 | 2.490 | 0.000 |
| | 11.765 | 2.490 | 7.045 |
| | 11.765 | 5.144 | 7.045 |
| | 11.765 | 5.144 | 0.000 |

Surface 14: Floor - 1 Carpet

| Vertex data | X | Y | Z |
|---|---|---|---|
| | 0.000 | 0.000 | 1.271 |
| | 2.610 | 0.000 | 0.990 |
| | 2.610 | 0.000 | 0.000 |
| | 4.286 | 0.000 | 0.000 |
| | 4.286 | 0.000 | 7.045 |
| | 2.610 | 0.000 | 7.045 |
| | 2.610 | 0.000 | 6.055 |
| | 0.000 | 0.000 | 5.774 |

Surface 15: Step 0 Riser - Carpet

| Vertex data | X | Y | Z |
|---|---|---|---|
| | 4.286 | 0.000 | 0.000 |
| | 4.286 | 0.000 | 7.045 |
| | 4.286 | 0.318 | 7.045 |
| | 4.286 | 0.318 | 0.000 |

Surface 16: Step 1 Tread - Carpet

| Vertex data | X | Y | Z |
|---|---|---|---|
| | 4.286 | 0.318 | 0.000 |
| | 4.286 | 0.318 | 7.045 |
| | 5.124 | 0.318 | 7.045 |
| | 5.124 | 0.318 | 0.000 |

Surface 17: Stair 1 Riser - Carpet

| Vertex data | X | Y | Z |
|---|---|---|---|
| | 5.124 | 0.318 | 0.000 |
| | 5.124 | 0.318 | 7.045 |
| | 5.124 | 0.648 | 7.045 |
| | 5.124 | 0.648 | 0.000 |

Surface 18: Stair 2 Tread - Carpet

| Vertex data | X | Y | Z |
|---|---|---|---|
| | 5.124 | 0.648 | 0.000 |
| | 5.124 | 0.648 | 7.045 |
| | 5.962 | 0.648 | 7.045 |
| | 5.962 | 0.648 | 0.000 |

Surface 19: Stair 2 Riser - Carpet

| Vertex data | X | Y | Z |
|---|---|---|---|
| | 5.962 | 0.648 | 0.000 |
| | 5.962 | 0.648 | 7.045 |
| | 5.962 | 0.991 | 7.045 |
| | 5.962 | 0.991 | 0.000 |

Surface 20: Stair 3 Tread - Carpet

| Vertex data | X | Y | Z |
|---|---|---|---|
| | 5.962 | 0.991 | 0.000 |
| | 5.962 | 0.991 | 7.045 |
| | 6.800 | 0.991 | 7.045 |
| | 6.800 | 0.991 | 0.000 |

Surface 21: Stair 3 Riser - Carpet

| Vertex data | X | Y | Z |
|---|---|---|---|
| | 6.800 | 0.991 | 0.000 |
| | 6.800 | 0.991 | 7.045 |
| | 6.800 | 1.347 | 7.045 |
| | 6.800 | 1.347 | 0.000 |

| Surface 22: | Stair 4 Tread - Carpet | | |
|---|---|---|---|
| Vertex data | X | Y | Z |
| | 6.800 | 1.347 | 0.000 |
| | 6.800 | 1.347 | 7.045 |
| | 7.638 | 1.347 | 7.045 |
| | 7.638 | 1.347 | 0.000 |

| Surface 23: | Stair 4 Riser - Carpet | | |
|---|---|---|---|
| Vertex data | X | Y | Z |
| | 7.638 | 1.347 | 0.000 |
| | 7.638 | 1.347 | 7.045 |
| | 7.638 | 1.715 | 7.045 |
| | 7.638 | 1.715 | 0.000 |

| Surface 24: | Stair 5 Tread - Carpet | | |
|---|---|---|---|
| Vertex data | X | Y | Z |
| | 7.638 | 1.715 | 0.000 |
| | 7.638 | 1.715 | 7.045 |
| | 8.476 | 1.715 | 7.045 |
| | 8.476 | 1.715 | 0.000 |

| Surface 25: | Stair 5 Riser - Carpet | | |
|---|---|---|---|
| Vertex data | X | Y | Z |
| | 8.476 | 1.715 | 0.000 |
| | 8.476 | 1.715 | 7.045 |
| | 8.476 | 2.096 | 7.045 |
| | 8.476 | 2.096 | 0.000 |

| Surface 26: | Stair 6 Tread - Carpet | | |
|---|---|---|---|
| Vertex data | X | Y | Z |
| | 8.476 | 2.096 | 0.000 |
| | 8.476 | 2.096 | 7.045 |
| | 9.314 | 2.096 | 7.045 |
| | 9.314 | 2.096 | 0.000 |

| Surface 27: | Stair 6 Riser - Carpet | | |
|---|---|---|---|
| Vertex data | X | Y | Z |
| | 9.314 | 2.096 | 0.000 |
| | 9.314 | 2.096 | 7.045 |
| | 9.314 | 2.490 | 7.045 |
| | 9.314 | 2.490 | 0.000 |

| Surface 28: | Floor Rear | | |
|---|---|---|---|
| Vertex data | X | Y | Z |
| | 9.314 | 2.490 | 0.000 |
| | 9.314 | 2.490 | 7.045 |
| | 11.760 | 2.490 | 7.045 |
| | 11.760 | 2.490 | 0.000 |

| Surface 29: | Bio-Box Front - Glass | | |
|---|---|---|---|
| Vertex data | X | Y | Z |
| | 9.314 | 2.490 | 2.957 |
| | 9.314 | 2.490 | 4.080 |
| | 9.314 | 5.241 | 4.080 |
| | 9.314 | 5.241 | 2.957 |

| Surface 30: | Bio-Box Left - Ply | | |
|---|---|---|---|
| Vertex data | X | Y | Z |
| | 9.314 | 2.490 | 2.957 |
| | 9.314 | 5.241 | 2.957 |
| | 10.640 | 5.180 | 2.957 |
| | 10.640 | 2.490 | 2.957 |

| Surface 31: | Bio-Box Right - Ply | | |
|---|---|---|---|
| Vertex data | X | Y | Z |
| | 9.314 | 2.490 | 4.080 |
| | 10.640 | 2.490 | 4.080 |
| | 10.640 | 5.180 | 4.080 |
| | 9.314 | 5.241 | 4.080 |

| Surface 32: | Bio-Box Back - Ply | | |
|---|---|---|---|
| Vertex data | X | Y | Z |
| | 10.640 | 2.490 | 2.957 |
| | 10.640 | 5.180 | 2.957 |
| | 10.640 | 5.180 | 4.080 |
| | 10.640 | 2.490 | 4.080 |

| Surface 33: | Lectern Front - Timber | | |
|---|---|---|---|
| Vertex data | X | Y | Z |
| | 1.200 | 0.000 | 2.520 |
| | 1.200 | 0.000 | 4.650 |
| | 1.200 | 0.690 | 4.650 |
| | 1.200 | 0.690 | 2.520 |

| Surface 34: | Lectern Left - Timber | | |
|---|---|---|---|
| Vertex data | X | Y | Z |
| | 1.200 | 0.000 | 2.520 |
| | 1.200 | 0.690 | 2.520 |
| | 1.810 | 0.690 | 2.520 |
| | 1.810 | 0.000 | 2.520 |

| Surface 35: | Lectern Right - Timber | | |
|---|---|---|---|
| Vertex data | X | Y | Z |
| | 1.200 | 0.000 | 4.650 |
| | 1.810 | 0.000 | 4.650 |
| | 1.810 | 0.690 | 4.650 |
| | 1.200 | 0.690 | 4.650 |

| Surface 36: | Lectern Back - Timber | | |
|---|---|---|---|
| Vertex data | X | Y | Z |
| | 1.810 | 0.000 | 2.520 |
| | 1.810 | 0.690 | 2.520 |
| | 1.810 | 0.690 | 4.650 |
| | 1.810 | 0.000 | 4.650 |

| Surface 37: | Lectern Top - Timber | | |
|---|---|---|---|
| Vertex data | X | Y | Z |
| | 1.200 | 0.690 | 2.520 |
| | 1.200 | 0.690 | 4.650 |
| | 1.810 | 0.690 | 4.650 |
| | 1.810 | 0.690 | 2.520 |

| Surface 38: | Row 1 Panel | | |
|---|---|---|---|
| Vertex data | X | Y | Z |
| | 3.448 | 0.000 | 0.995 |
| | 3.448 | 0.000 | 6.062 |
| | 3.573 | 0.830 | 6.062 |
| | 3.573 | 0.830 | 0.995 |

| Surface 39: | Row 2 Panel | | |
|---|---|---|---|
| Vertex data | X | Y | Z |
| | 4.286 | 0.318 | 0.995 |
| | 4.286 | 0.318 | 6.062 |
| | 4.411 | 1.148 | 6.062 |
| | 4.411 | 1.148 | 0.995 |

| Surface 40: | Row 3 Panel | | |
|---|---|---|---|
| Vertex data | X | Y | Z |
| | 5.124 | 0.648 | 0.995 |
| | 5.124 | 0.648 | 6.062 |
| | 5.249 | 1.478 | 6.062 |
| | 5.249 | 1.478 | 0.995 |

| Surface 41: | Row 4 Panel | | |
|---|---|---|---|
| Vertex data | X | Y | Z |
| | 5.962 | 0.991 | 0.995 |
| | 5.962 | 0.991 | 6.062 |
| | 6.087 | 1.821 | 6.062 |
| | 6.087 | 1.821 | 0.995 |

| Surface 42: | Row 5 Panel | | |
|---|---|---|---|
| Vertex data | X | Y | Z |
| | 6.800 | 1.347 | 0.995 |
| | 6.800 | 1.347 | 6.062 |
| | 6.925 | 2.171 | 6.062 |
| | 6.925 | 2.171 | 0.995 |

| Surface 43: | Row 6 Panel | | |
|---|---|---|---|
| Vertex data | X | Y | Z |
| | 7.638 | 1.715 | 0.995 |
| | 7.638 | 1.715 | 6.062 |
| | 7.763 | 2.545 | 6.062 |
| | 7.763 | 2.545 | 0.995 |

| Surface 44: | Row 7 Panel | | |
|---|---|---|---|
| Vertex data | X | Y | Z |
| | 8.476 | 2.096 | 0.995 |
| | 8.476 | 2.096 | 6.062 |
| | 8.601 | 2.926 | 6.062 |
| | 8.601 | 2.926 | 0.995 |

| Surface 45: | Row 8 Panel | | |
|---|---|---|---|
| Vertex data | X | Y | Z |
| | 9.314 | 2.490 | 0.995 |
| | 9.314 | 2.490 | 6.062 |
| | 9.439 | 3.320 | 6.062 |
| | 9.439 | 3.320 | 0.995 |

| Surface 46: | Row 9 Panel Left | | |
|---|---|---|---|
| Vertex data | X | Y | Z |
| | 10.152 | 2.490 | 0.965 |
| | 10.152 | 2.490 | 2.965 |
| | 10.277 | 3.320 | 2.965 |
| | 10.277 | 3.320 | 0.965 |

| Surface 47: | Row 9 Panel Right | | |
|---|---|---|---|
| Vertex data | X | Y | Z |
| | 10.152 | 2.490 | 4.115 |
| | 10.152 | 2.490 | 6.110 |
| | 10.277 | 3.320 | 6.110 |
| | 10.277 | 3.320 | 4.115 |

| Volume | 308.0000 |
|---|---|

## *Absorption Data*

| | | | Frequency | | | | | | |
|---|---|---|---|---|---|---|---|---|---|
| No. | Description | Area | 125 | 250 | 500 | 1000 | 2000 | 4000 | Source |
| 1 | Screen Wall - Chalkboard | 15.2697 | 0.20 | 0.28 | 0.26 | 0.09 | 0.12 | 0.11 | 1 |
| 2 | Screen Left - Ply | 9.5514 | 0.20 | 0.28 | 0.26 | 0.09 | 0.12 | 0.11 | 1 |
| 3 | Screen Right - Ply | 9.5514 | 0.20 | 0.28 | 0.26 | 0.09 | 0.12 | 0.11 | 1 |
| 4 | Screen Ceiling - Ply | 12.7088 | 0.20 | 0.28 | 0.26 | 0.09 | 0.12 | 0.11 | 1 |
| 5 | Upper Screen - Plaster | 11.3597 | 0.02 | 0.03 | 0.04 | 0.06 | 0.06 | 0.03 | 1 |
| 6 | Ceiling - Plaster | 63.1340 | 0.02 | 0.03 | 0.04 | 0.06 | 0.06 | 0.03 | 1 |
| 7 | Front Left Screen - Ply | 3.8471 | 0.20 | 0.28 | 0.26 | 0.09 | 0.12 | 0.11 | 1 |
| 8 | Front Right Screen - Ply | 3.8471 | 0.20 | 0.28 | 0.26 | 0.09 | 0.12 | 0.11 | 1 |
| 9 | Wall - Left Ply | 29.8590 | 0.20 | 0.28 | 0.26 | 0.09 | 0.12 | 0.11 | 1 |
| 10 | Wall - Right Ply | 29.8590 | 0.20 | 0.28 | 0.26 | 0.09 | 0.12 | 0.11 | 1 |
| 11 | Rear Left - Perforated Ply | 6.6238 | 0.16 | 0.47 | 0.87 | 0.86 | 0.63 | 0.58 | 2 |
| 12 | Rear Right - Perforated Ply | 6.6238 | 0.16 | 0.47 | 0.87 | 0.86 | 0.63 | 0.58 | 2 |
| 13 | Rear Wall - Perforated Ply | 18.6974 | 0.16 | 0.47 | 0.87 | 0.86 | 0.63 | 0.58 | 2 |
| 14 | Floor - 1 Carpet | 24.2937 | 0.05 | 0.08 | 0.20 | 0.30 | 0.35 | 0.40 | 3 |
| 15 | Step 0 Riser - Carpet | 2.2403 | 0.05 | 0.08 | 0.20 | 0.30 | 0.35 | 0.40 | 3 |
| 16 | Step 1 Tread - Carpet | 5.9037 | 0.05 | 0.08 | 0.20 | 0.30 | 0.35 | 0.40 | 3 |
| 17 | Stair 1 Riser - Carpet | 2.3249 | 0.05 | 0.08 | 0.20 | 0.30 | 0.35 | 0.40 | 3 |
| 18 | Stair 2 Tread - Carpet | 5.9037 | 0.05 | 0.08 | 0.20 | 0.30 | 0.35 | 0.40 | 3 |
| 19 | Stair 2 Riser - Carpet | 2.4164 | 0.05 | 0.08 | 0.20 | 0.30 | 0.35 | 0.40 | 3 |
| 20 | Stair 3 Tread - Carpet | 5.9037 | 0.05 | 0.08 | 0.20 | 0.30 | 0.35 | 0.40 | 3 |
| 21 | Stair 3 Riser - Carpet | 2.5080 | 0.05 | 0.08 | 0.20 | 0.30 | 0.35 | 0.40 | 3 |
| 22 | Stair 4 Tread - Carpet | 5.9037 | 0.05 | 0.08 | 0.20 | 0.30 | 0.35 | 0.40 | 3 |
| 23 | Stair 4 Riser - Carpet | 2.5926 | 0.05 | 0.08 | 0.20 | 0.30 | 0.35 | 0.40 | 3 |
| 24 | Stair 5 Tread - Carpet | 5.9037 | 0.05 | 0.08 | 0.20 | 0.30 | 0.35 | 0.40 | 3 |
| 25 | Stair 5 Riser - Carpet | 2.6841 | 0.05 | 0.08 | 0.20 | 0.30 | 0.35 | 0.40 | 3 |
| 26 | Stair 6 Tread - Carpet | 5.9037 | 0.05 | 0.08 | 0.20 | 0.30 | 0.35 | 0.40 | 3 |
| 27 | Stair 6 Riser - Carpet | 2.7757 | 0.05 | 0.08 | 0.20 | 0.30 | 0.35 | 0.40 | 3 |
| 28 | Floor Rear | 17.2321 | 0.05 | 0.08 | 0.20 | 0.30 | 0.35 | 0.40 | 3 |
| 29 | Bio-Box Front - Glass | 3.0894 | 0.20 | 0.15 | 0.10 | 0.07 | 0.05 | 0.05 | 3 |
| 30 | Bio-Box Left - Ply | 3.6074 | 0.20 | 0.28 | 0.26 | 0.09 | 0.12 | 0.11 | 1 |
| 31 | Bio-Box Right - Ply | 3.6074 | 0.20 | 0.28 | 0.26 | 0.09 | 0.12 | 0.11 | 1 |
| 32 | Bio-Box Back - Ply | 3.0209 | 0.20 | 0.28 | 0.26 | 0.09 | 0.12 | 0.11 | 1 |
| 33 | Lectern Front - Timber | 1.4697 | 0.03 | 0.25 | 0.20 | 0.17 | 0.15 | 0.10 | 3 |
| 34 | Lectern Left - Timber | 0.4209 | 0.03 | 0.25 | 0.20 | 0.17 | 0.15 | 0.10 | 3 |
| 35 | Lectern Right - Timber | 0.4209 | 0.03 | 0.25 | 0.20 | 0.17 | 0.15 | 0.10 | 3 |
| 36 | Lectern Back - Timber | 1.4697 | 0.03 | 0.25 | 0.20 | 0.17 | 0.15 | 0.10 | 3 |
| 37 | Lectern Top - Timber | 1.2993 | 0.03 | 0.25 | 0.20 | 0.17 | 0.15 | 0.10 | 3 |
| 38 | Row 1 Panel | 4.2530 | 0.05 | 0.15 | 0.40 | 0.80 | 0.65 | 0.60 | 3 |
| 39 | Row 2 Panel | 4.2530 | 0.05 | 0.15 | 0.40 | 0.80 | 0.65 | 0.60 | 3 |
| 40 | Row 3 Panel | 4.2530 | 0.05 | 0.15 | 0.40 | 0.80 | 0.65 | 0.60 | 3 |
| 41 | Row 4 Panel | 4.2530 | 0.05 | 0.15 | 0.40 | 0.80 | 0.65 | 0.60 | 3 |
| 42 | Row 5 Panel | 4.2230 | 0.05 | 0.15 | 0.40 | 0.80 | 0.65 | 0.60 | 3 |
| 43 | Row 6 Panel | 4.2530 | 0.05 | 0.15 | 0.40 | 0.80 | 0.65 | 0.60 | 3 |
| 44 | Row 7 Panel | 4.2530 | 0.05 | 0.15 | 0.40 | 0.80 | 0.65 | 0.60 | 3 |
| 45 | Row 8 Panel | 4.2530 | 0.05 | 0.15 | 0.40 | 0.80 | 0.65 | 0.60 | 3 |
| 46 | Row 9 Panel Left | 1.6787 | 0.05 | 0.15 | 0.40 | 0.80 | 0.65 | 0.60 | 3 |
| 47 | Row 9 Panel Right | 1.6745 | 0.05 | 0.15 | 0.40 | 0.80 | 0.65 | 0.60 | 3 |
| | Air Absorption | | 0.00 | 0.00 | 0.00 | 0.003 | 0.007 | 0.020 | |

### Source of Absorption Data

1. Bradford Insulation Catalogue. *("Compiled from works of such authorities as P.V. Bruel, L.L. Beranek, J.E.R. & K.H. Constable, V.O. Knudsen and others, and also from manufacturers' data")*
2. Davern (1977, pg87) Figure 1. 11% perforation
3. Public Works Department, W.A. Environmental Design Section Data (1984)

## Case Study 2

Note: The volume and surface areas are computed by the program.

The dimensional data is in metres.

### *Input Geometric Data*

Surface 1: Floor - Carpet

| Vertex data | X | Y | Z |
|---|---|---|---|
| | 0.855 | 0.000 | 0.000 |
| | 0.000 | 0.000 | 0.862 |
| | 0.000 | 0.000 | 5.007 |
| | 0.862 | 0.000 | 5.869 |
| | 4.729 | 0.000 | 5.869 |
| | 5.959 | 0.000 | 4.639 |
| | 5.959 | 0.000 | 0.809 |
| | 5.150 | 0.000 | 0.000 |
| | 0.855 | 0.000 | 0.000 |

Surface 2: Front Wall - Plaster

| Vertex data | X | Y | Z |
|---|---|---|---|
| | 0.855 | 0.000 | 0.000 |
| | 5.150 | 0.000 | 0.000 |
| | 5.150 | 3.245 | 0.000 |
| | 0.855 | 3.245 | 0.000 |

Surface 3: Front Left Wing - Plaster

| Vertex data | X | Y | Z |
|---|---|---|---|
| | 0.000 | 0.000 | 0.855 |
| | 0.855 | 0.000 | 0.000 |
| | 0.855 | 3.245 | 0.000 |
| | 0.000 | 3.245 | 0.855 |

Surface 4: Front Right Wing - Plaster

| Vertex data | X | Y | Z |
|---|---|---|---|
| | 5.150 | 0.000 | 0.000 |
| | 5.959 | 0.000 | 0.809 |
| | 5.959 | 3.245 | 0.809 |
| | 5.150 | 3.245 | 0.000 |

Surface 5: Side Right - Plaster

| Vertex data | X | Y | Z |
|---|---|---|---|
| | 5.959 | 0.000 | 0.809 |
| | 5.959 | 0.000 | 4.639 |
| | 5.959 | 3.245 | 4.639 |
| | 5.959 | 3.245 | 2.379 |
| | 5.959 | 2.935 | 2.379 |
| | 5.959 | 2.935 | 2.069 |
| | 5.959 | 3.245 | 2.069 |
| | 5.959 | 3.245 | 0.809 |
| | 5.959 | 0.000 | 0.809 |

Surface 6: Side Left - Plaster

| Vertex data | X | Y | Z |
|---|---|---|---|
| | 0.000 | 0.000 | 0.855 |
| | 0.000 | 3.245 | 0.855 |
| | 0.000 | 3.245 | 2.069 |
| | 0.000 | 2.935 | 2.069 |
| | 0.000 | 2.935 | 2.379 |
| | 0.000 | 3.245 | 2.379 |
| | 0.000 | 3.245 | 5.007 |
| | 0.000 | 0.000 | 5.007 |

Surface 7: Back Right Wing - Plaster

| Vertex data | X | Y | Z |
|---|---|---|---|
| | 0.000 | 0.000 | 5.007 |
| | 0.000 | 2.375 | 5.007 |
| | 0.862 | 2.375 | 5.869 |
| | 0.862 | 0.000 | 5.869 |

| Surface 8: | Back Left Wing - Plaster | | |
|---|---|---|---|
| Vertex data | X | Y | Z |
| | 4.729 | 0.000 | 5.869 |
| | 4.729 | 2.375 | 5.869 |
| | 5.591 | 2.375 | 5.007 |
| | 5.591 | 3.245 | 5.007 |
| | 5.959 | 3.245 | 4.639 |
| | 5.959 | 0.000 | 4.639 |

| Surface 9: | Back Wall - Plaster | | |
|---|---|---|---|
| Vertex data | X | Y | Z |
| | 0.862 | 0.000 | 5.869 |
| | 0.862 | 2.375 | 5.869 |
| | 4.729 | 2.375 | 5.869 |
| | 4.729 | 0.000 | 5.869 |

| Surface 10: | Beam Bottom - Concrete | | |
|---|---|---|---|
| Vertex data | X | Y | Z |
| | 0.000 | 2.935 | 2.069 |
| | 5.959 | 2.935 | 2.069 |
| | 5.959 | 2.935 | 2.379 |
| | 0.000 | 2.935 | 2.379 |

| Surface 11: | Beam Front - Concrete | | |
|---|---|---|---|
| Vertex data | X | Y | Z |
| | 0.000 | 2.935 | 2.069 |
| | 0.000 | 3.245 | 2.069 |
| | 5.959 | 3.245 | 2.069 |
| | 5.959 | 2.935 | 2.069 |

| Surface 12: | Beam Back - Concrete | | |
|---|---|---|---|
| Vertex data | X | Y | Z |
| | 0.000 | 2.935 | 2.379 |
| | 5.959 | 2.935 | 2.379 |
| | 5.959 | 3.246 | 2.379 |
| | 0.000 | 3.245 | 2.379 |

| Surface 13: | Ceiling Front - Vermiculite | | |
|---|---|---|---|
| Vertex data | X | Y | Z |
| | 0.000 | 3.245 | 0.855 |
| | 0.855 | 3.245 | 0.000 |
| | 5.150 | 3.245 | 0.000 |
| | 5.959 | 3.245 | 0.809 |
| | 5.959 | 3.245 | 2.069 |
| | 0.000 | 3.245 | 2.069 |

| Surface 14: | Ceiling Back - Vermiculite | | |
|---|---|---|---|
| Vertex data | X | Y | Z |
| | 0.000 | 3.245 | 2.379 |
| | 5.959 | 3.245 | 2.379 |
| | 5.959 | 3.245 | 4.639 |
| | 5.591 | 3.245 | 5.007 |
| | 0.000 | 3.245 | 5.007 |

| Surface 15: | Bulkhead Side - Plaster | | |
|---|---|---|---|
| Vertex data | X | Y | Z |
| | 0.000 | 2.375 | 5.007 |
| | 0.000 | 3.245 | 5.007 |
| | 5.591 | 3.245 | 5.007 |
| | 5.591 | 2.375 | 5.007 |

| Surface 16: | Bulkhead Base - Plaster | | |
|---|---|---|---|
| Vertex data | X | Y | Z |
| | 0.000 | 2.375 | 5.007 |
| | 5.591 | 2.375 | 5.007 |
| | 4.729 | 2.375 | 5.869 |
| | 0.862 | 2.375 | 5.869 |

| Volume | 101.0000 |
|---|---|

## *Absorption Data*

| No. | Description | Area | Frequency 125 | 250 | 500 | 1000 | 2000 | 4000 | Source |
|---|---|---|---|---|---|---|---|---|---|
| 1 | Floor - Carpet | 33.1497 | 0.05 | 0.08 | 0.20 | 0.30 | 0.35 | 0.40 | 3 |
| 2 | Front Wall - Plaster | 13.9373 | 0.02 | 0.03 | 0.04 | 0.06 | 0.06 | 0.03 | 1 |
| 3 | Front Left Wing - Plaster | 3.9237 | 0.02 | 0.03 | 0.04 | 0.06 | 0.06 | 0.03 | 1 |
| 4 | Front Right Wing - Plaster | 3.7126 | 0.02 | 0.03 | 0.04 | 0.06 | 0.06 | 0.03 | 1 |
| 5 | Side Right - Plaster | 12.3322 | 0.02 | 0.03 | 0.04 | 0.06 | 0.06 | 0.03 | 1 |
| 6 | Side Left - Plaster | 13.3771 | 0.02 | 0.03 | 0.04 | 0.06 | 0.06 | 0.03 | 1 |
| 7 | Back Right Wing - Plaster | 2.8952 | 0.02 | 0.03 | 0.04 | 0.06 | 0.06 | 0.03 | 1 |
| 8 | Back Left Wing - Plaster | 4.5840 | 0.02 | 0.03 | 0.04 | 0.06 | 0.06 | 0.03 | 1 |
| 9 | Back Wall - Plaster | 9.1841 | 0.02 | 0.03 | 0.04 | 0.06 | 0.06 | 0.03 | 1 |
| 10 | Beam Bottom - Concrete | 1.8473 | 0.01 | 0.01 | 0.02 | 0.02 | 0.02 | 0.03 | 1 |
| 11 | Beam Front - Concrete | 1.8473 | 0.01 | 0.01 | 0.02 | 0.02 | 0.02 | 0.03 | 1 |
| 12 | Beam Back - Concrete | 1.8503 | 0.01 | 0.01 | 0.02 | 0.02 | 0.02 | 0.03 | 1 |
| 13 | Ceiling Front - Vermiculite | 11.6364 | 0.10 | 0.13 | 0.19 | 0.33 | 0.45 | 0.40 | 3 |
| 14 | Ceiling Back - Vermiculite | 15.5925 | 0.10 | 0.13 | 0.19 | 0.33 | 0.45 | 0.40 | 3 |
| 15 | Bulkhead Side - Plaster | 4.8642 | 0.02 | 0.03 | 0.04 | 0.06 | 0.06 | 0.03 | 1 |
| 16 | Bulkhead Base - Plaster | 4.0764 | 0.02 | 0.03 | 0.04 | 0.06 | 0.06 | 0.03 | 1 |
| | Air Absorption | | 0.00 | 0.00 | 0.00 | 0.003 | 0.007 | 0.020 | |

### Source of Absorption Data

1. Bradford Insulation Catalogue. *("Compiled from works of such authorities as P.V. Bruel, L.L. Beranek, J.E.R. & K.H. Constable, V.O. Knudsen and others, and also from manufacturers' data")*
2. Davern (1977, pg87) Figure 1. 11% perforation
3. Public Works Department, W.A. Environmental Design Section Data (1984)